Molecular Requirements for RIF1 Role in DNA Double-Strand Break End Protection

Inaugural-Dissertation to obtain the academic degree

Doctor rerum naturalium (Dr. rer. nat.)

submitted to the Department of Biology, Chemistry, Pharmacy

of Freie Universität Berlin

by

Matteo Andreani

2020

This study was performed from February 2015 to August 2019 under the supervision of Prof. Dr. Michela Di Virgilio at "Max Delbrück-Center for Molecular Medicine" in the Helmholtz Association, in Berlin.

1st Reviewer:	Prof. Dr. Michela Di Virgilio Max Delbrück Center for Molecular Medicine
2nd Reviewer:	Prof. Dr. Oliver Daumke Freie Universität Berlin - Max Delbrück Center for Molecular Medicine

Date of the defense: 12.03.2020

Table of Contents

List of figures

List of tables

Abstract

Mammalian Rap1-interacting factor 1 (RIF1) is a multifunctional protein required for DNA replication timing, restart of stalled replication forks, resolution of anaphase bridges and non-homologous end joining (NHEJ) repair of DNA double-strand breaks (DSBs). NHEJ repair is essential in certain contexts but can be detrimental in others. On one hand, defective NHEJ hampers the ability of B lymphocytes to undergo antibody class switch recombination (CSR) and leads to life-threatening immunodeficiencies. On the other hand, the predominance of NHEJ over homologous recombination (HR) in HR-deficient cells can cause the accumulation of mutations, genomic aberrations, and tumorigenesis. DSB end resection is an important step in the DSB repair pathway choice and RIF1 promotes NHEJ repair partly by protecting DSB ends from extensive resection. How the process of DSB end protection is regulated, especially in the context of CSR, remains unclear. Specifically, the full picture of interactor proteins, as well as the post-translational modifications (PTMs) that may regulate RIF1 function in DSB repair, have not been defined yet.

Therefore, the characterization of RIF1 interacting partners and PTMs will be instrumental for our understanding of the mechanisms underlying DSB end protection during CSR in B cells and genomic instability in HR-deficient cells. To this aim, first I conducted a loss-of-function screen to test the involvement of potential RIF1 interactors in isotype switching. I identified ARPC1A, a protein involved in actin polymerization, as a factor affecting CSR upon bulk somatic targeting. ARPC1A, whose function in CSR has not been reported yet, may represent a link between these two processes that so far were considered unrelated. Second, I assessed the requirement for DSB end protection of three RIF1 conserved, clustered SQ motifs that we found to be phosphorylated in primary B lymphocytes undergoing CSR. To investigate if the phosphorylation status of these sites contributed to modulate RIF1 function during DSB end protection, I generated and tested the ability of RIF1 phosphomutant cell lines to undergo CSR. I proved that the phosphorylation status of the conserved SQ cluster does not affect RIF1 ability to support CSR. Furthermore, RIF1 phosphomutants failed to rescue genomic instability in a *BRCA1*-deficient background. These findings indicate that the phosphorylation of the conserved SQ sites is dispensable for RIF1 role in DSB end protection.

Zusammenfassung

Das Rap1-interacting factor 1 (RIF1) ist ein multifunktionales Protein, welches unter anderem den Prozess der DNA-Replikation zeitlich koordiniert sowie am Neustart blockierter Replikationsgabeln, der Auflösung von Anaphase-Brücken und der Nicht-homologen Endverknüpfung (non-homologous end joining, NHEJ) von DNA-Doppelstrangbrüchen (DNA double-strand breaks, DSBs) beteiligt ist. Die NHEJ Reparatur ist in bestimmten Zusammenhängen unerlässlich, kann jedoch in anderen nachteilig sein. Einerseits beeinträchtigen Defekte in der NHEJ die Fähigkeit von B Lymphozyten, einen Antikörper-Isotypen-Wechsel (class switch recombination, CSR) durchzuführen, was zu lebensbedrohlicher Immundefizienz führen kann. Andererseits kann eine Prädominanz des NHEJ im Vergleich zur homologen Rekombination (homologous recombination, HR) in HR-defizienten Zellen zur Akkumulation von Mutationen, genomischen Aberrationen und zur Tumorigenese führen. DSB-Endresektion ist ein wichtiger Schritt im Signalweg der DSB-Reparatur und das RIF1 Protein fördert die NHEJ teils durch den Schutz der DSB-Enden vor extensiver Resektion. Wie der Schutz der DSB-Enden genau reguliert ist, vor allem im Kontext des CSR ist bisher nicht untersucht. Insbesondere ist bisher nichts über die Gesamtheit aller Interaktionspartner sowie die post-translationalen Modifikationen bekannt, welche die Funktion von RIF1 im Prozess der DSB-Reparatur regulieren könnten.

Die Charakterisierung der Interaktionspartner von RIF1 sowie die Untersuchung seiner post-translationalen Modifikationen wird daher entscheidend zum Verständnis der Mechanismen, die der DSB-Endprotektion während des CSR in B Zellen sowie der genomischen Instabilität in HR-defizienten Zellen unterliegen, beitragen. Folglich habe ich in dieser Studie zunächst ein Loss-of-Function Screen zur Untersuchung potentieller RIF1-Interaktionspartner im Prozess des CSR durchgeführt. Hierbei habe ich ARPC1A als ein Faktor identifiziert, welcher den CSR beeinflusst. ARPC1A ist ein Protein, welches in die Polymerisation von Aktin involviert ist und für welches bisher keine Funktion im Prozess des CSR beschrieben wurde; als solches könnte ARPC1A jedoch einen ersten Link zwischen diesen beiden Prozessen, die bisher als unzusammenhängend angesehen wurden, darstellen.

Zudem habe ich den Einfluss dreier konservierter, geclusterter SQ Motive von RIF1 im Prozess der DSB-Endprotektion untersucht, bei welchen zuvor eine spezifische Phosphorylierung während des CSR in primären B Zellen festgestellt wurde.

Um zu untersuchen, ob der Phosphorylierungs-Status dieser Abschnitte die Funktion von RIF1 im Prozess der DSB-Endprotektion beeinflusst, habe ich RIF1-phosphomutante Zelllinien

generiert und deren Fähigkeit des CSR durchzuführen, untersucht. Hierbei konnte ich zeigen, dass der Phosphorylierungs-Status der konservierten SQ Cluster die Funktion von RIF1 im CSR nicht beeinflusst. Des Weiteren konnten die generierten RIF1-Phosphomutanten die genomische Instabilität in einem HR-defizienten Hintergrund nicht verhindern. Aus diesen Ergebnissen ist zu schließen, dass die Phosphorylierung der konservierten SQ Abschnitte keinen entscheidenden Einfluss auf die Rolle des RIF1 Proteins in der DSB-Endprotektion hat.

1. Introduction

1.1 The threats to genome stability and the importance of its maintenance

The deoxyribonucleic acid (DNA) is the carrier of the genetic information in all cellular organisms. The way an organism develops, functions (by adapting and responding) and finally declines in a specific environment is dictated by its DNA. The extremely complex processes involved in these steps are coordinated *via* the finely regulated expression of the genetic code. In fact, in the course of evolution, reproduction and survival of the fittest organisms are permitted by their adaptations, which are then transferred to the following generations in the form of changes in the genetic code (mutations) and in the accessibility of specific genes (epigenetic marks). As we all know, these changes occur slowly in the course of millennia.

Nonetheless, on a shorter timescale, the survival of an organism during its life is strictly dependent on the maintenance of the integrity of its genome. Despite the great stability of the DNA molecule[1], its stability is put at risk by endogenous sources even in physiological conditions[2,3]. In fact, it was estimated that approximately 70,000 spontaneous DNA lesions occur in each human cell every day[4]. These aberrations can arise from heat, reactive oxygen species (ROS) generated during metabolic processes, mismatches introduced during DNA replication, spontaneous depurination/deamination, and many other endogenous sources[2-4]. Furthermore, exposition to environmental sources such as ultraviolet (UV) radiation, ionizing radiation (IR) and various chemical agents increase the risk to accumulate DNA damage[5,6]. Specifically, these sources create adducts that can hamper replication and transcription or cause base losses and DNA single-strand breaks (SSBs). The most deleterious type of damage, namely DNA double-strand

breaks (DSBs), occurs when the replication fork encounters a SSB or when two SSB nicks on complementary strands are in close proximity to each other[7].

Any unrepaired damage to the DNA not only can cause cell death or apoptosis but, if accumulated, it can cause mutations leading to cellular dysfunctions and ultimately to tumorigenesis. Additionally, during the physiological processes that rely on genetic rearrangements (i.e. those required for antibody diversification in B lymphocytes), cells need to specifically induce and repair DNA damage. Hence, a prompt DNA damage response (DDR) is necessary for preserving the genetic material and the physiology of the organism.

1.2 DNA double-strand breaks

DSBs represent one of the major cytotoxic DNA lesions contributing to genomic instability. These specific lesions can lead to the buildup of genetic abnormalities such as chromosome translocations, point mutations, insertion, and deletions. Hence, cells developed specific types of machinery intended to timely identify and repair them[8].

Once a DSB has been located, the configuration of its ends ("blunt" or "5' overhang"), the high order structure of the surrounding chromatin (euchromatin or heterochromatin) and, most prominently, the affected genes and the stage of the cell cycle, dictate how it will be repaired[5,9-11]. As it will be later described, cells can choose between different DSB repair pathways and an adequate choice is needed to avoid the accumulation of genomic instability as well as to ensure the positive outcome of those physiological processes that require programmed DSBs.

1.2.1 Sensing the break: the beginning of the DDR

Considering the amount of DNA damage that a cell needs to deal with each day, it is not surprising to know that, besides the repair mechanisms, the complexity of

the DDR lays in those factors dedicated to the "genome integrity and cell cycle surveillance". In fact, the earliest stages of DSB sensing remain unclear, but most recent studies suggest that PARP1 (Poly(ADP-ribose) polymerase-1), MRN (MRE11-RAD50-NBS1) and Ku (Ku70/80) complexes are the primary DSB sensors[12,13] (Fig. 1A).

PARP1 is an abundant protein involved in many cellular processes besides the DDR, namely RNA metabolism, DNA replication, and transcription[14,15]. PARP1 can bind DSBs via its zinc-fingers[16] and polymerize Poly(ADPribose) (PAR) branches (a process called "PARylation"). PAR chains promote chromatin relaxation and histone displacement[17] as well as the recruitment of DDR factors, especially NBS1 (Nijmegen breakage syndrome 1) and MRE11 (meiotic recombination 11 homolog 1), two subunits of the MRN complex[18] (Fig. 1B). Additionally, Ku70/80 recruits DNA-dependent protein kinase catalytic subunit (DNA-PKcs) to the damage site, which in turn activates Ataxia-telangiectasia mutated (ATM) kinase (Fig. 1B). ATM is the major kinase of the DDR and besides phosphorylating and activating many DDR downstream factors, it activates G1/S and G2/M cell cycle checkpoints upon DNA damage[19]. ATM phosphorylates histone H2A.X (S139), forming γH2AX, the main DNA damage histone mark[20]. The kinase activity of ATM is enhanced by its interaction with PAR branches and NBS1, along with its consecutive autophosphorylation[21]. Collectively, PARP1 (via PAR chains), MRN, ATM, and other factors form a positive feedback loop spreading the DDR signal to the surrounding chromatin, which in turn augments its accessibility and facilitates the recruitment of DSB repair factors[19] (Fig. 1C). The additional factors and post-translational modifications (PTMs) involved in the DDR signaling cascade will be mentioned in paragraph 1.2.3.2.

Both Ku70/80 and MRN have also been postulated to sense the DSB and have shown to compete for binding to DNA ends *in vitro*[22]. How these two complexes, which have an apparently redundant function and are recruited to DSB sites within seconds[23,24], affect each other is still an open question.

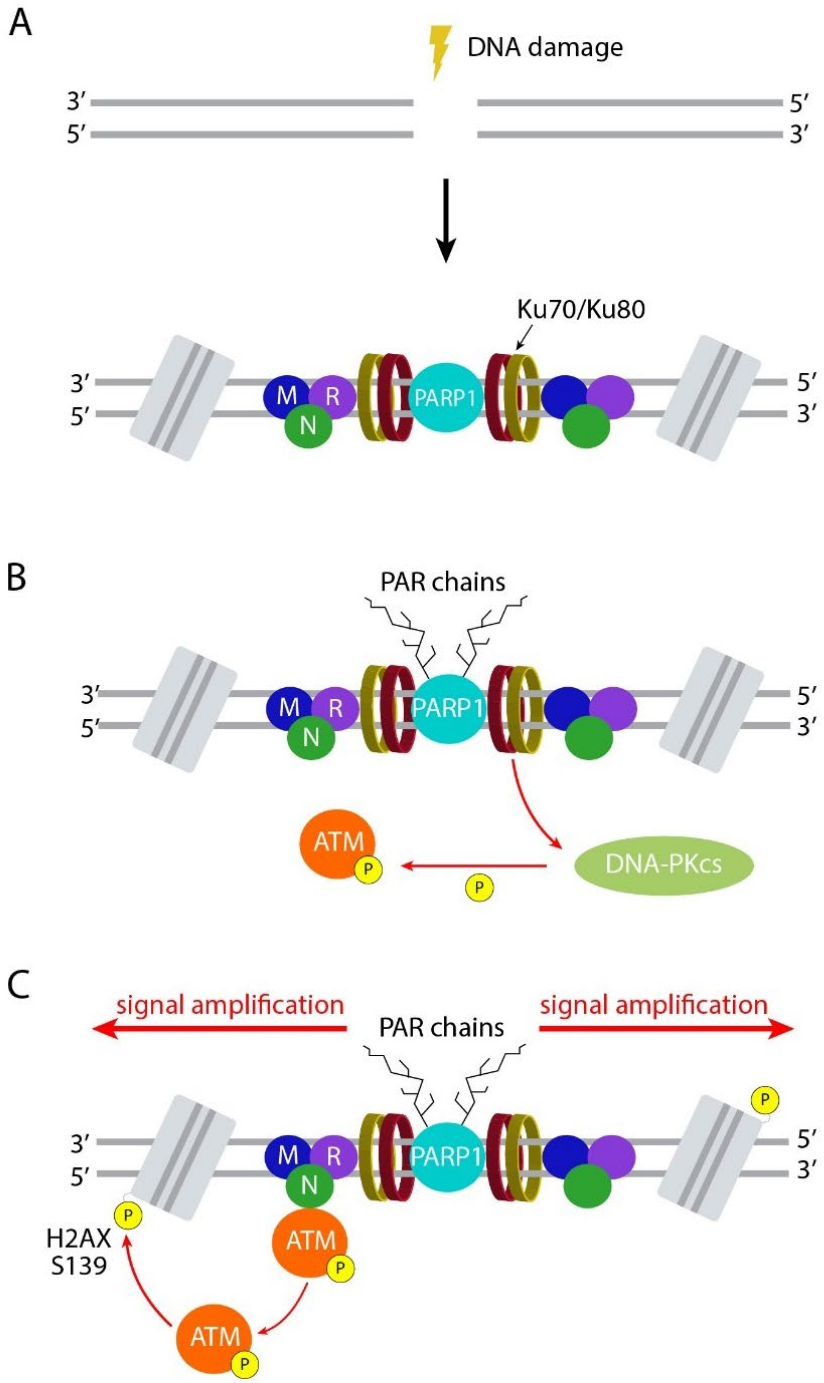

Figure 1: **Present model of DSB sensing and amplification of the DDR signal. (A)** Upon DNA damage formation by a spontaneous or exogenous source, the three sensor proteins PARP1, Ku70/80 and MRN are recruited to the break. **(B)** PARP1 polymerizes PAR chains (PARylation) that contribute to chromatin accessibility and to the recruitment of DSB repair factors. The Ku complex recruits DNA-PKcs, which phosphorylates and activates ATM. **(C)** ATM phosphorylates S139 of H2AX, generating the major histone mark of the DDR which, together with ATM autophosphorylation and PARP1-mediated PARylation, amplifies the DDR signal.

It is suggested that the residency of Ku70/80 and MRN at DSB sites depends on the cell cycle stage and on the DSB structure. For instance, the Ku70/80 heterodimer, which is highly abundant throughout the cell cycle, has a high affinity to blunt DSB ends but low affinity for ssDNA[25-27]. On the other hand, MRN is much lesser abundant than Ku70/80 but it is able, via its nuclease subunit MRE11 activity coupled to CtIP (CtBP-interacting protein) (both activated by cyclin-dependent-kinases 1/2, CDK1/CDK2), to displace Ku70/80 from DSB in S and G2/M phases[28].

1.2.2 Repairing the break

The two predominant DSB repair pathways are non-homologous end joining (NHEJ), active throughout the cell cycle, and homologous recombination (HR), only active in S/G2 phase. Both of these multi-step processes have been object of intense studies for more than two decades but continue to be investigated, as new factors involved in their regulation and execution are identified. These pathways are regulated at different steps and when both are active and competing in S/G2 phase, the coordination of factors and enzymes allows one or the other to prevail[29] (Fig. 2).

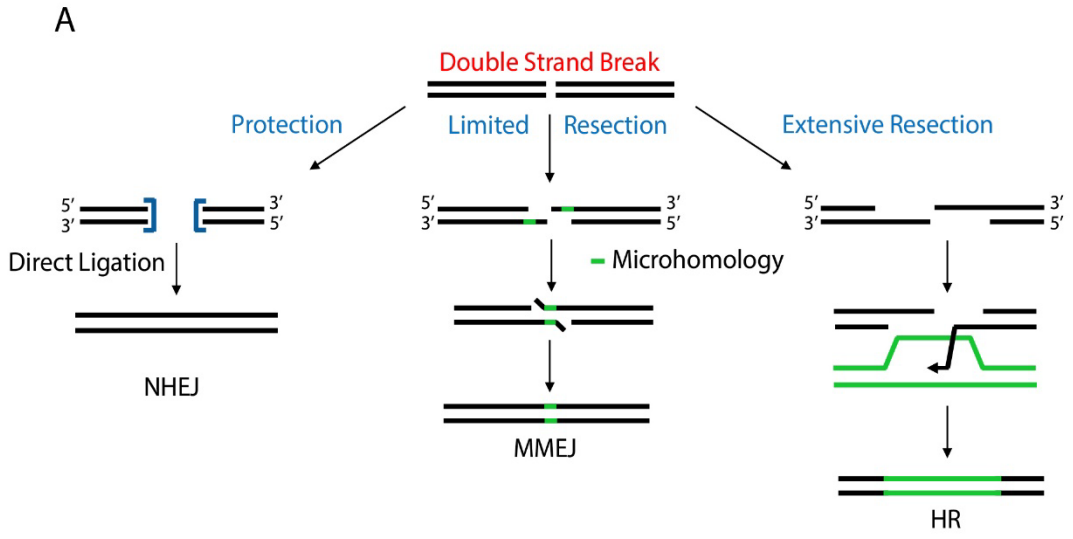

(Fig. 2 continued on page 6)

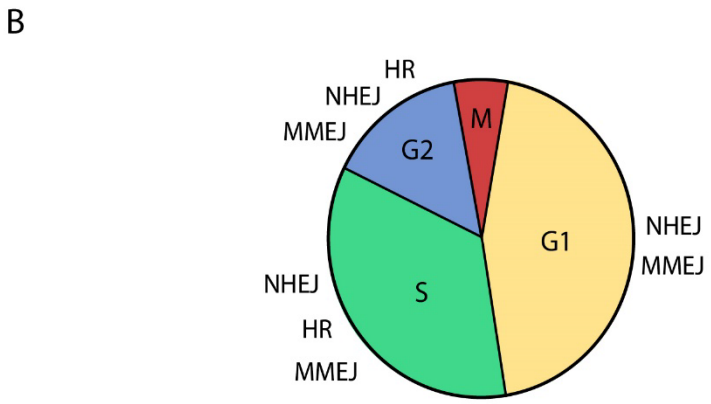

Figure 2: The three main DNA DSB repair pathways. (A) Schematic representation of the NHEJ, HR and MMEJ pathways. **(B)** Scheme indicating the phases of the cell cycle in which each pathway is active.

1.2.2.1 Non-homologous end joining

NHEJ is a rapid, error-prone mechanism, whose mutagenic potential is dictated by the structure of DSB ends rather than by the repair process itself[30-32]. NHEJ quickly repairs breaks in G0/G1 and G2 and is required for the completion of the recombinational processes leading to antigen receptor formation and antibody isotype switching in mature B lymphocytes[33-37] (described in paragraph 1.3.3). Because of its fast kinetics, the process is thought to be the first attempt of a cell to repair multiple breaks and avoid their accumulation[8].

NHEJ starts with the recognition and binding to DSBs by the Ku70/Ku80 heterodimer, followed by the recruitment of DNA-PKcs[38]. The newly formed DNA-PK complex promotes the formation of filaments composed of XRCC4 (X-ray repair cross complementing 4) and XLF (XRCC4-like factor)[39]. The XRCC4/XLF filaments, together with Ku and MRN complexes, aid the stabilization and synapsis of the two DSB ends[40,41]. Finally, re-joining occurs via the restoration of the phosphodiester bond between the free 5' phosphate and 3' hydroxyl groups by the XRCC4-DNA ligase IV (LIG4) complex with no loss of genetic material[40]. Since this type of repair does not require DSB end processing, it is called "resection-independent NHEJ"[42].

A more complex subset of DSBs, like those induced by chemicals or ionizing radiation, does not expose the LIG4 substrates required for ligation. Hence, the repair of these breaks requires minimal end processing (up to 4 bases) by the nuclease Artemis coupled to DNA-PK[42,43]. This type of repair is called "resection-dependent NHEJ". In summary, NHEJ is an efficient process that can directly repair blunt DSBs but, due to its mutagenic repair of complex DSB, its inhibition in S phase is essential for faithful replication of the DNA.

1.2.2.2 Homologous recombination

In contrast to NHEJ, HR is a slow, error-free repair pathway that relies on the availability of intact homologous sequences on sister chromatids for templated DNA synthesis. Thus, this mechanism can be productive only in late S/G2 phases of the cell cycle[44] (Fig. 2). Thanks to its fidelity, HR is required for the repair of DSB occurring in highly transcribed genes or in repetitive sequences present in the heterochromatin[44]. Furthermore, HR is required for the repair of one-ended DSBs resulting from replication fork stalling or collapse[45]. HR heavily relies on extensive 5'-3' nucleolytic processing of the DSB ends (referred also as "nucleolytic digestion" or – more often – as "resection"), in order to permit synapsis and invasion of the homologous donor strand of the sister chromatid, prior to DNA synthesis and repair[46].

The initial step of HR is represented by an "end-clipping" event carried out by MRE11 and CtIP, which first form a nick *via* their 3'-5' exonuclease activity, followed by short-range 5'-3' endonucleolytic processing (50-100 bases)[47]. Long-range resection (> 100 bases) is then performed by DNA2 (DNA replication helicase/nuclease 2), EXO1 (exonuclease 1) and CtIP exonucleases in concert with BLM (Bloom syndrome RecQ like helicase) helicase, forming long ssDNA filaments on both DSB ends[48]. The two ssDNA threads are then bound with high affinity and stabilized by RPA (replication protein A). RPA is subsequently

replaced by RAD51 via BRCA2 (breast cancer type 2 susceptibility protein), which forms a nucleofilament adept to homology search and strand invasion[49]. Upon D-loop formation of the 3'-end of the invading strand with the template strand and annealing of the second DSB mediated by RAD52, a double Holliday junction (dHJ) is generated by the filling activity of DNA polymerase. After crossover or non-crossover events mediated by Resolvase A, DNA polymerase and DNA ligase restore the DNA duplex[50].

1.2.2.3 Microhomology-mediated end joining

A third repair pathway that will be mentioned in this monograph is the microhomology-mediated end joining (MMEJ) also called alternative end joining (A-EJ). The molecular mechanism of this pathway remains unclear but its harmful effects on genomic integrity are well recognized. In fact, upon nucleolytic digestion of that exposes regions of microhomology (1-20 bases), DSB ends can be re-ligated with loss of genetic material[51] (Fig. 2). Importantly, MMEJ has the tendency to join DSBs in different chromosomes, thus causing chromosomal translocations[52,53].

1.2.3 The DSB repair pathway choice: to protect or not to protect the ends

Several pieces of evidence led to the concept that NHEJ is the first pathway of choice for prompt repair of most DSBs[46,54-56]. In support of this concept, it was estimated that 80% of IR-induced DSB occurring outside of the S phase are repaired by NHEJ[54]. It is suggested that when NHEJ is not active (in S phase) or fails to repair a DSB, the slower HR repair process takes place (if sister chromatids are available), while the more imprecise MMEJ type of repair is activated only as a

"last resort"[8]. In the extreme case in which the degree of DNA damage goes beyond repair capacity, additional signaling networks induce apoptosis in order to avoid the tumorigenic consequences of genomic instability.

Nonetheless, the estimated residual 20% of DSBs may require faithful repair by HR and, as it will be later discussed, the interplay between the two main repair pathways is tightly regulated by a complex network of factors. In fact, cells developed DDR signaling pathways that are dynamically activated and modulated based on (1) the structure of the DSB breaks[57-59], (2) the phase of the cell cycle[46,60] and (3) the chromatin structure in which the DSB occur[61,62]. These different contexts can simultaneously affect the decision of the DSB pathway choice, which can be revoked at early, mid or late stages of the DDR. This suggests that the engagement of a repair pathway is not consolidated until the ends are ligated[30].

Resection of DSB ends is a pivotal and rigorously regulated step to direct the repair towards NHEJ or HR. In support of this notion, the nucleases involved in DSB end resection (MRE11, EXO1, and DNA2), as well as the end protection factors, are well conserved from yeast to human[63].

The following paragraphs will focus on the most important factors that prevent long-range resection, thus allowing the repair to occur *via* NHEJ. For the purpose of coherence, also the factors promoting resection will be mentioned.

1.2.3.1 The early barrier to DSB resection

In all phases of the cell cycle, two ring-shaped Ku70/Ku80 monomers bind to a DSB a few seconds after the damage is formed[12] (Fig. 1). The Ku complex, besides promoting the loading of early NHEJ factors via the recruitment of DNA-PKcs, makes the DSB ends resistant to the long-range resection nucleases EXO1 and DNA2[64,65]. In G0/G1, this blockage prevents the formation of ssDNA stretches, which would otherwise become, due to the absence of sister chromatids for faithful HR repair, substrates for the aberrant MMEJ repair and potentially lead to

chromosomal translocations[64]. Ku70/80-dependent resection inhibition is mainly occurring in G1. In S/G2, CDKs activate MRE11/CtIP nucleases that, via their early 5'-3' endonuclease and 3'-5' exonuclease activities (as described in 1.2.2.2), displace Ku heterodimers from the ends[64,66]. The protecting role of Ku complex is strongly supported by studies in yeast, but observations in mice indicate that downstream effectors wield more repression on DSB end processing[67,68].

1.2.3.2 The late barriers to DSB resection

A more complex situation, in which the early barrier is bypassed, is the repair of staggered DSBs formed in G1 phase. Ku70/80 has no affinity to such DNA ends and minimal resection is required before NHEJ can take place[42]. Accordingly, MRN, along with CtIP, creates small stretches of ssDNA. Meanwhile, as described in paragraph 1.2.1, ATM mediates the spreading of the DNA damage signal γH2AX through the interaction with the MRN subunit NBS1[20] (Fig. 3A). γH2AX binds to MDC1 (mediator of DNA damage checkpoint 1), which is stabilized by ATM phosphorylation[69,70] and interacts with the NBS1 subunit of MRN, retaining the complex on γH2AX-marked chromatin[71]. Phosphorylated MDC1 promotes the ubiquitin E3 ligase activity of RNF8 (ring finger protein 8), which polyubiquitylates histone 1 on lysine 63 (H1K63ub)[72] (Fig. 3B, step 1). A second ubiquitin ligase, RNF168 (ring finger protein 168), ubiquitylates lysine 15 on H2A histones (H2AK15ub). H2AK15ub epigenetic mark, together with the ubiquitous H4K20me2 mark, recruits another essential NHEJ factor, the p53-binding protein (53BP1)[73] (Fig. 3B, step 2). Thanks to its ubiquitylation-dependent recruitment (UDR) motif and Tudor domain, 53BP1 stably binds to H2AK15ub and H4K20me2 marks, respectively[74,75] (Fig. 3B, step 3).

Experiments in mice showed that 53BP1 has a higher inhibitory effect on resection than Ku70/80[67]. This may be due to the fact that multiple 53BP1 moieties can form a "chromatin barrier" around the damage and not bind to the DSB end

alone, as in the case of Ku70/80. For this reason, NHEJ is often referred to as a 53BP1-dependent pathway[68,73,76-78]. Nonetheless, 53BP1 and its downstream effectors (introduced below) are not NHEJ core components. In fact, the end-protection function of 53BP1 is also important in other cellular contexts: it modulates the extent of resection in S phase[79], protects DNA from degradation in the context of stalled replication forks[80,81] and deprotected telomeres[82,83].

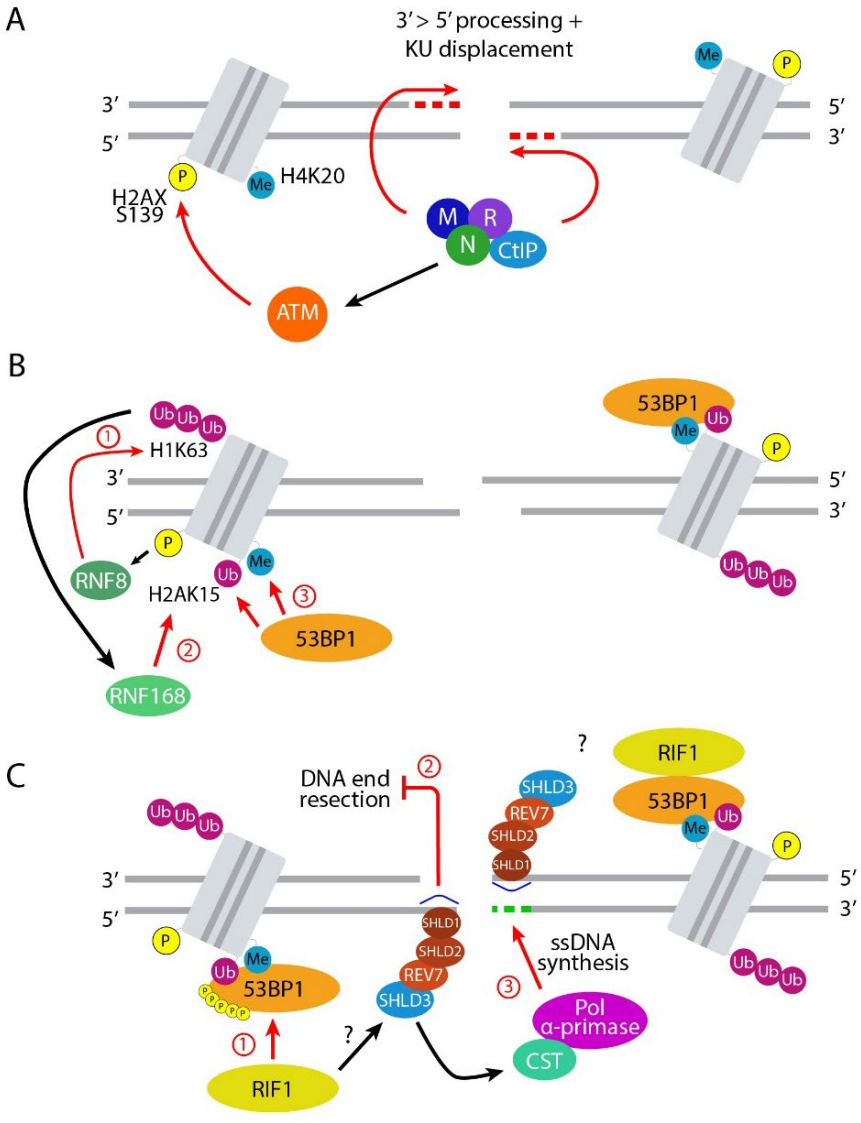

(*Figure 3 continued on page 12*)

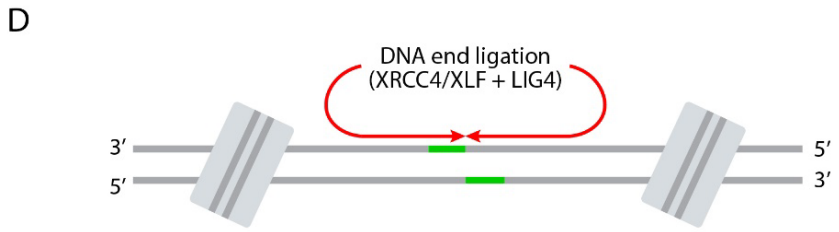

Figure 3: Model of the DSB end protection machinery leading to NHEJ repair in G1. **(A)** After sensing of the DSB, an endonucleolytic cut is introduced by CtIP together with MRN and extended towards the 5' end of the DSB *via* the 3'-5' exonucleolytic activity of MRE11. The nucleolytic activities expose short tracts of ssDNA. Simultaneously, NSB recruits ATM, which in turn phosphorylates Ser139 of the H2AX nucleosomes surrounding the DSB. **(B)** MDC1 (not shown) along with γH2AX promotes the polyubiquitylation of K1K63 by RNF8, which in turn recruits RNF168. RNF168 creates the H2AK15ub mark that together with the constitutive H4K20me2 mark allows the interaction of 53BP1 with the chromatin. **(C)** Phosphorylation of 53BP1 N-terminus by ATM is required for the recruitment of RIF1 and PTIP (not shown). RIF1 is required for the recruitment of the Shieldin complex, composed of REV7 and SHLD1-3. The complex is suggested to prevent extensive resection by DNA2/BLM and EXO1. In turn, the complex recruits CST and Pol α-primase, which creates blunt ends. **(D)** The blunt DSB can be then repaired by NHEJ, through LIG4 activity supported by XRCC4/XLF. Red and green dashed lines indicate DNA resection and synthesis activities, respectively. The steps indicated in the text are labeled in red and accompanied by red arrows.

As the response to DSB formation proceeds, ATM phosphorylates the N-terminus of 53BP1 on 28 specific SQ/TQ phosphorylation sites. These phosphorylation events are essential for the recruitment and stable interaction of 53BP1 with the downstream factors (PAX transcription activation domain interacting protein (PTIP)[84] and Rap1-interacting factor 1 (RIF1)[68,85-88] (Fig. 3C, step 1). The two proteins act independently to inhibit resection and their association with DSBs depends on the phosphorylation of specific SQ/TQ sites[89]. Accordingly, the mutation of the eight most N-terminal sites abrogated PTIP recruitment and enhanced RIF1 recruitment[90]. Conversely, in a 53BP1 mutant in which seven different SQ/TQ sites downstream of those required for PTIP activity were mutated to alanine, the association of 53BP1 with RIF1 was abolished while the one with PTIP was augmented[89]. Data from a recent study support a model in which 53BP1, by interacting with RIF1 and PTIP, antagonizes HR at the level of

RAD51-mediate recombination and at the level of long-range resection, respectively[90].

RIF1 is required for the recruitment of additional downstream factors of the 53BP1-dependent pathway, namely REV7 (also termed MAD2L2, mitotic arrest deficient 2 like 2)[91,92], C20orf196, FAM35A, CTC-534A2.2[93-97]. The latter three proteins, for simplification named SHLD1, SHLD2, and SHLD3, respectively, were discovered after REV7, whose direct interaction with RIF1 remained unconfirmed[91]. SHLD1/2/3 appear to form a stable complex with REV7, even in the absence of DNA damage[98]. Loss of the so-called "Shieldin complex" (REV7-SHLD1/2/3) was shown to affect many functions dependent on DSB end protection, such as resistance to ionizing radiation, etoposide (a topoisomerase II inhibitor that prevents re-ligation of DNA strands) and bleomycin (a radiomimetic drug that causes DNA damage by free radicals formation) treatments[78,93-97]. These data confirm the requirement of the 53BP1-RIF1-Shieldin axis to prevent the nucleolytic degradation of DSB ends (Fig. 3C, step 2).

Of note, the studies that dissected the function of each Shieldin component were in agreement with a potential biochemical property of SHLD2. The predicted C-terminal domain of SHLD2 was in fact predicted to be similar to that of RPA1 (subunit of the RPA complex), which confers ssDNA-binding ability[78,93,96,97]. This suggests that Shieldin competes with RPA for the binding to ssDNA generated by the short-range 3'-5' exonuclease activity of MRE11, thus preventing further long-range resection mediated by EXO1 and DNA2 and HR repair[99]. Eventually, this roadblock would then promote the conversion of resected DSB ends into appropriate NHEJ substrates. In agreement with this model, Mirman et al. demonstrated that DSB end protection machinery recruits and interacts with the CST complex (CTC1, STN1, TEN1) which, together with its partner polymerase α-primase (Pol α-primase), fills-in the DNA initially resected by MRE11-CtIP and further prevents its extensive processing by EXO1 and DNA2[100] (Fig. 3C, step 3). In summary, the barrier to resection established by the 53BP1-RIF1-Shieldin axis

allows DSBs to be protected but also remodeled in order to be repaired by NHEJ *via* XRCC4/XLF and LIG4 activities (Fig. 3D). Nonetheless, the link between resection inhibition functions of 53BP1 and RIF1 and the apparent ssDNA-binding function of the Shieldin complex remains puzzling and partly unexplained, especially at the interface between RIF1 and Shieldin complex[99].

1.2.3.3 The importance of PTMs in the DSB repair pathway choice

As anticipated in paragraph 1.2.3.2, different factors regulate the role of DDR proteins at DSBs by modulating their binding to chromatin. Phosphorylation of 53BP1 by ATM kinase is an example of PTM affecting the function of DDR proteins. The DSB repair pathway choice is also controlled by different chromatin writers and erasers creating or disrupting specific epigenetic marks.

For instance, positive regulation of 53BP1 residency at sites of damage strongly depends on the ubiquitylation of histone H2A by RNF168 (ring finger protein 168)[72,74,101]. The levels of the H4K20me2 mark are reduced during S phase, repressing 53BP1 interaction with chromatin[102]. Additionally, the H4K20me2-53BP1 interaction can be repressed by the simultaneous activity of L3MBTL1 (lethal(3)malignant brain tumor-like protein 1) and JMJD2 (lysine-specific demethylase 4A), which mask and demethylate the H4K20 histone mark, respectively[101,103]. 53BP1 binding to chromatin can also be hampered by the antagonistic binding of TIRR (Tudor-interacting repair regulator protein) to its Tudor domain[104-106].

Acetylation is another post-translational modification that modulates 53BP1 activity at DSBs. In fact, the acetyltransferase TIP60 (histone acetyltransferase KAT5) acetylates lysine 16 on histone H4, thus interfering with 53BP1 binding to the chromatin[107,108]. A recent report showed that yeast ortholog of Rif1 is acetylated on its N-terminus by Pfa4 (a palmitoyl acetyltransferase of the DHHC

family)[109]. This modification was shown to promote Rif1 recruitment to DSB and its anti-resection function in the context of NHEJ repair.

The mutual antagonism between 53BP1 and BRCA1 (breast cancer type 1 susceptibility protein) is another key regulatory step in the DSB repair pathway choice, which further contributes to the dynamic nature of this process. In fact, in response to DNA damage ATM can also phosphorylate and activate BRCA1[110], whose role in promoting HR is well described[85]. BRCA1 promotes the ubiquitylation of the C-terminal lysines of H2A histones *via* its interaction with BARD1 (BRCA1-associated RING domain protein 1) E3 ubiquitin ligase[111,112]. BRCA1-BARD1 activity was shown to stimulate the accumulation and activity of SMARCAD1 (SWI/SNF-related matrix-associated actin-dependent regulator of chromatin subfamily A containing DEAD/H box 1) chromatin remodeler, which mobilizes 53BP1 from the damage site and restores resection[113]. It is postulated that, when HR is required, different chromatin remodelers create an environment that is more favorable to BRCA1 rather than to 53BP1 binding, thus inhibiting the formation of the end-protection machinery and promoting long-range resection. Once RIF1 is recruited to DSBs by 53BP1, BRCA1 can as well antagonize (partly or completely) its anti-resection function by two different mechanisms. In one mechanism, CDK2 (active in S phase) phosphorylates UHRF1 (ubiquitin like with PHD and ring finger domains 1), which is then recruited to the DSB by BRCA1. UHRF1, in turn, ubiquitylates RIF1, causing its displacement from chromatin[114]. A second report described BRCA1-mediated dephosphorylation of 53BP1 N-terminus by PP4C (Serine/threonine-protein phosphatase 4 catalytic subunit), which also induces RIF1 release from chromatin[115,116]. Finally, RIF1 is outcompeted by SCAI (suppressor of cancer cell invasion) in the binding with 53BP1 during S-phase, promoting BRCA1 accumulation[117].

The complex cellular response to DSBs summarized herein, is composed of dynamic and reversible processes. Due to the considerable amount of endogenous damage a cell encounters each day (see 1.1), the fine coordination between

different repair pathways, the ongoing nuclear processes as well as the control of cell cycle is essential for cell survival. As described in the previous paragraphs, the modification of both histone proteins and repair factors plays an important role in the restoration of genomic stability. In this dissertation, only some of the PTMs involved in the DSB repair pathway choice have been mentioned (Table 1).

Effector	Target	Function
Acetylation		
TIP60	Histone H4 (K16)	Negative regulation of 53BP1 binding to chromatin
Pfa4 (yeast ortholog)	Rif1 (yeast ortholog)	Promoting Rif1 recruitment to DSB and its function in NHEJ
PARylation		
PARP1	PARP1 (autoPARylation)	Amplification of the DDR signal
Phosphorylation		
ATM	ATM (autophosphorylation)	Amplification of the DDR signal
ATM	Histone H2AX (S139)	Mark of the DSB site, extension of the DSB repair signal, recruitment of downstream DDR proteins
ATM	MDC1	Recruitment of RNF8
ATM	53BP1	Recruitment of RIF1 and PTIP
CDK1/CDK2	CtIP, EXO1	Cell-cycle-dependent activation of CtIP and EXO1 (promoting HR)
CDK2	UHRF1	Displacement of RIF1 from chromatin
Ubiquitylation		
RNF8	Histone 1 (K63)	Recruitment of RNF168
RNF168	Histone H2AX (K15)	Recruitment of 53BP1
BRCA1/BARD 1	Histone H2A (K125, K127, K129)	Negative regulation of 53BP1 binding to chromatin

Table 1: List of the post-translational modifications of DDR factors and histone variants mentioned in this dissertation.

Nonetheless, the landscape of protein and chromatin modifications of the DDR signaling as well as those involved in the interface between DSB end resection/protection is much broader[118-120]. Importantly, a precise and controlled response is also required upon formation of programmed DSBs, as in the case of meiosis and immunoglobulin loci rearrangement. The specific process of immunoglobulin class switch recombination (CSR) was exploited in this study and is described in paragraph 1.3.2.

1.3 The adaptive immune response

Antibody production is an important step of the immune response to a wide variety of pathogens and foreign molecules (such as toxins and allergens)[121]. Through the essential role of other immune cells that are assigned to patrolling the body, identifying threats and executing the primary immune response (defined as innate immune response), B lymphocytes (also called "B cells") take advantage of specific peptides present on the foreign entities (called antigens) to execute, in coordination with T lymphocytes, the adaptive immune response[121]. B cells and T cells have antigen-specific receptors on their surfaces that allow them to bind to foreign threats with high affinity and specificity. This is achieved through a specific recombination process acting on the antigen receptor genes, called V(D)J recombination[122]. Antigen receptors are basically antibodies that have not been secreted. One of the main differences between T and B cells is that only the latter owns the ability to secrete antibodies. In this dissertation, importance is given to a second recombination process that allows to produce different types of secreted antibodies; for this reason, B lymphocytes will come into focus.

1.3.1 Antibody structure and isotype switching

Antibodies, also called immunoglobulins (Igs), are composed of two heavy (IgH) and light (IgL) chains encoded by genes on two different loci, *IgH* and *IgL*,

respectively. Both IgHs and IgLs are characterized by a variable region, which is the antibody portion that specifically recognizes and binds an antigen (Fig. 4).

The high affinity of the variable region for an antigen is initially achieved, during B cell maturation, *via* the V(D)J recombination. In this process, the variable (*V*), diversity (*D*) and joining (*J*) genes are rearranged through the activity of recombination activating genes 1 and 2 (RAG1 and RAG2)[123]. Higher affinity is then obtained through somatic hypermutation (SHM), in which point mutations are introduced in the *V(D)J* genes. SHM occurs when B cells reach specific structures in the secondary lymphoid organs called germinal centers (GCs). Here, SHM and other maturation processes are induced by cytokine-based stimuli released by T cells[122]. Additionally, in these compartments antigens are presented to B cells, which in turn are selected for their antigen-binding ability[122,124]. Selected B lymphocytes are then released in the bloodstream, where they secrete antibodies in order to bind and inactivate foreign substances (like viruses and toxins) or defeat bacteria via complement activation or phagocytosis[123].

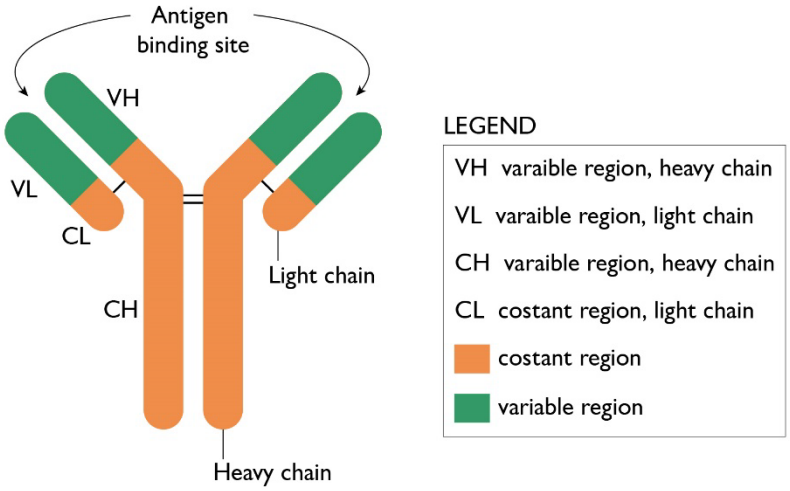

Figure 4: Representative scheme of an antibody monomer.

The effective B cell response does not only depend on the affinity of their antibodies for specific foreign antigens[124]. In fact, specific antigen-defined antibodies can have distinct effector functions and are defined as antibody

isotypes: IgMs, IgDs, IgGs, IgAs, and IgEs. In mice, IgGs are divided into four subclasses (IgG1, IgG2a, IgG2b, IgG3). The isotype of an immunoglobulin (its effector function) is defined by the constant region (C_H) of its heavy chains (Fig. 4). The C_H can be encoded by one of the eight different constant (C_H) genes present downstream of the *V(D)J* genes in the *IgH* locus (Fig. 5). Of note, an enhancer region (*Eμ*) is present between the variable and the constant region genes and is essential for *IgH* expression. Each C_H gene is preceded by an independent inducible promoter, an intervening exon (I-exon) and a 1-10 kb long, repetitive intronic sequence (termed "switch" region), with the exception of the *Cμ* and *Cδ* genes that are co-transcribed (*Cδ* is expressed only as a result of alternative splicing)[125,126] (Fig. 5).

Before receiving cytokine stimulation by T cells in GCs, B cells express mainly IgMs (or IgDs), whose gene is directly downstream the *V(D)J* genes. In order to express different immunoglobulin isotypes, the *Cμ/Cδ* genes must be exchanged with a different C_H gene (*Cγ, Cε* or *Cα*). This is achieved by class switch recombination (CSR): a deletional-recombination reaction occurring between the donor switch region upstream the *Cμ* gene (S*μ*) and the acceptor switch region upstream another C_H gene [126].

1.3.2 CSR: an example of programmed DSB induction

The T cell cytokine stimulus induces two main CSR events: germline transcription (GLT) and the mutagenic activity of activation induced deaminase (AID) (Fig. 5). GLT, initiating at each inducible promoter, does not produce coding transcripts but is essential for CSR[127,128]. In fact, the temporary exposure of ssDNA filaments during transcription allows AID to exert its enzymatic activity, by which it deaminates cytidines to uracils, generating dU:dG mismatches. These mismatches activate the base excision repair (BER) pathway, in which Uracil-DNA glycosylase (UNG) removes dU bases, creating apurinic sites that are then converted into

ssDNA nicks. As a consequence of the fact that AID can induce several mutations in each S-region, ssDNA nicks created simultaneously and in close proximity to each other can be converted into 5' overhang DSBs. Blunt DSBs are then obtained by the filling activity of DNA polymerase[126].

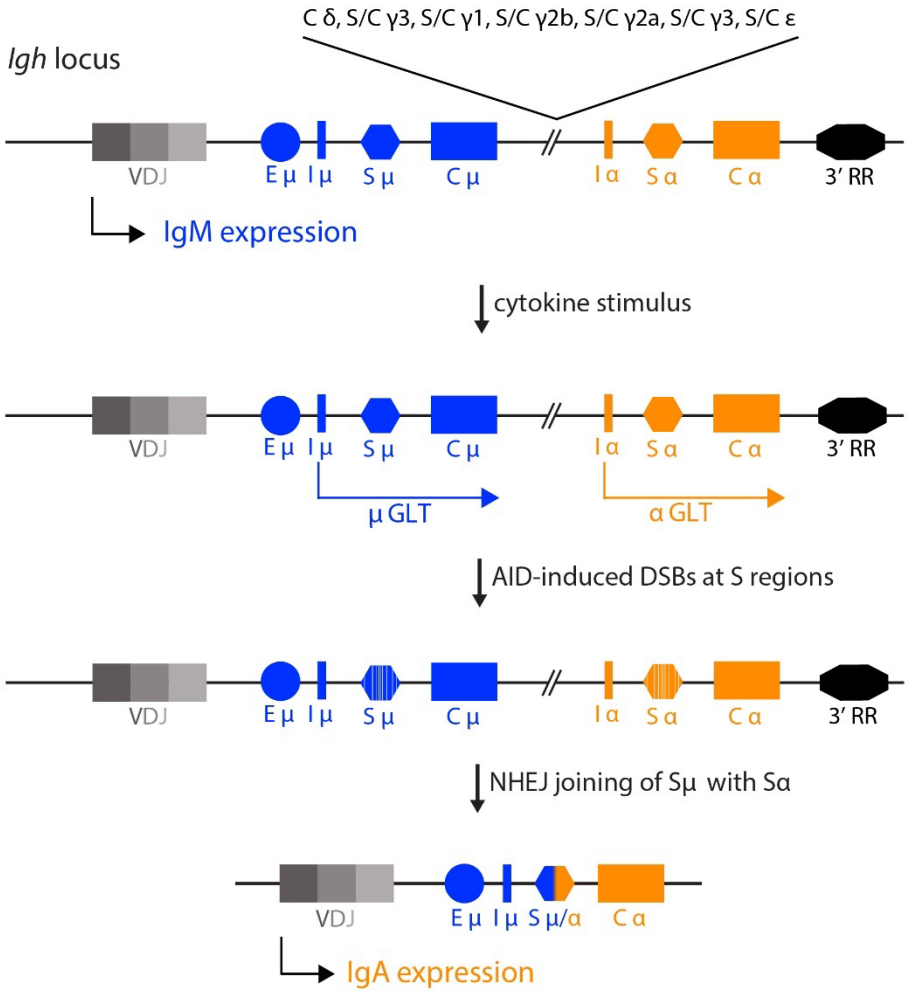

Figure 5: Steps of class switch recombination leading to expression of IgA antibody isotypes.

Importantly, AID-targeted sequences are more concentrated in the central portion (core) of switch regions. For this reason, to increase the chances that a DSBs are also formed away from the S-regions cores, AID-induced mismatches can also activate the mismatch repair (MMR) pathway. In this case, nicks are generated directly at the DNA 5' of the mismatch by endonucleolytic cleavage, followed by 5'-3' endonucleolytic processing. As a consequence, strands processed in the

vicinity of a nick on the opposite strand can create a 5' overhang DSB, which are usually not further processed[126].

The deletional-recombination reaction is then completed by ligation of one DSB end formed in Sμ with a DSB end on the S-region of a specific downstream C gene (as dictated by the cytokine-induced GLT allowing AID-mediated DSBs).

1.3.3 NHEJ is the pathway of choice for the repair of CSR breaks

The induction of DSBs at the S-regions of C_H genes is regulated by the cell cycle and occurs in G1. In support of this notion, different studies showed that the stability and activity of both AID and UNG are higher in G1 than in S/G2[129,130]. These observations are in agreement with the detection of DNA damage at the *IgH* locus in G1 phase[131].

Similar to unprogrammed DSBs, S-region DSBs resulting from AID activity are recognized by Ku70/80 and MRN, which initiate the DDR signaling cascade involving ATM-mediated phosphorylation of H2AX and other downstream factors (see 1.2.1 and 1.2.3.1)[132]. Eventually, the NHEJ pathway (and to a lesser extent, MMEJ) ligates the S-region DSBs. Hence, productive antibody isotype switching is dependent on the NHEJ repair factors, as shown by the moderate defects in antibody isotype switch in Ku70/80, LIG4 and XRCC4 knock-outs (up to 50% reduction)[33,34,133-135]. The residual switching of NHEJ-deficient cells led to the hypothesis that the other repair pathway active in G1, MMEJ, may be involved in the repair of AID-induced breaks[133,135]. This hypothesis is supported by the evidence that staggered DSBs generated by the MMR pathway, which exposes short regions of microhomology (1-20 nt), are favorably repaired by MMEJ[136].

In the context of AID-induced DSBs, the DNA end-protection function of 53BP1, RIF1, and the other downstream NHEJ-promoting factors (see 1.2.3.2) is required for productive CSR as well as for the stability of the I*gH* locus and cell survival[88,91,93,94,97,98,137-139]. Specifically, but not uniquely, protection of the DNA

ends from resection is a major requirement[124]. As a matter of the fact, deficiency in the 53BP1-dependent pathway causes uncontrolled resection of S-region DSBs, which promotes MMEJ over NHEJ repair and the ensuing unproductive internal switch deletions (ISDs)[137-141]. MMEJ can also mediate the formation of oncogenic translocations upon joining of homologous sequences in the S-regions with those present in other chromosomes[135,140,142].

In summary, the deletional-recombination of the *IgH* constant genes occurring in mature B cells strictly requires protection of AID-induced DSB ends by NHEJ-promoting factors. Nonetheless, chances that unproductive ISDs or aberrant recombination between *IgH* and non-*IgH* genes occur are high, considering the large amount of DSBs occurring at each S-region[124].

1.3.4 The roles of the 53BP1-dependent pathway in CSR

As anticipated, the requirement of 53BP1-RIF1 downstream effector REV7 and the recently discovered Shieldin complex (described in 1.2.3.2) for productive CSR has been demonstrated in many studies[68,78,85,88,89,91-94,98,137,143]. Some of the authors proposed Shieldin to be the ultimate DSB end protection factor, involved in the NHEJ-dependent processes supported by 53BP1 and RIF1. This was proved by the reduction of deprotected telomeres fusion[92-94], the rescue of HR in *Brca1*-null cells[78,93] and the increased sensitivity to different genotoxic drugs[97] upon depletion of the complex. Nonetheless, the epistasis of Shieldin components is not consistent and their specific role in these different contexts remains unclear[99].

The requirement of additional functions, besides DSB end-protection, for productive CSR has been often considered, especially in studies related to 53BP1 and RIF1. In fact, the comparably profound CSR deficiency of 53BP1-deficient lymphocytes (over 95% reduction) is suggested to be due to additional events upstream the ligation S-region DSBs. In fact, 53BP1 was shown to be involved in the synapsis of distant S-regions, the removal of the intervening region as well as

the preservation of C_H genes directionality, all necessary conditions for effective isotype switching[144-146].

According to RIF1 requirement for protection of DSB ends from resection (see 1.2.3.2), *Rif1*-deficient lymphocytes are characterized by up to 85% reduction in CSR efficiency, as well as accumulation of genomic instability in the form of *IgH* chromosomal breaks and translocations[68,85,86,88]. Recent work from our lab suggested that RIF1, similarly to 53BP1, has additional roles in CSR. In fact, a novel RIF1 interactor, the chromatin reader ZMYND8 (Zinc Finger MYND-Type Containing 8), was identified as a CSR-promoting factor *via* a functional screen. The data indicated that ZMYND8, but not RIF1, regulates the transcription and the activity of the 3' *IgH* enhancer. Experimental evidence led to the conclusion that the RIF1-ZMYND8 interaction is not required for the repair of AID-associated breaks in B lymphocytes, but may be required for other CSR-promoting processes yet to be elucidated[147]. In the same study, several transcriptional regulators were identified, hinting at the involvement of RIF1 in transcriptional processes required for CSR. Additionally, Sundaravinayagam et al. raised the interesting possibility that the 53BP1-RIF1-dependent DSB end protection function might not be essential, but only partly required for productive CSR. This idea was supported by data indicating that 53BP1-dependent recruitment of RIF1 to DSBs is necessary for resection inhibition, but not for the generation of newly switched antibody heavy chains[148].

These and other studies underline the requirement to further investigate RIF1 function in CSR and, more generally, in DSB end protection.

1.4 RIF1

RIF1 is a conserved protein present from yeast to mammals. It was initially discovered in yeast as a Rap1-associated protein involved in the negative regulation of telomere length[149]. Years later, the mouse ortholog was identified[150]. In contrast to the yeast ortholog, mammalian RIF1 had no role in telomere maintenance but was reported to be recruited at DSBs[151] and at stalled replication forks[152]. Structural comparison between yeast and mammalian orthologs highlights divergence at the primary structure levels[85,152-155]. Nonetheless, high eukaryotes orthologs share key features with yeast Rif1, which will be discussed in the following paragraph (1.4.1). Mammalian RIF1 has evolved numerous functions involved in the maintenance of genomic stability. In fact, the protein is involved in the regulation of intra-S-phase checkpoint[151], resolution of anaphase ultrafine bridges (UFBs), control of abscission timing[156,157], HR-mediated repair of stalled replication forks[153,154], and replication origin firing[158-162].

The ability of RIF1 to regulate the timing of replication in different chromatin contexts is explained by its interaction with protein phosphatase 1 (PP1). PP1 once docked on chromatin-bound RIF1, dephosphorylates the helicases activated by DDK (DBF4-dependent kinase), thus preventing the firing of replication origins[160-162]. An additional, non-exclusive, explanation of this mechanism relies on RIF1 ability to relocate late-replicating regions of the genome to the nuclear periphery[163]. The RIF1/PP1 interaction was recently shown to be inhibited by CDK1-mediated phosphorylation of RIF1 and promoted by ATR/CHK1 (checkpoint kinase 1) kinase signaling[164]. RIF1 role in replication origin firing has also been well described in studies in yeast and fruit fly[165-168]. Interestingly, the interplay between RIF1 and PP1 is also required for the resolution of UFBs both in fission yeast[169] and in human cells[157].

Along with the different roles mentioned above, RIF1 maintains the stability of the genome by preventing extensive resection of DSB ends and promoting prompt repair by NHEJ[85-87] (see 1.2.3.2). As a consequence of this activity, RIF1 is also required for mature B lymphocytes to produce different sets of immunoglobulins and contribute to the response to pathogens[68,88] (as mentioned in 1.3.4).

At the beginning of this study, the molecular mechanism of DSB end protection by RIF1 was unknown. To date, in spite of the studies that led to the recent discoveries of the Shieldin complex and other factors regulating DNA resection and CSR[99], the explanation of how RIF1 exerts its function is still missing. Furthermore, the presence of a yet-to-be-defined accessory factor(s) that further support the 53BP1-RIF1 and RIF1-Shieldin interactions cannot be excluded [73,91,98] (see 1.2.3.2). Finding novel proteins acting at the 53BP1-RIF1 and RIF1-REV7 interfaces, as well as unveiling the mechanism of action of RIF1 at DSB sites, may offer the missing links in the understanding of the 53BP1-dependent pathway.

1.4.1 RIF1 structure

Murine RIF1 has been identified 15 years ago as a large protein characterized by 2426 amino acid residues and a molecular weight of around 270 kDa[150]. Previous bioinformatic analyses identified two main key structural features that are conserved from yeast to mammals: at the N-terminus, the HEAT (Huntingtin, Elongation factor 3, protein phosphatase 2A, Tor1)-like repeats domain[151], and at the C-terminus the RVxF-SILK motifs[155]. An additional feature, which has a strong similarity to the C-terminal domain of the bacterial RNA polymerase α subunit (CTD), is called CTD domain[154] (Fig. 6). The CTD domain is only present in vertebrates (and partially conserved in fruit fly and yeast).

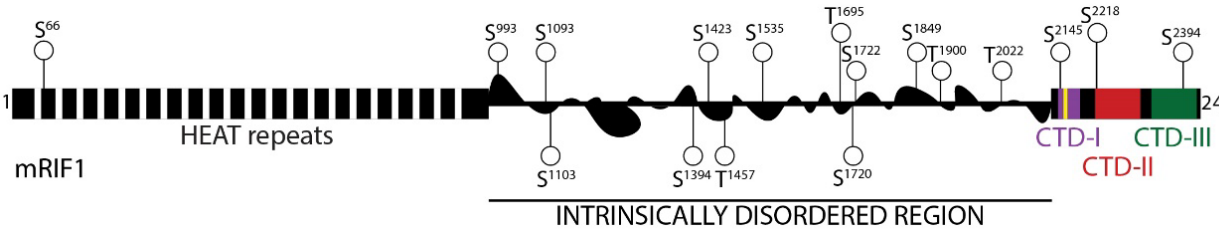

Figure 6: Structure of murine RIF1. Schematic representation of RIF1 protein (NP_780447.4). Predicted domains are indicated with boxes: 21 N-terminal HEAT repeats domain (dashed black); C-terminal CTD-I (RVxF/SILK motif, purple), CTD-II (DNA binding domain, red) and CTD-III (BLM interaction domain, green). Balloons indicate serine (S) and threonine (T) residues within putative ATM/ATR phosphorylation sites (SQ/TQ).

The N-terminal HEAT-repeat domain was the first one to be identified in murine RIF1 and it shares the highest sequence similarity to the yeast ortholog[151]. Generally, HEAT-repeats mediate protein-protein interactions in different contexts[170], including the DNA damage response[171]. The domain, composed of 21 HEAT-repeats, is indispensable for the accumulation of murine RIF1 at DSBs and, in the context of DSB end protection, is also required for inhibition BRCA1 accumulation at DSB site in G1[85]. In two recent studies, researchers managed to purify full-length murine RIF1 and several deletion variants, demonstrating that the HEAT-repeats domain, together with the C-terminal portion, is required for RIF1 binding to G-quadruplex secondary DNA structures (G4) and for oligomer formation[172]. The RVxF-SILK motifs are required for the interaction of RIF1 with PP1[162,173], and this interaction is important for RIF1-mediated regulation of replication timing[160].

The CTD domain was first characterized almost a decade ago[154]. In vertebrates, it is divided into three portions: CTD-I, CTD-II, CTD-III. CTD-I contains the mammalian RVxF-SILK motif and is predicted to be unfolded[174]. CTD-II was shown to have DNA-binding properties *in vitro*[154]. CTD-III is the minimum structural requirement for the interaction between RIF1 and BLM helicase[154] and, with the contribution of CTD-II, it promotes RIF1-mediated resistance to replication stress[153,154]. RIF1-BLM interaction is essential for stalled replication

forks restart [153,154] and resolution of anaphase ultrafine bridges[156], two roles of RIF1 that are independent of its interaction with 53BP1.

Technical challenges hamper the study of RIF1 structural requirements for its numerous functions. For instance, the fact that mammalian RIF1 is bound to the insoluble nuclear matrix complicates the study of RIF1 binding to DNA *in vivo*, as well as the purification of sufficient quantities of endogenous protein[158,159]. The necessary *in vitro* studies have also been limited because of the difficulties in producing recombinant material[174].

Nonetheless, recent crystal structure analyses contributed to further dissect RIF1 C-terminus and eventually outline overlapping functions between yeast and mammal orthologs[172,174-176]. The first ortholog to be crystalized was yeast Rif1, whose CTD domain seemed to function as a tetramerization module[176] and was later shown to mediate the binding to G4 structures[175]. Conversely, the successful generation of soluble murine RIF1 fragments indicated that the C-terminal CTD domain enables RIF1 binding to different structures: DNA cruciforms[174]. Nonetheless, a later study in which murine full-length RIF1, as well as deletion mutants, were successfully purified, confirmed the ability of both N-terminal and C-terminal RIF1 segments to interact with DNA G4-quadruplexes and the binding was enhanced by their oligomerization[172]. The biological significance of these observations remains unclear, but the interaction between RIF1 and specific DNA structures may indicate that RIF1 functions in structure-specific contexts.

Apart from the HEAT-repeats domain, the connection between the other RIF1 conserved domains and its function at DSBs is still missing, especially in the context of CSR. Shedding light on these aspects of such large, multifunctional protein may help understanding its essential role in the protection of DSB ends generated upon spontaneous or AID-induced damage, as well as eventually unveiling its as-yet-unknown additional functions.

1.4.2 RIF1 disorder and phosphorylation

As anticipated, the importance of phosphorylation during the DDR signaling as well for the control of the cell cycle is well described[19]. Specifically, ATM phosphorylates a range of proteins involved in both processing and protection of DSB ends[70,110,177-179]. Modification of specific SQ/TQ motifs in 53BP1 N-terminus by ATM kinase is a strict requirement for its DSB end protection function and therefore ATM inhibition impacts CSR in primary B cells. Accordingly, it was also shown that mutation of specific 53BP1 N-terminal SQ/TQ sites affected different molecular events, such as recruitment of RIF1 and PTIP to DSBs[73]. Of note, 53BP1 N-terminus represents an intrinsically disordered region (IDR).

IDRs are portions of protein sequences that do not adopt any stable and defined secondary or tertiary structure. Fully or partially disordered proteins can switch between different conformational states, which can ultimately affect their functions and interactions with other proteins or with chromatin[180-183]. Intriguingly, phosphorylation of residues within IDRs is known to affect both protein folding and function in a variety of biological contexts[184,185].

RIF1 also presents a large IDR, accounting for more than half of its length (Fig. 6). Interestingly, three clusters of SQ/TQ sites are present in the unstructured region and the serine residue of one of these sites (S^{1525}) was found to be phosphorylated upon IR-induced DNA damage in a large-scale phosphoproteomic study[186]. For many years, the phosphorylation of RIF1 ATM/ATR consensus sites, as well as its IDR, have been disregarded. Only two recent studies in yeast Rif1 showed that a single SQ site, present in a 100 aa-long SQ/TQ cluster, was phosphorylated by ATM and that this phosphorylation was increased upon telomere damage[187,188]. Additionally, mimicking the phosphorylation of all sites of this cluster appeared to increase telomere length, in accordance with the reported function of yeast Rif1 in telomere length regulation[188]. Despite this evidence, no information regarding the structural and functional consequences of mammalian RIF1 phosphoregulation by

ATM is available. We hypothesized that the phosphorylation of specific serines of the SQ/TQ clusters governs the conformational changes of RIF1 IDR, which in turn modulate RIF1 functions and interactions with other proteins in the context of DSB end protection. To test this, I studied the DNA damage-induced phosphorylation of conserved SQ/TQ sites and their involvement in the protection of AID-induced DSB ends in B lymphocytes.

1.5 The aberrant NHEJ repair in *Brca1*-deficient cells

BRCA1 was identified as a common breast and ovarian cancer gene[189]. The aberrant NHEJ repair of DNA replication-associated DSBs resulting from BRCA1 loss drives the accumulation of cancerogenic mutations and genomic aberrations typical of these tumors[190]. Inhibitors of PARP1 (PARPi), the essential protein involved in DSB sensing (see 1.2.1) and SSB repair[191], showed high efficacy in early trials[192]. Several PARPi treatments are FDA-/EMA-approved monotherapies or combination therapies for *BRCA*-mutated tumors[193].

The ability of PARPi to preferentially kill *BRCA*-deficient cells relies on the so-called concept of "synthetic lethality". Generally, this concept represents a situation in which depletion of either protein "A" or protein "B" is not lethal to cells, but the simultaneous loss of both protein "A" and protein "B" leads to cell death. In this case, we talk about the abrogation of the physiological function of PARP1 by PARPi treatment, in an HR-deficient setting caused by BRCA1 loss. In fact, the mechanism of action of PARPi relies on the "trapping" of PARP1 molecules bound to DNA *via* zinc finger domains[193]. One of the most supported models of synthetic lethality implies that PARP1 moieties trapped at SSBs during S phase cause replication blockages and formation of single-ended DSBs upon replication fork collapse. The lack of functional BRCA1 prevents the faithful HR

repair of replication-associated DSBs, leading to aberrant repair, accumulation of genomic instability and finally cell death[194].

Unfortunately, tumors often develop resistance to PARPi treatments. Short progression-free survival (PFS) and overall survival (OS) of some triple-negative breast cancers patients were reported to correlate with low BRCA1 and 53BP1 protein levels[195]. This and other observations unraveled a resistance mechanism named "HR rewiring": in the absence of functional BRCA1 protein, HR activity was restored by 53BP1 depletion[195-197]. Further reports confirmed that also loss of other NHEJ-promoting factors, such as RIF1[68,85-88], REV7[91,92], and the other Shieldin components[78,93,94,98], causes the reestablishment of HR, hence a drastic reduction of genomic instability and consequent cancer cell survival.

Depletion of 53BP1 in *Brca1*-deficient cells leads to higher rescue of HR levels as compared to its downstream effectors. This was initially explained by the separation of function of 53BP1, in which the independent phospho-interaction with RIF1 or PTIP mediates a productive or aberrant NHEJ repair, respectively[89]. The duality of 53BP1 pro-NHEJ activity has been further dissected in a recent report, in which PTIP and RIF1 seemed to efficiently deregulate HR at two different steps: nucleolytic processing and RAD1-mediated recombination, respectively[90].

Collectively, a better understating of the mechanism of action of RIF1 may contribute to consolidating a model in which this multifunctional protein favors, in a 53BP1-dependent manner, NHEJ by inhibiting HR at specific steps.

2. Aims of the study

Protection and nucleolytic processing of DSB ends are two counterposed processes during DSB repair that promote NHEJ and HR, respectively. RIF1 and BRCA1 contribute to the balance between these DSB repair pathways, which is required for the maintenance of genome stability and for the physiological outcome of specific nuclear processes.

RIF1 is an important pro-NHEJ factor, whose involvement in different molecular processes may underlie complex mechanisms of action as well as specific regulatory events. With regards to the role of RIF1 in the repair of both spontaneous and programmed DSBs, these aspects remain unclear. The identification of yet-to-be-defined RIF1 interactors, as well as the structural features and PTMs required for RIF1 contribution to DSB end protection, could potentially help to elucidate how RIF1 function during DSB repair is regulated.

In the first part of this dissertation, I describe how I investigated RIF1 interactome by the use of a CSR loss-of-function screen, exploiting a list of potential RIF1 interactor candidates generated in the lab at the beginning of this project.

In the second part, I present the achievements, discoveries, and challenges derived from my efforts to understand the structural requirements for RIF1 function in DSB end protection as well as its ATM-dependent regulation.

3. Material and Methods

3.1 Material

Oligonucleotides, PCR programs and gRNAs

gRNA	Protospacer sequence	Application
g*Rif1*-3	**AAGTCTCCAGAAGCGGCTCC (-)**	Generation of *Rif1*$^{-/-}$-1 CH12 clones
g*Rif1*-4	**GAAGACCCCTCGGTGCCTCC (+)**	
g*Rif1*-5	**ACTCTTAATGATACCATTCA (-)**	Generation of *Rif1*$^{-/-}$-2 CH12 clones
g*Rif1*-6	**TGTGTGTACCAGGGCACTGT (+)**	
gRNA_3xHAKI#1	**GCGACCTGGGGCCGTCATGT (-)**	Generation of *NLS-3xHA-Rif1* / *3xHA-Rif1* CH12 clones
PhoMut_gRNA#1	**AAACACTCCGACGGTCTTCG (+)**	Generation of *Rif1*$^{S>A}$/ *Rif1*$^{S>D}$ CH12 clones
PhoMut_gRNA#2	**CGACTTGTCTAGATTGTCCA (-)**	

Table M1: List of gRNAs used for the indicated CRISPR/Cas9 applications.

Primer	Sequence	Application
MDV_p130	**TGGATTGGCTCGAGCCTCTC**	gDNA analysis *Rif1*$^{-/-}$ clone 1
MDV_p131	**AACCCACTAACTCCGGATCG**	
MDV_p126	**TTCCTTCCCTCAGTAGAGTTG**	gDNA analysis *Rif1*$^{-/-}$ clone 2
MDV_p129	**AAATGCCAGCCCTGTTGC**	
MDV_p232	**GGCCGTGCTGCCTGGGAAGCG**	Screen / gDNA analysis *NLS-3xHA-Rif1* clones
MDV_p233	**GGCCCGCCTCACCTGGTCAGAGT**	
MDV_p282	**GCGGTGCTTGAACTTCAGGG**	Screen / gDNA analysis *Rif1*$^{-S>A}$ / *Rif1*$^{-S>D}$ clones
MDV_p286	**GCTGCGTGCTCAGTCTCAAC**	

Table M2: List of primers used for genotyping and screening PCR of single cell clones.

Rif1$^{-/-}$ clone 1	*Rif1*$^{-/-}$ clone 2	*NLS-3xHA-Rif1*$^{-/-}$	*Rif1*$^{S>A}$ / *Rif1*$^{S>D}$
95°C 12 min. **x1**	95°C 12 min. **x1**	98°C 30 sec. **x1**	98°C 30 sec. **x1**
95°C 2 min. 52°C 35 sec. **x32** 72°C 30 sec.	95°C 2 min. 56°C 30 sec. **x32** 72°C 3 min.	98°C 10 sec. 68°C 15 sec. **x32** 72°C 10 sec.	98°C 10 sec. 68°C 15 sec. **30x** 72°C 3 min.
72°C 5 min **x1**	72°C 5 min. **x1**	72°C 5 min. **x1**	72°C 5 min. **x1**
HotStar Taq Pol, 10% DMSO	HotStar Taq Pol, 3% DMSO	Phusion Pol, 10% DMSO	Phusion Pol, 3% DMSO

Table M3: List of PCR programs and specific reagents used for genotyping and screening CH12 single cell clones.

Other reagents and materials

Name	Source	Cat. #
Plasmids		
pX458G (pSpCas9(BB)-2A-GFP)	Addgene	48138
pX330G (pX330-T2A-GFP)	V.T. Chu (K. Rajewsky's lab)	N/A
pX330Gn (Cas9^{D10A})	M. Andreani	N/A
pMA-NLS-3xHA #1	M. Andreani (GeneArt)	N/A
pMA-3xHA #1	M. Andreani (GeneArt)	N/A
pMA-PhoMim	M. Andreani (GeneArt)	N/A
pMA-PhoNull	M. Andreani (GeneArt)	N/A
Recombinant proteins and chemicals		
LPS	Sigma-Aldrich	L2630
IL-4 (mouse recombinant)	Sigma-Aldrich	I1020
TGFβ-1 (mouse recombinant)	R&D Systems	7666-MB-00
FBS	Sigma-Aldrich	F7524
RPMI 1640	Thermo Fisher Scientific	21875091
HEPES	Thermo Fisher Scientific	15630056
Sodium Pyruvate	Thermo Fisher Scientific	11360039
Antibiotic Antimycotic	Thermo Fisher Scientific	15240062
L-Glutamine	Thermo Fisher Scientific	25030024
2-Mercaptoethanol	Thermo Fisher Scientific	21985023

Name	Source	Cat. #
NuPage LDS Sample buffer	Thermo Fisher Scientific	NP0008
Proteinase K	Peqlab	3375501
Phenol:Chloroform:Isoamyl alcohol	Roth	A156.3
PARPi Olaparib/AZD2281, Ku-0059436	Selleckchem	S1060
Colcemid	Sigma-Aldrich	1029589200
KaryoMAX Giemsa Stain Solution	Gibco	10092013
Gurr Buffer Tablets	Gibco	10582013
Kits, enzymes and other reagents		
PureLink HiPure Plasmid Filter Midiprep Kit	Thermo Fisher Scientific	K2100-15
PureLink HiPure Plasmid Filter Maxiprep Kit	Thermo Fisher Scientific	K210017
Stbl2 Competent *E. coli*	Thermo Fisher Scientific	10268019
Stbl3 Competent *E. coli*	Thermo Fisher Scientific	C737303
TOP10 Competent *E. coli*	Thermo Fisher Scientific	C404003
Neon Transfection System, 100 mL Kit	Thermo Fisher Scientific	MPK10025
TOPO TA Cloning Kit	Thermo Fisher Scientific	450641
NucleoSpin DNA Purification Kit	Macherey-Nagel	740499
Gibson assembly cloning kit	NEB	E5510S
QuickExtract Solution	Epicentre	QE09050
HotStarTaq DNA Polymerase	Qiagen	203205
Phusion High-Fidelity DNA Polymerase	Thermo Scientific	F530L
Taq DNA Polymerase with ThermoPol Buffer	NEB	M0267
T4 DNA Ligase	NEB	M0202
T7 DNA Ligase	NEB	M0318
Phase Lock Gel tubes	VWR	2302820
Software		
FACS Diva	BD	N/A
FlowJo v.10	Treestar	N/A
MacVector v15.0	MacVector, Inc.	N/A
Prism v.6	GraphPad	N/A

Name	Source	Cat. #
Bioinformatic tools		
CRISPRgold[198]	https://crisprgold.mdc-berlin.de	N/A
CRISPRdesign	https://crispr.mit.edu	N/A
CRISPOR[199]	https://bio.tools/crispor	N/A
ExPASy translate tool[200]	https://web.expasy.org/translate	N/A
Clustal Ω (v.1.2.4)[201]	https://www.ebi.ac.uk/Tools/msa/clustalo	N/A

3.2 Methods

3.2.1 Cell culture

In the present study, the following CH12 cell lines were used: wild-type CH12 (CH12F3, Nakamura 1996), *Rif1*$^{-/-}$ CH12, *Rif1*$^{S>A}$ CH12, *Rif1*$^{S>D}$ CH12 (this study). Cells were grown in RPMI 1640 medium supplemented with 10% fetal bovine serum (FBS), 10 mM HEPES, 1 mM Sodium Pyruvate, 1X Antibiotic Antimycotic, 2 mM L-Glutamine, and 1X 2 Mercaptoethanol at 37°C and 5% CO_2 levels.

3.2.2 I-DIRT

I-DIRT was performed as previously described[147]. Briefly, splenocytes from *Rif1*$^{FH/FH}$ and WT mice were isolated and cultured in SILAC medium supplemented with either labeled (heavy medium, *Rif1*$^{FH/FH}$ culture) or unlabeled (light medium, WT culture) L-arginine and L-lysine.

Upon 96 h culture, cells were exposed to 20 Grays of IR and then frozen in liquid nitrogen, after 45 min. of recovery at 37°C. RIF1 immunocomplexes were isolated from a 1:1 mix of frozen *Rif1*$^{FH/FH}$ and WT cells, upon sub-stoichiometric treatment with glutaraldehyde to preserve labile interactions and without altering

the native composition of protein complexes. RIF1 and co-precipitating proteins were pulled down using anti-FLAG conjugated magnetic beads. Immunocomplexes were purified and analyzed by LC-MS/MS. Peptide identification and quantification were performed using the MaxQuant software[202].

3.2.3 Flow cytometry

For CSR assay, 5 x10^4 cell/mL CH12 cells were cultured for 40 h in RPMI 1640 supplemented with 5-15 mg/mL αCD40L (BioLegend), 5 ng/ml TGFβ and 5 ng/ml of mouse recombinant IL-4 to induce the expression of IgA antibodies. Cell suspensions were collected, washed once in PBS and incubated for 20 min. at 4°C on a rotator with fluorochrome-conjugated anti-IgA antibodies (Southern Biotech). Stained cells were again washed and resuspended in 200 µL PBS 3% FBS. Samples were acquired on an LSRFortessa cell analyzer (BD-Biosciences). For single cell and bulk sorting, cells were collected 24-48 h after transfection and the portion of cells with highest GFP expression (top 3-5 %) were sorted using a BD FACSAria cell sorter (BD-Biosciences, MDC FACS Core facility).

3.2.4 CRISPR/Cas9 genome editing

For all CRISPR/Cas9-based applications, 2 to 7 guide RNAs (gRNAs) per target region were selected based on efficiency/off-target scores generated by three different gRNA design tools, namely CRISPRgold[198] (https://crisprgold.mdc-berlin.de), CRISPRdesign (https://crispr.mit.edu) and CRISPOR[199] (https://bio.tools/crispor) (gRNAs listed in Table S1). gRNAs were cloned in different Cas9-expressing plasmids using a cloning strategy adapted from a protocol developed by Zhang's lab[203]. Cloned plasmids were amplified in TOP10 competent cells (Thermo Fisher Scientific) and then purified by midi-/maxiprep (Thermo Fisher Scientific). To test the efficiency of different gRNAs to mediate

Cas9 cut, the ability of activated CH12 cells to perform CSR was assessed upon expression of different Cas9-gRNAs expressing constructs. In all applications, cell transfection was performed *via* electroporation with Neon Transfection System (Thermo Fisher Scientific) and was tested based on the depletion of RIF1 function, as represented by the reduction of CSR levels of activated B cells. The sequences of the gRNAs employed in these studies are listed in Table M1 and Table S1.

In both knock-out and knock-in applications, 6 selected clones per genotype were validated at the protein expression level, from which 3 clones expressing physiological RIF1 protein levels were further validated at the genomic level. Genomic analysis involved the amplification of the region of interest by PCR, followed by TOPO cloning (Thermo Fisher Scientific) and Sanger sequencing of TOPO plasmids amplified from individual TOP10 competent cells (Thermo Fisher Scientific) colonies. To make sure both copies of *Rif1* gene were analyzed, up to 10 vectors were sequenced. The primers and PCR programs employed in these experiments are listed in Tables M2 and M3. Controls were either WT CH12 or cells nucleofected with gRNAs against random sequences absent in the mouse genome. The scheme of *Rif1* genomic locus in Figures 10, 12 and 16 is adapted from Ensembl ENSMUSG00000036202 (GRCm38:CM000995.2).

3.2.4.1 Knock-out cell lines

To generate the knock-out cell lines, the selected gRNAs were cloned into tandem U6 cassettes of a pX330Gn (Cas9 nickase) plasmid. pX330Gn was created by introducing an additional U6 cassette *via* Gibson Assembly (NEB) to a pX330-T2A-GFP plasmid (kind gift of V.T. Chu, K. Rajewsky's lab). CH12 cells were transfected with the selected Cas9^{D10A}-gRNAs expressing constructs via electroporation with Neon Transfection System (Thermo Fisher Scientific) and single-sorted for GFP-positive cells after 40 h. After ca. 12 days, single cell colonies of discrete size were collected in a "mother" 96-well plate, let grow for

additional 48 h and split in replica plates. Replica plates were used for either culture, cryostorage or screening of the clones. Clones were selected *via* a large-scale CSR assay employing an HTS (High-throughput sampler) coupled to an LSRFortessa cell analyzer (BD-Biosciences).

3.2.4.2 Knock-in cell lines

To generate knock-in cell lines, the selected gRNAs were cloned into a single U6 cassette of a pX458G (wild-type Cas9) plasmids. CH12 cells were co-electroporated with the required pX458G plasmid and a circular donor plasmid carrying the knock-in template. The knock-in template was synthesized by GeneArt (Thermo Fisher Scientific) included the necessary mutations and 600-1000 bp of homology arms (HA). The top 3-4% of GFP-positive cells were single cell-sorted into 96-well plates and allowed to grow for ca. 12 days before selection and expansion. For the purpose of performing a large-scale selection and cryostorage of the clones in the 96-well plate format, each plate was divided into replica plates. Knock-in clones were selected *via* a PCR-based screen. Briefly, gDNA was extracted from up to 140 single cell clones from each 96-well replica plate using Quick Extract solution (Epicentre) to resuspend cell pellets which were then heated up at 68°C for 6 min. and then at 98°C for 2 min. 96-well plate PCR reactions were set-up using primers annealing with genomic sequences outside the homology arms. Positive *3XHA* / *NLS-3XHA-Rif1* clones were identified by a unique, discrete bands of 368bp / 395bp.

To identify positive *Rif1*$^{S>A}$ / *Rif1*$^{S>D}$ single cell clones, unpurified PCR products obtained from 96-well plate PCR reactions were directly digested overnight using 10 units of NheI restriction enzyme (NEB, #R0131) and visualized on agarose gel. The primers and PCR programs employed in the PCR screens are listed in Tables M2 and M3.

3.2.5 Genotyping

Genomic DNA (gDNA) was extracted from ca. $1x10^6$ cells. Cell pellets after overnight incubation at 55°C with 0.5 mL Proteinase K (20mg/mL) diluted in Proteinase K buffer (100mM Tris pH 8, 0.2% SDS, 200 mM NaCl, 5 mM EDTA). Lysed cells were transferred in Phase Lock Gel tubes (VWR) and vigorously mixed 1:1 with Phenol:Chloroform:Isoamyl alcohol (Roth). After centrifugation at 16,000 g for 20 min. at room temperature, the aqueous phase was transferred to a new 1.5 mL tube and the procedure was repeated. The aqueous phase was then mixed with 2.5X volumes of 100 % ethanol, 10% Sodium Acetate pH 5.2 and 0.05 µg/µL glycogen. The tube was gently inverted until gDNA clumped and stored for at least 30 min. at -20°C. After gentle mixing followed by centrifugation at 18,000 g for 15 min. at 4°C, the precipitated gDNA was washed three times in 0.5 mL 70 % ethanol. After discarding the 70 % ethanol, the pellet was dried for 10 min. to allow the residual ethanol to evaporate. gDNA was then eluted in TA buffer (Thermo Fisher Scientific) pre-warmed at 55°C. In most cases, amplification was carried out using 0.4 units Phusion High-Fidelity Polymerase (Thermo Scientific), 1x HF Phusion buffer, 40 mM dNTPs, 3% DMSO, 20 mM of each primer. Primers and PCR programs designed for each target sequence and application are listed in Tables M2 and M3.

3.2.6 Western blot analysis

Western blot analysis of protein levels was performed on whole cell lysates prepared by lysis in RIPA buffer (Sigma) supplemented with complete EDTA free proteinase inhibitors (Roche) and DDT (Roth). Proteins were mixed with 3.5X NuPAGE loading dye (Thermo Fisher Scientific) and separated by SDS gel electrophoresis (SDS-PAGE) using NuPAGE Tris-Acetate 3-8% gradient gels (Thermo Fisher Scientific). Protein separation was carried out in Tris-Acetate SDS running buffer (Thermo Fisher Scientific) at 150 V for 1 h. Up to 40ug of whole

cell extract were transferred on a PDVF membrane activated for 1 min. with 100% methanol. Wet protein transfer was performed at 220mA for 2 h in transfer buffer (25 mM TRIS, 192 mM glycine, 20% methanol). Membranes were blocked with 3% BSA (bovine serum albumin) in PBS-t (1X PBS + 0.1% Tween 20). Primary antibody incubation was carried out at 4°C overnight (alternatively, for 1 h). Following 3 washes in PBS-t, incubation of the membranes with secondary antibodies was carried out at RT for 1 h. The primary antibodies used were anti-RIF1[88] (1:5000; #2034) and anti-β Actin (1:10.000; Sigma-Aldrich). Secondary HRP-conjugated antibodies (1:20.000; Jackson ImmunoResearch) were used. ECL solution (GE Healthcare) was used to activate HRP and chemiluminescence signals were used to impress Amersham Hyperfilm ECL (GE Healthcare).

3.2.7 Metaphase analysis

CH12 cells were seeded at a concentration of $8x10^4$ cells/ml in 25mL complete RPMI. After 24 h, PARPi (Olaparib, previously dissolved in DMSO) was added to the culture media at a final concentration of 1 μM. On the following day, 45 min. before harvesting, cells were treated with 1% colcemid to block cells in the metaphase stage of mitosis. Exactly after 24 h of PARPi treatment cells were collected and gently resuspended in 1 mL of pre-warmed 0.075 M KCl at 37ºC. Once the pellet was fully resuspended, additional 40 mL of pre-warmed 0.075 M KCl were added dropwise, while vortexing the tube in order to avoid the formation of clumps. Cell suspensions were incubated at 37ºC for 15 min. to perform a hypotonic shock, inverting the tube after the first half of the incubation. Samples were subsequently washed with 1mL of freshly prepared fixative solution (methanol/glacial-acetic acid – 3:1 v/v). Additional 40 mL of fixative solution were added slowly while shaking the tube, because after hypotonic shock cells were swollen and tending to clump. Samples were fixed for 30 min. at room temperature (RT). After two additional washes, cells were resuspended again in fixative solution

and kept at 4ºC. Metaphase spreads were prepared by dropping fixed cells on tilted microscope slides with a Pasteur pipette from at least 30 cm height distance. Slides were placed on a humidifier for 1-2 min., air-dried and incubated at 42ºC for 1 h. Giemsa staining was performed by treating slides first with KaryoMAX Giemsa stain solution for 2 min., then with Gurr buffer solution and lastly washed with ddH_2O. Drying was performed overnight at RT. Metaphases were acquired with the Automated Metaphase Finder System Metafer4 at 63X magnification. Chromatid breaks and chromosome radials were manually counted from at least 50 metaphases per sample.

3.2.8 Statistical analysis

Statistical analysis *via* Mann-Whitney U test was performed using GraphPad Prism software. Results were considered statistically significant when P-values were less than 0.05 (* represents $p < 0.05$, ** represents $p < 0.01$, *** represents $p < 0.001$, **** represents $p < 0.0001$). Quantitative data were represented with either median or mean values ± standard error of the mean (SEM) unless otherwise stated.

4. Results

4.1 A SILAC-based pull-down coupled to a CSR screen allows studying RIF1 interactome

In recent years, novel NHEJ-promoting factors have been discovered, some of which have been proposed to be the ultimate downstream effectors of the 53BP1-dependent DSB end protection pathway[99]. Their involvement in NHEJ-dependent events, like B cell CSR[124], fusion of unprotected telomeres[76] and generation of genomic instability in *Brca1*$^{-/-}$ cells[193], has been largely described. Despite this, their connection to the upstream factors 53BP1 and RIF1, as well as the specific DSB end protection mechanism, leave many questions unanswered. This suggests that additional uncharacterized proteins may be involved, further expanding this protein network.

As part of the lab's effort to identify new effector proteins contributing to DSB end protection, this work focused on the study of RIF1 interactome in the specific context of B cells antibody class switching.

4.1.1 iDIRT identifies 41 possible RIF1 interactor candidates

To identify RIF1 interactors involved in DSB end protection during CSR, Isotopic Differentiation of Interactions as Random or Targeted (I-DIRT) was used in primary cultures of splenocytes undergoing CSR. I-DIRT is a technique used to isolate affinity-tagged protein complexes, which is coupled to a SILAC (stable isotope labeling by amino acids in cell culture) approach[204]. I-DIRT has the important advantage of discriminating between specific and aspecific protein interactions prior to enrichment, while in other immunoisolation techniques protein specificity is monitored during enrichment, thus being compromised by

artifacts. Furthermore, I-DIRT allows isolating protein complexes under native conditions, limiting the enrichment of aspecific contaminants while retaining specific protein-protein interactions[204]. I-DIRT was performed by Daniel Rosen and Brian Chait (The Rockefeller University, New York), as part of a collaborative project[147]. In this experiment, *Rif1*$^{FH/FH}$ C57B6 mice were employed[159]. These mice were generated by crossing heterozygous mice in which a 1xFLAG-2xHA (influenza hemagglutinin) tag was knocked-in at the N-terminal portion of RIF1. The ability of *Rif1*$^{FH/FH}$ mature B cell to undergo CSR was proven to be comparable to *Rif1*$^{+/+}$ mice[147]. Splenocytes from both *Rif1*$^{+/+}$ and *Rif1*$^{FH/FH}$ strains were isolated, stimulated to undergo CSR to IgG1 with an activation cocktail (LPS, IL-4, RP/14) and grown in either light (L, *Rif1*$^{+/+}$) or heavy (H, *Rif1*$^{FH/FH}$) isotopic medium (Fig. 7).

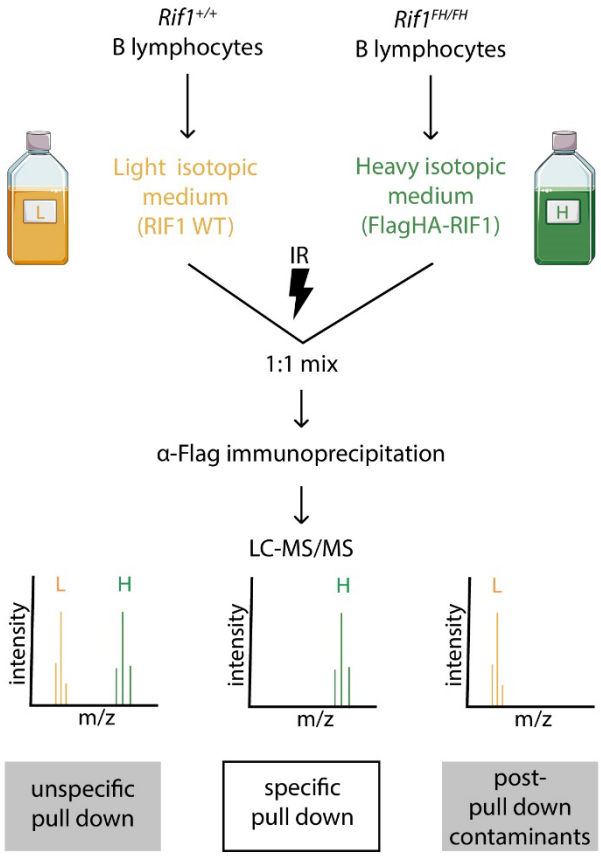

Figure 7: SILAC-based pull down (I-DIRT) for the identification of new RIF1 interactors in primary B lymphocytes. Scheme representing RIF1 I-DIRT. FH: 1xFLAG-2xHA tag; IR: ionizing radiation; LC-MS/MS: liquid chromatography-tandem mass spectrometry. For details see 3.2.2.

Cells were then treated with IR to induce additional DSBs and amplify RIF1 recruitment to damage sites. A 1:1 cell mixture was then subjected to anti-Flag immunoprecipitation followed by liquid chromatography (LC) tandem mass spectrometry (MS/MS). Upon analysis of the MS data, 41 candidates were selected based on the following criteria: SILAC ratio (H/H+L) of at least 2 standard deviations (SD) higher than the mean of the H/H+L distribution (0.49); number of identified peptides greater than three; a posterior error probability (PEP) lower than $1x10^{-4}$ (Table 2).

Gene name	H/H+L.	Pept. count
4x SD		
CD36	0.89	16
MGA	0.88	57
LY6D	0.87	7
3x SD		
BACH2	0.83	14
PLD4	0.80	7
EIF5	0.80	6
CHMP5	0.79	6
AHNAK	0.78	5
RNF31	0.78	7
CD55	0.78	7
POLE1	0.78	11
SPCS2	0.77	5
CPM	0.77	17
2x SD		
TLK2	0.76	5
EIF2B5	0.76	7
COX5B	0.75	5
TEX10	0.75	8
LAS1L	0.74	6
MS4A4C	0.74	8
PDLIM2	0.74	4
PHYN1	0.74	9
EXOSC8	0.73	4

Gene name	H/H+L	Pept. count
2x SD		
SYK	0.73	4
GBAS	0.73	4
PSMD4	0.72	6
IFIH1	0.71	5
DPP4	0.71	15
APRT	0.71	6
ARPC1A	**0.71**	**13**
SLC2A1	0.71	4
TCEB1	0.70	4
NAA50	0.69	4
RNF2	0.69	4
NDUFB7	**0.69**	**5**
IGLV2	0.69	4
TIMELESS	0.69	4
GBP3	0.69	4
BMP2K	0.69	4
PAG1	0.68	7
CISD1	0.68	5
ZRANB2	0.68	5

Table 2: List of the 41 RIF1 interaction candidates selected. The criteria used are mean SILAC ratio (H/H+L), number of identified peptides (Pept. count) and PEP (not shown).

4.1.2 ARPC1A and NDUFB7 are potential RIF1 interactors during CSR in B lymphocytes

To test whether the candidates had a role in CSR, I used a CRISPR/Cas9-based loss-of-function screen. For each of the 41 candidates, I designed three different guide RNAs (gRNAs) based on their activity and off-target scores obtained from different *in silico* tools (Table S1). All gRNAs were individually cloned in Cas9-T2A-GFP-expressing plasmids (pX330G-T2A-GFP) and co-transfected in CH12 cells (Fig. 8) (see 3.2.4 for more details).

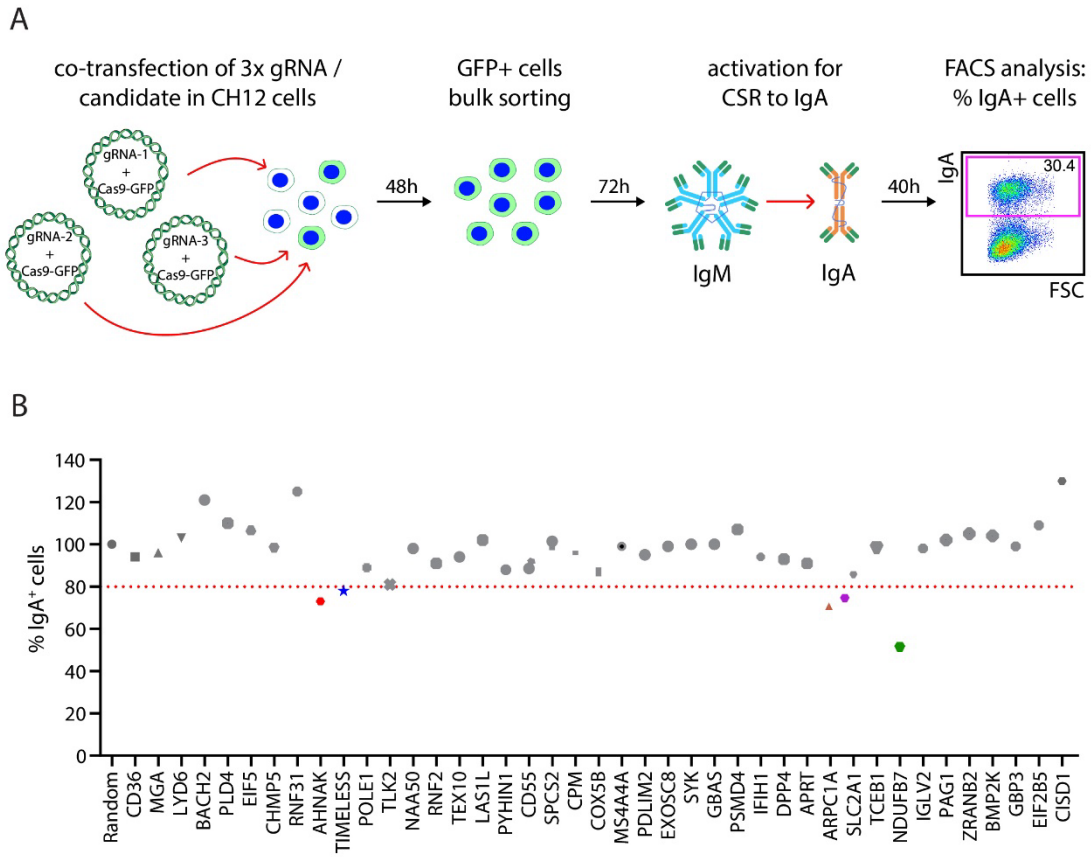

Figure 8: A loss-of-function screen allows to study the involvement of RIF1 interactor candidates in CSR. (A) Scheme representing the workflow of the loss-of-CSR-function screen employed to test the 41 potential RIF1 interactors. **(B)** Dot-plot showing the percentage of IgA^+ cells upon somatic targeting of the indicated candidate genes by CRISPR/Cas9. Control cell lines (Random) were CH12 cells transfected with gRNAs that do not target any region of the murine genome. Mean CSR value of the controls was set to 100% and used to normalize the data. Five candidates (AHNAK, red; TIMELESS, blue; ARPC1A, brown; SLC2A1, purple; NDUFB7, green) that displayed more than 20 % reduction of CSR levels are indicated.

Efficiently transfected cells (10-25% GFP^+ cells) were then analyzed for the ability to undergo CSR to IgA upon specific stimulation. I performed the loss-of-function screen in multiple experiments, where the CSR levels of each sample were normalized to those of wild-type CH12 cells transfected with Cas9 and "random" gRNAs, which do not target any sequence in the murine genome (defined in this manuscript as "Random" or "gRandom" controls). The normalized CSR levels were then compared to cells in which 53BP1 was transiently knocked-out using a previously optimized gRNA (CSR-deficient controls). Collectively, results showed that most of the targeted genes are dispensable for CSR. Only the depletion of 5 proteins out of 41 caused a reduction in CSR efficiency of more than 20% (Fig. 8B). To further test the requirement of these proteins (AHNAK, TIMELESS, ARPC1A, SLC1A and NFUFB7) for antibody switching, the assay was repeated. In this case, transient knock-outs were induced by using both pooled and individual gRNAs to rule out the possibility that none of the gRNAs was causing off-target effects and to simultaneously test the efficiency of individual gRNAs. AHNAK, TIMELESS, and SLC1A resulted to be dispensable for CSR (Fig. 9A-C). Targeting of *Ndufb7* (Fig. 9D) and *Arpc1a* (Fig. 9E) resulted in a mild, but reproducible, CSR deficiency. Based on these preliminary results, we conclude that NDUFB7 and ARPC1A are affecting, directly or indirectly, antibody isotype switching in B lymphocytes. Nonetheless, I decided not to pursue the investigation of their potential role in B cell antibody class switching because of the lack of experimental evidence hinting at a direct role in the process. and because of time constraints (see 5.1).

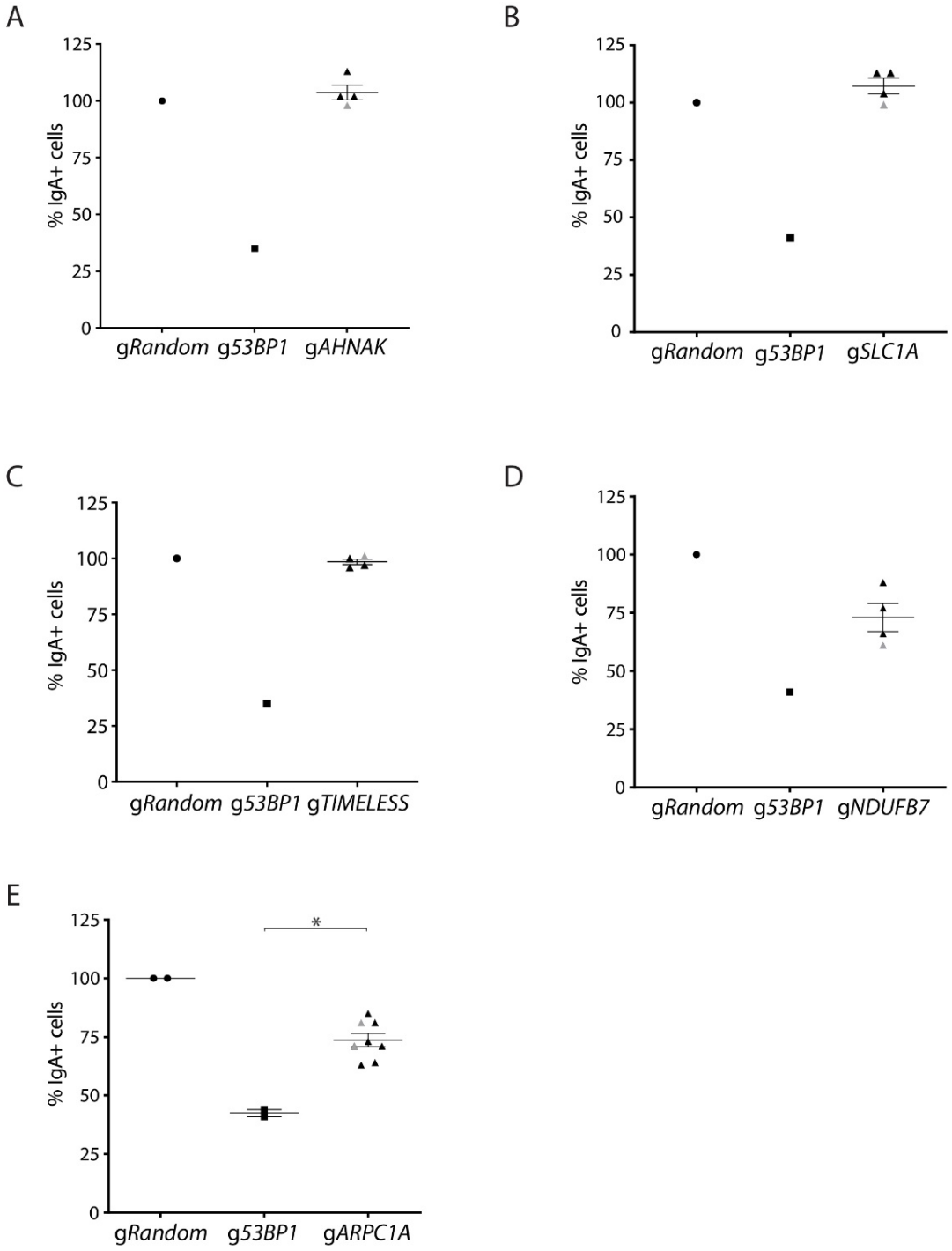

Figure 9: ARPC1A and NDUFB7 are two potential RIF1 interactors affecting CSR in CH12 cells. Graphs summarizing the mean percentage of IgA^+ cells upon somatic targeting of ANHAK **(A)**, SLC1A **(B)**, TIMELESS **(C)**, NDUFB7 **(D)** and ARPC1A **(E)** with single (black symbols) and pooled (grey symbol) gRNAs. Significance in panel E was calculated with the Mann–Whitney U test (*: $p \leq 0.05$). Error bars in the graphs represent SEM.

4.2 Phosphorylation at conserved and clustered SQ sites does not affect RIF1 role in productive and aberrant NHEJ

Recently, independent studies aimed elucidating further the process of DSB end protection converged into the discovery of the Shieldin complex, claimed to be the ultimate effector of the 53BP1-dependent pathway[78,93-98,100]. Nonetheless, the exact molecular mechanism of DSB end protection and, specifically, the actual contribution of RIF1 to this process remain unclear. The lack of catalytic domains in most of the proteins of the 53BP1-dependent pathway could suggest that RIF1 may function as a simple scaffold protein. However, the predicted protein-protein interaction domain as well as the DNA binding domain[154], together with other structural features (Fig. 6), may indicate that RIF1 orchestrate the recruitment of downstream factors while interacting with the chromatin surrounding the DSB site. This idea is in accordance with recent reports depicting RIF1 as an organizer of chromatin architecture during replication timing in both yeast and mammals[158,163,172]. Hence, further unraveling the structural features of RIF1 may help to define its function in the context of resection inhibition. To do so, I exploited the direct implications of DSB end protection in the repair of CSR breaks in the B murine lymphoma CH12 cell line[205].

4.2.1 Knock-out by CRISPR/Cas9 corroborates RIF1 requirement for CSR in murine CH12 cells

Rif1 deficiency was reported to impair CSR and lead to immunodeficiency in mice[88]. In the CH12 cell line, *Rif1* downregulation achieved by RNAi led to a minor CSR deficiency compared to the *in vivo* system, most likely due to residual RIF1 protein levels[85]. To confirm that CH12 is an ideal model system to study the regulation of RIF1 function in CSR, I generated *Rif1*-deficient clones by employing CRISPR/Cas9 (see 3.2.4.1 for details).

To minimize undesired off-target effects, Cas9 nickase ($Cas9^{D10A}$) was employed[206]. Seven gRNAs targeting either exon 2 or exon 5 were designed and tested for their ability to efficiently reduce CSR in CH12 by knocking-out RIF1 (Fig. 10A-B). Based on the results, two gRNA pairs (g*Rif1*-3/4 and g*Rif1*-5-6, Fig.10A) were selected to induce RIF1 knock-out by $Cas9^{D10A}$.

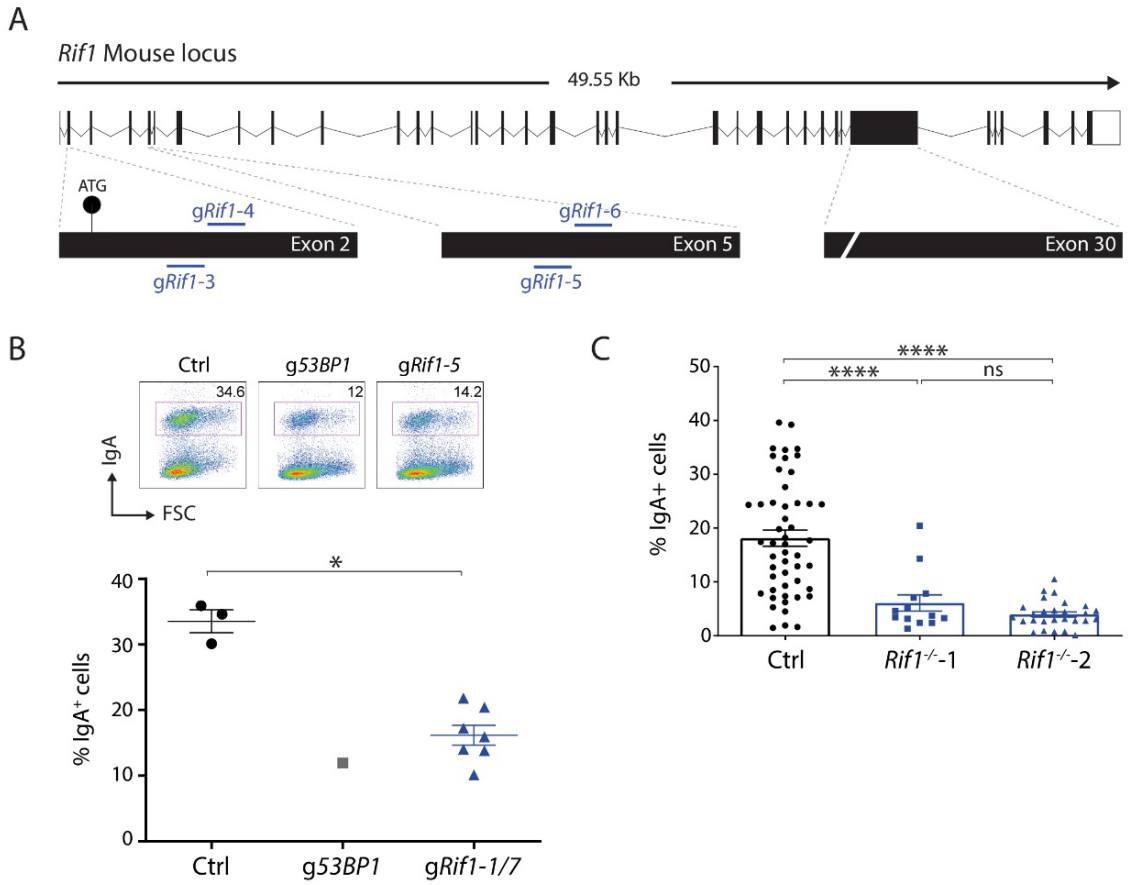

Figure 10: CRISPR/Cas9-mediated *Rif1* knock-out recapitulates CSR deficiency in the B cell lymphoma CH12 cell line. (A) Scheme of murine *Rif1* genomic locus and location of the gRNAs selected for gene editing (adapted from Ensembl Rif1-201ENSMUST00000112693.9). **(B)** gRNAs validation experiment. (top) Representative FACS plot indicating the percentage of IgA^+ CH12 cells. (bottom) Dot plot representing the mean percentage of IgA-switched cells upon targeting with 7 different gRNAs (ctrl: untransfected cells and cells transfected with two different random gRNAs). **(C)** Summary from the large-scale CSR screen performed on single cell clones targeted with one of the indicated nickase gRNA pairs and spCas9D10A (ctrl: single cell clones targeted with a random gRNA pair). Significance in panel B and C was calculated with the Mann–Whitney U test (ns: non-significant, *: $p \leq 0.05$, ****: $p \leq 0.0001$). Error bars in the graphs represent SEM.

Compared to control clones, *Rif1*-deficient single cell clonal derivatives showed an overall drastic decrease of CSR even prior to selection (Fig. 10C), indicating the high efficiency of the CRISPR/Cas9-based system used. Misleading phenotypes due to clonality issues or eventual Cas9 off-target cuts can arise also upon use of Cas9 nickase-mediated gene editing[207]. For this reason, I selected and further characterized two independent CSR-deficient clones (one per gRNA pair) (Fig. 11A-C).

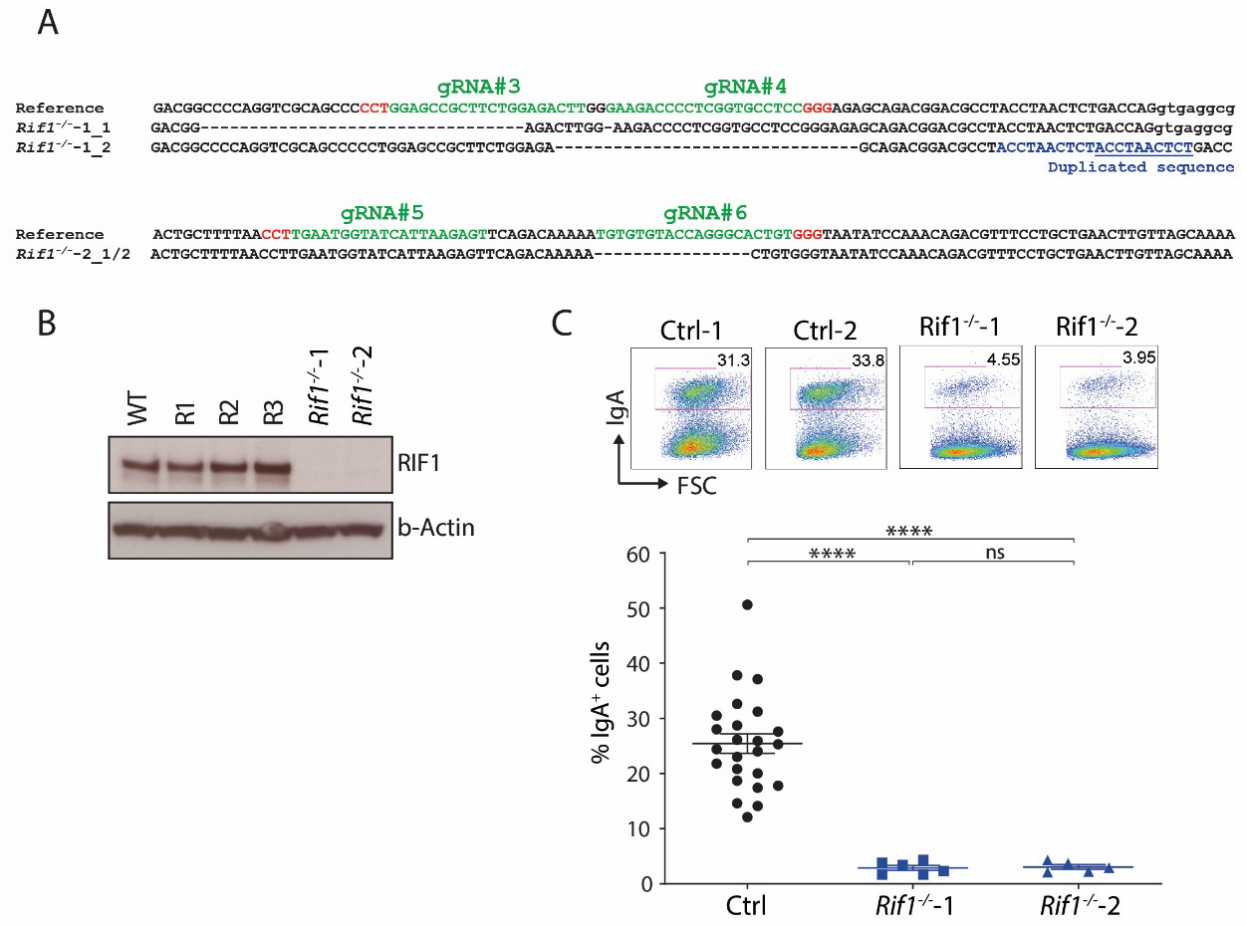

Figure 11: Characterization of the *Rif1*$^{-/-}$ CH12 clones. (A) Genomic scar analysis. Reference sequence (wild-type *Rif1*) shows gRNA protospacers (green) and PAM sequences (red). *Rif1*$^{-/-}$ clone 1 presents on one allele a sequence duplication (blue). *Rif1*$^{-/-}$ clone 2 presents the same deletion on both alleles. **(B)** Western blot analysis of selected *Rif1*$^{-/-}$ clones. **(C)** Representative FACS plots (left) and dot plot (right) summarizing 7 independent experiments confirming CSR levels of the selected clones. Significance in panel C was calculated with the Mann–Whitney U test (ns: non-significant, ****: $p \leq 0.0001$). Error bars in the graphs represent SEM.

To confirm the efficient targeting on both *Rif1* alleles, TOPO cloning was performed using gDNA extracted from both clonal derivatives (*Rif1*$^{-/-}$-1 and *Rif1*$^{-/-}$-2). Sanger sequencing confirmed the presence of various deletions inducing biallelic frameshift mutations on both clones (Fig. 11A). Accordingly, western blot analysis confirmed the loss of RIF1 protein expression, potentially by nonsense-mediate mRNA decay (Fig. 11B). As expected, both *Rif1*-deficient clones consistently displayed CSR deficiency (Fig. 11C). We conclude that RIF1 is essential for CSR in CH12 cells, thus indicating the suitability of this model system to study of RIF1 functions in CSR.

4.2.2 Minimal RIF1 protein levels in the *NLS-3xHA-Rif1* cell lines are sufficient to support CSR

The generation of small constructs (suitable for B cell nucleofection) for expressing full-length and mutant versions of RIF1 in *Rif1*$^{-/-}$ CH12 cells, was consistently hindered by bacterial toxicity (not shown). This experimental obstacle could have been overcome by directly generating RIF1 deletion mutant cell lines. To this end, it was first necessary to generate a stable cell line expressing an epitope-tagged version of RIF1 (as later discussed in paragraph 5.2). I envisaged to use anti-HA tag antibodies, which are widely used and continuously optimized, to eventually: study RIF1 interactome *via* pull-down approaches; test the ability of RIF1 mutants to interact with its effector 53BP1 or to form ionizing radiation-induced foci (IRIF) *via* proteomic approaches or immunofluorescence techniques, respectively. Considering that some of the RIF1 mutants may have lost the predicted nuclear localization sequence (NLS)[151], I decided to add to RIF1 N-terminus a simian virus 40 (SV40) large T antigen sequence, which is known to act as NLS[208,209].

To generate a cell line expressing both the NLS and the 3xHA peptides, I took advantage of CRISPR/Cas9 to knock-in the required coding sequences directly

downstream RIF1 start codon. gRNAs were designed as close as possible to the ATG sequence, which is present on exon 2 of *Rif1* gene (Fig. 12A).

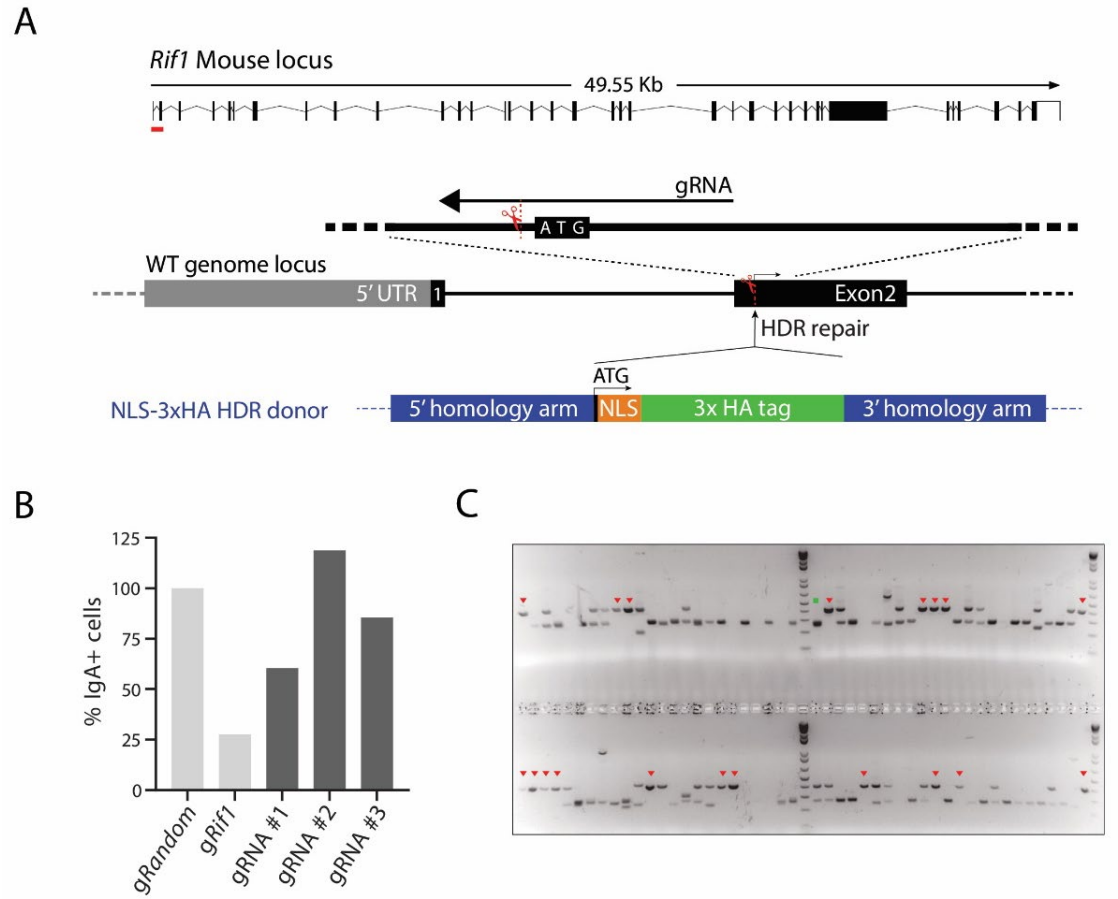

Figure 12: Generation of the *NLS-3xHA-Rif1* CH12 cell line. (A) (top) *Rif1* genomic locus, the targeted exon (2) is indicated by a red line. (bottom) Schematic representation of the CRISPR/Cas9 knock-in strategy used to introduce a NLS-3xHA tag to RIF1 N-terminus in CH12 cells. The Cas9 cut at *Rif1* start codon (ATG) is indicated by a scissor. The selected gRNA and its orientation are indicated by a backward arrow **(B)** Graph representing the gRNA validation experiment. The efficiency of each gRNA to induce a Cas9 cut at *Rif1* exon 2 was measured indirectly by assessing the cells' ability to perform CSR to IgA. Controls used were a gRNA targeting any region of the murine genome (gRandom) and the most efficient gRNA used for RIF1 somatic targeting, targeting exon 5 (*gRif1*). The levels of IgA^+ cells were normalized to the gRandom control. **(C)** Representative agarose gel of a large-scale genomic screening showing amplification of the 5' sequence of *Rif1* exon 2. Potential *NLS-3xHA-Rif1* homozygous knock-in clones are indicated by red arrowheads. Wild-type CH12 gRNA used as control (green square).

Three candidate gRNAs were tested *via* loss-of-CSR-function assay and the gRNA showing the strongest reduction of IgA^+ cells was chosen (gRNA #1, Fig. 12B). A synthetic gene containing the NLS-3xHA coding sequence and 600 bp of

homology arms was co-transfected with a Cas9/gRNA expressing vector in wild-type CH12 cells (see 3.2.4.2 for details). Single cell clones were screened for successful homozygous editing *via* a PCR-based screen, in which amplicons generated from knock-in alleles were 96 bp-longer than those deriving from wild-type alleles. Out of 85 clones tested, 19 showed a single and discrete band (22% homozygous knock-in efficiency) (Fig. 12C). Three independent clones were selected after a confirmatory PCR-based screen. The presence of the intact NLS-3xHA sequence on both alleles and the lack of unwanted mutations were assessed by Sanger sequencing (data not shown). To confirm that the newly introduced peptides did not affect RIF1 function in CSR, the clonal derivatives were stimulated with cytokines and their ability to undergo CSR to IgA was tested. Although variable, CSR efficiencies were comparable to that of a control cell line (Fig. 13A). In parallel, to make sure that NLS-3xHA-RIF1 was expressed at physiological levels, western blotting on whole cell extracts from clonal and control cell lines was performed. Surprisingly, at standard conditions that allow for clear visualization of endogenous RIF1, none of the clones seemed to express the protein. Nonetheless, by over-exposition, the expected RIF1 band appeared in all clones (Fig. 13B).

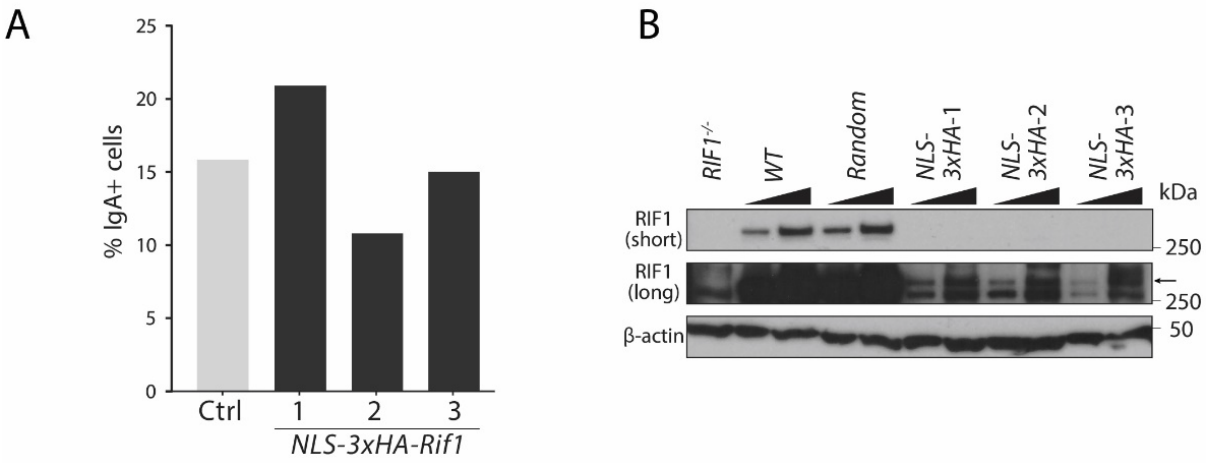

Figure 13 continued on page 55

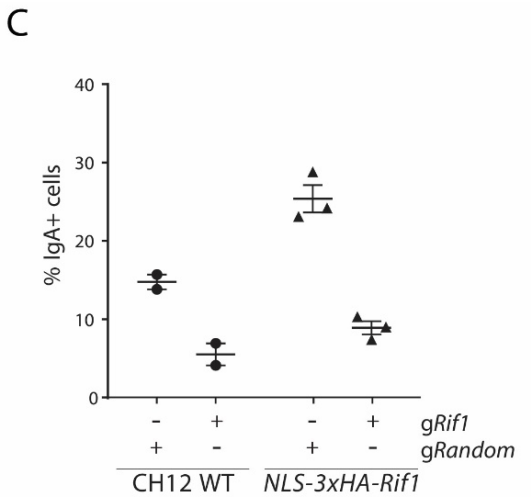

Figure 13: *NLS-3xHA-Rif1* CH12 cells undergo CSR despite showing reduced RIF1 protein expression. (A) Graph representing the ability of three selected *NLS-3xHA-Rif1* clones to undergo CSR to IgA upon activation. Ctrl: CH12 cells nucleofected with a random gRNA not targeting any sequence in the murine genome. **(B)** Western blot analysis of RIF1 protein levels. Apart from *Rif1*$^{-/-}$ control, 1 mg/mL and 3 mg/mL of whole cell lysate were used for each sample. The arrow indicates specific RIF1 antibody binding. **(C)** Loss-of-CSR-function assay. Control and *NLS-3xHA-Rif1* cell lines were transfected with either an established gRNA targeting *Rif1* at exon 5 or a random gRNA, and then activated for CSR to IgA.

Considering the results of the characterization experiments (Fig. 13A-B) and the fact that the epitope of the antibody used for western blot was located towards the C-terminus of the protein, one could argue that probably trace amounts of RIF1 are enough for B cells to produce IgA antibodies. To test this hypothesis, I performed a loss-of-function experiment, targeting the poorly expressed protein with an established gRNA targeting exon 5. The results confirmed that the levels of NLS-3xHA-RIF1 support CSR (Fig. 13C). Remarkably, the same phenomenon was observed in two independent single cell clones expressing 3xHA-RIF1, which were created and tested in parallel to the *NLS-3xHA-Rif1* cell lines (data not shown).

We conclude that minimal levels of RIF1 molecules are sufficient to promote NHEJ repair of AID-induced DSBs, thus allowing CH12 cells to produce IgA antibodies at physiological levels.

4.2.3 Three conserved SQ phosphorylation motifs in murine RIF1 are phosphorylated *in vivo*

Many aspects of 53BP1 function during DSB repair are dependent on the phosphorylation of specific SQ/TQ motifs located at its intrinsically disordered N-terminus[68,85,88,137].

Similar to its phosphorylation-dependent interactor, murine RIF1 displays 17 SQ/TQ sites, some of which are organized in clusters spanning 100-200 aa (Fig. 14). Notably, these clusters are also localized within an IDR, which accounts for more than half of RIF1 length, as predicted by PrDOS[210] (Fig. 14) and Phyre2[211] (data not shown) servers.

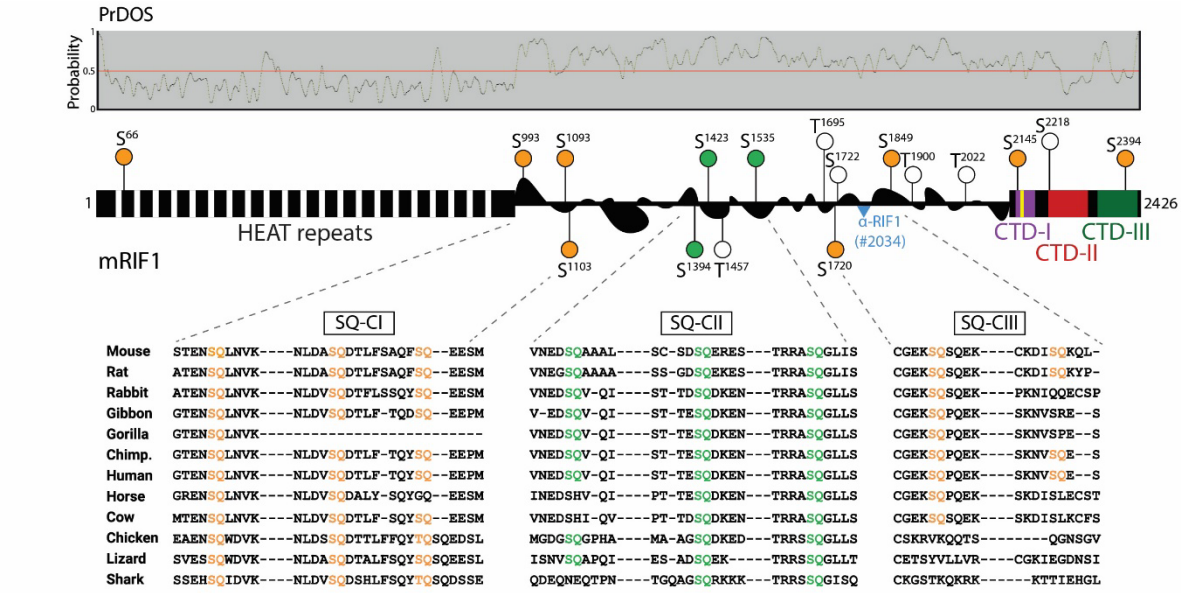

Figure 14: RIF1 displays a large intrinsically disordered region characterized by clusters of conserved SQ sites. (Top) Graph representing RIF1 protein disorder prediction (performed using PrDOS[210]), where probability values >0.5 indicate disordered regions. (Middle) Schematic representation of RIF1 protein (NP_780447.4). Predicted domains are indicated with boxes: N-terminal HEAT repeats domain (dashed black); C-terminal CTD-I (RVxF/SILK motif, purple), CTD-II (DNA binding domain, red) and CTD-III (BLM interaction domain, green). Balloons indicate serine (S) and threonine (T) residues within putative ATM/ATR phosphorylation sites (SQ/TQ). White balloons: non-conserved sites; orange balloons: moderately conserved sites; green balloons: sites that are conserved and phosphorylated in vivo (I-DIRT). (Bottom) Protein sequence alignment between different species showing conservation of three SQ clusters (performed using ClustalOmega[201]).

To date, the role of ATM-mediated phosphorylation of mammalian RIF1 remains undescribed. Therefore, I decided to investigate how ATM-mediated phosphorylation within RIF1 IDR affects its function in DSB end protection.

To narrow down the SQ/TQ sites that are potentially involved in RIF1 regulation, the degree of conservation was assessed first. Out of 13 SQ/TQ sites localized in the IDR, 8 are highly conserved among mammals (Fig. 14). Because the IDR contains only conserved SQ motifs, the three corresponding clusters will herein be termed "SQ-C" (SQ clusters). DISPHOS (DISorder-enhanced PHOSphorylation site) tool was used to predict phosphorylation of RIF1 residues based on intrinsic disorder[184]. Intriguingly, two serines (S^{1423} and S^{1535}) included in SQ-CII were predicted to be phosphorylated with high confidence (Table 3).

Position	Residue	Score	Sequence
1423	Ser	0.886	SCSDSQERE
1535	Ser	0.776	TRRASQGLI
2145	Ser	0.505	GLKRSQEDE
2218	Ser	0.541	LSPGSQSSK

Table 3: Summary of DISPHOS 1.3 (Disorder-Enhanced Phosphorylation Sites Predictor). Results were filtered for serines (S) followed by glutamine (Q). Conserved SQ sites are indicated in red.

Next, I took advantage of the dataset generated *via* the I-DIRT proteomic pull-down performed on *Rif1*$^{FH/FH}$ splenocytes treated with IR (Fig. 7). Thanks to relatively high coverage (73%), phosphate-containing serines/threonines were identified with high confidence (Table 4). Among 31 identified phosphoresidues, only three phosphoserines (S^{1394}, S^{1423}, S^{1535}) were part of SQ motifs (Fig. 15). Remarkably, these ATM phosphosites belong to SQ-CII (Fig. 14). Remarkably, S^{1423} and S^{1535} were predicted to be phosphorylated (Table 3).

Interestingly, a larger number of identified residues were part of consensus CDK phosphorylation sites (S/T-P motifs) (Table 4). We conclude that murine RIF1 contains a highly conserved cluster of SQ sites (SQ-CII) that are phosphorylated *in vivo*.

Identified residues	Motif
S1394, S1423, S1535	SQ (ATM/ATR kinases)
S383, S394, S398, T1212, S1238, S1240, S1446, S1464, S1690, S1835, S1875, S2303	SP (CDK kinase)

Table 4: List of phosphorylated residues identified in *Rif1*$^{FH/FH}$ primary B cells. The list was filtered for residues that are targeted by either ATM/ATR or CDK kinases.

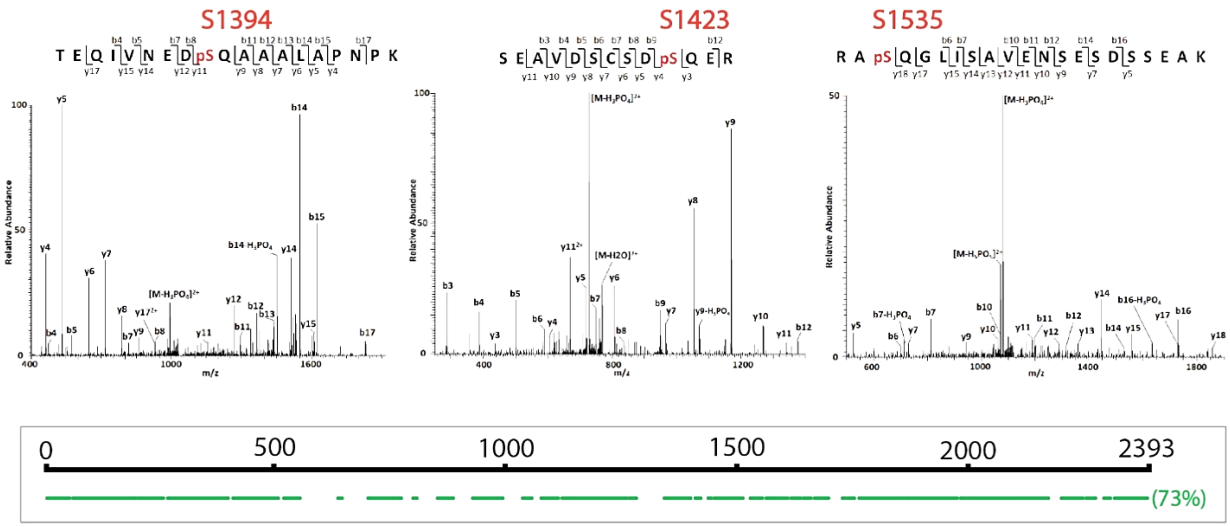

Figure 15: The conserved SQ/TQ cluster 2 within RIF1 intrinsically disordered region is phosphorylated in vivo. (top) Mass-spec spectra showing the identified phospho-residues corresponding to S^{1394}, S^{1423} and S^{1535}. (bottom) Scheme representing MS analysis coverage relative to RIF1 isoform 2 (XP_011237438.1). Max Quant analysis performed by W. Zhang (Chait Lab, Rockefeller University, NY).

4.2.4 An efficient CRISPR/Cas9 approach allows the simultaneous introduction of multiple point mutations into the CH12 genome

To investigate the role of RIF1 SQ-CII in DSB end protection, its phosphorylation was either abrogated or mimicked by simultaneous mutation of all serines to alanine (S → A) or aspartate (S → D), respectively. This was achieved by CRISPR/Cas9-mediated knock-in, which exploited HDR to replace the target sequence on exon 30 with a synthetic DNA sequence containing the desired alanine/aspartate codon mutations (HDR donor) (Fig. 16, Fig. S1). The presence of a 5' (gRNA 5') and a 3' (gRNA 3') Cas9 cut sites, together with 1000bp-long homology arms (HAs), would have allowed to "push" the cells to repair the two DSBs -occurring simultaneously on both alleles- by HR using the full synthetic gene as template[212]. Besides the nonsynonymous mutations, different silent mutations were needed to prevent spCas9 from further cutting the correctly knocked-in sequence (Fig. S1-S2). To do so, gRNAs with similar efficiency/off-target scores, were chosen based of the possibility to silently mutate both protospacer and PAM sequences, while keeping into consideration the existence of the two non-canonical spCas9 PAM sequences, NAG and NGA[213,214]. To test the efficiency of two selected gRNAs (gRNA 5' and gRNA 3'), CH12 cells transiently expressing two individual spCas9/gRNA constructs were activated and their ability to perform CSR was assessed. A reduction of IgA^+ cells up to 35% was observed (data not shown), confirming the suitability of the gRNAs for *Rif1* gene targeting. To discriminate between wild-type and edited genomes, a unique NheI restriction site was introduced in the HDR donor sequence by synonymous mutations (Fig. 16A, Fig. S1). As opposed to the selection of *Rif1*$^{-/-}$ clones *via* a large-scale CSR assay (Fig. 11C), unbiased selection of the homozygous knock-in clones was performed *via* a digestion/PCR-based genetic screen. After transfection with the required plasmids and single cell sorting, this large-scale screen allowed to select CH12 clones carrying the NheI restriction site on both alleles (Fig. 16B).

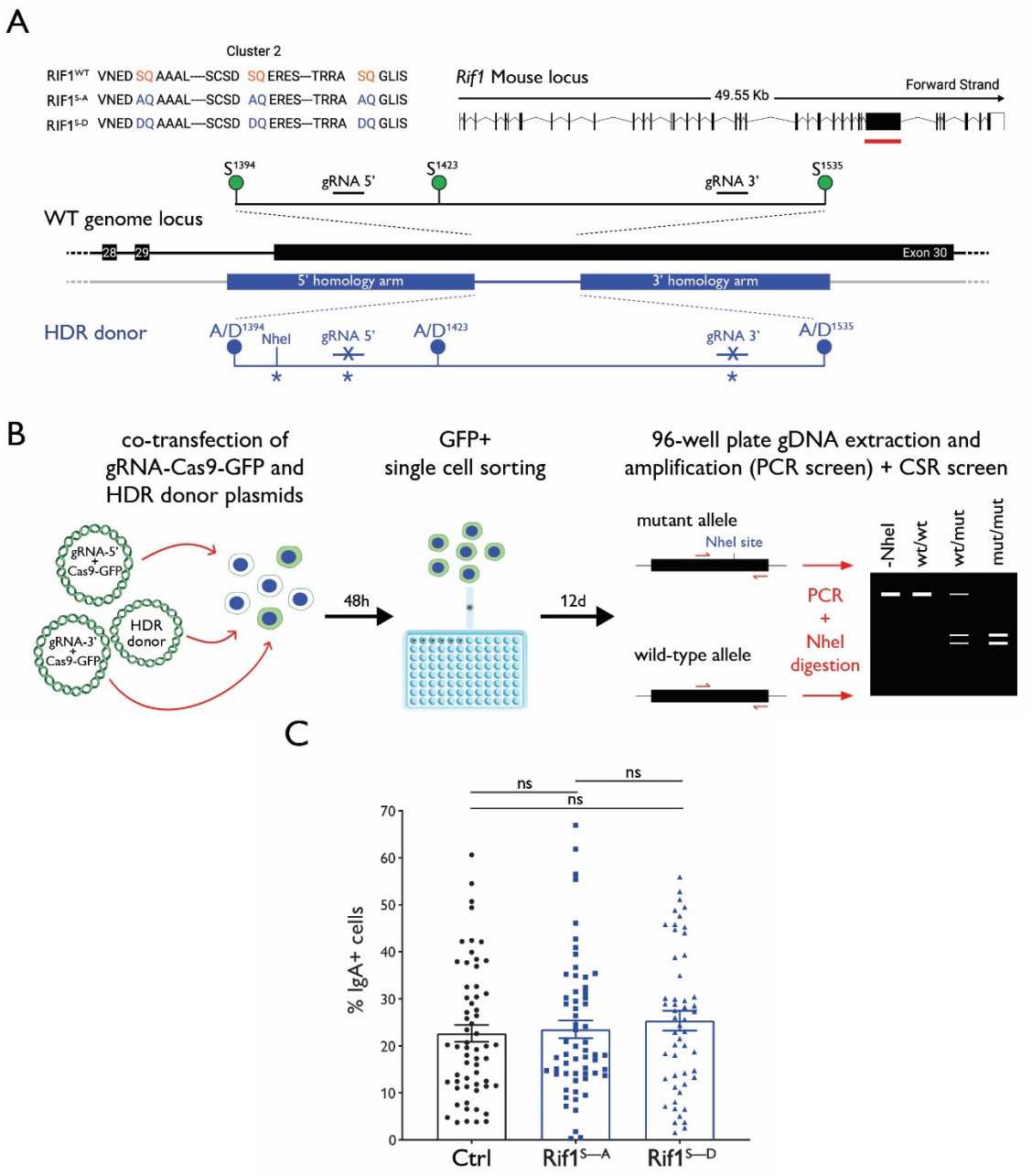

Figure 16: Simultaneous introduction of multiple point mutations by CRISPR/Cas9-mediated knock-in. (A) (top left) Expected protein sequence of SQ-CII upon mutation of the codons encoding for S1394, S1423 and S1535. (top right) *Rif1* genomic locus, the targeted exon is indicated by a red line. (bottom) Schematic representation of the CRISPR/Cas9 knock-in strategy used to mutate the serine of each of the three conserved SQ sites to either alanine (A) or to aspartate (D) in CH12 cells. Silent mutations are marked by an asterisk (*) **(B)** Schematic representation of the workflow for the generation and screening of knock-in single cell clones. **(C)** Summary from the large-scale CSR screen performed on single cell clones transfected with knock-in constructs (ctrl: single cell clones targeted with a random gRNA pair). Significance in panel C was calculated with the Mann–Whitney U test (ns: non-significant). Error bars in the graphs represent SEM.

To rule out the possibility that the knock-in sequence or other parts of the HDR donor were integrated in other regions of the genome, gDNA amplification was performed using primers annealing beyond the homology arms. The genomic screen of 61 *Rif1*$^{S \rightarrow A}$ and 53 *Rif1*$^{S \rightarrow D}$ clones showed homozygous knock-in efficiencies of 13% (8/61) and 23% (12/53), respectively (data not shown). Nonetheless, due to the availability and ease of use of the LSRFortessa analyzer coupled to an HTS module, I as well performed a large-scale CSR analysis, in parallel to the genetic screen. The preliminary results showed no significant differences in IgA^{+} cells of both genotypes compared to control single cell clones. However, no conclusion could be drawn, due to the unknown knock-in efficiency and the wide distribution of the clones that were analyzed (Fig. 16C).

4.2.5 Phosphorylation of RIF1 at the conserved SQ cluster is not required for the regulation of its function during CSR

Because CSR efficiency can be subjected to clonality-related issues, three clones of each genotype (*Rif1*$^{S \rightarrow A}$ and *Rif1*$^{S \rightarrow D}$) were selected and further characterized. To confirm the presence of the NheI site on both alleles, the digestion/PCR-based genetic screen was repeated. Amplification of the target region followed by NheI digestion showed the expected bands and no undigested (WT) DNA band in all 6 clones (Fig. 17A). Sanger sequencing of undigested PCR products confirmed the homozygous knock-in of the desired mutations in all selected clones. Western blot analysis showed that neither abrogation or mimicking of the SQ-CII phosphorylation affected negatively RIF1 protein folding and expression (Fig. 17B).

To finally test whether phosphorylation of SQ-CII regulates RIF1 role in DSB end protection, I stimulated the clones to express IgA on their surface. Surprisingly, both *Rif1*$^{S \rightarrow A}$ and *Rif1*$^{S \rightarrow D}$ cell lines preserved their ability to undergo CSR, despite the variable efficiencies (Fig. 17C). Considering that the three clones of each

mutagenesis were identical from a genetic as well as a protein expression point of view, the CSR results were grouped per genotype (Fig. 17D). This representation clearly showed that differences between control and RIF1 mutant cell lines were not significant, despite the variability observed among clones of the same genotype. We concluded that the phosphorylation of SQ-CII does not regulate RIF1 function in CSR.

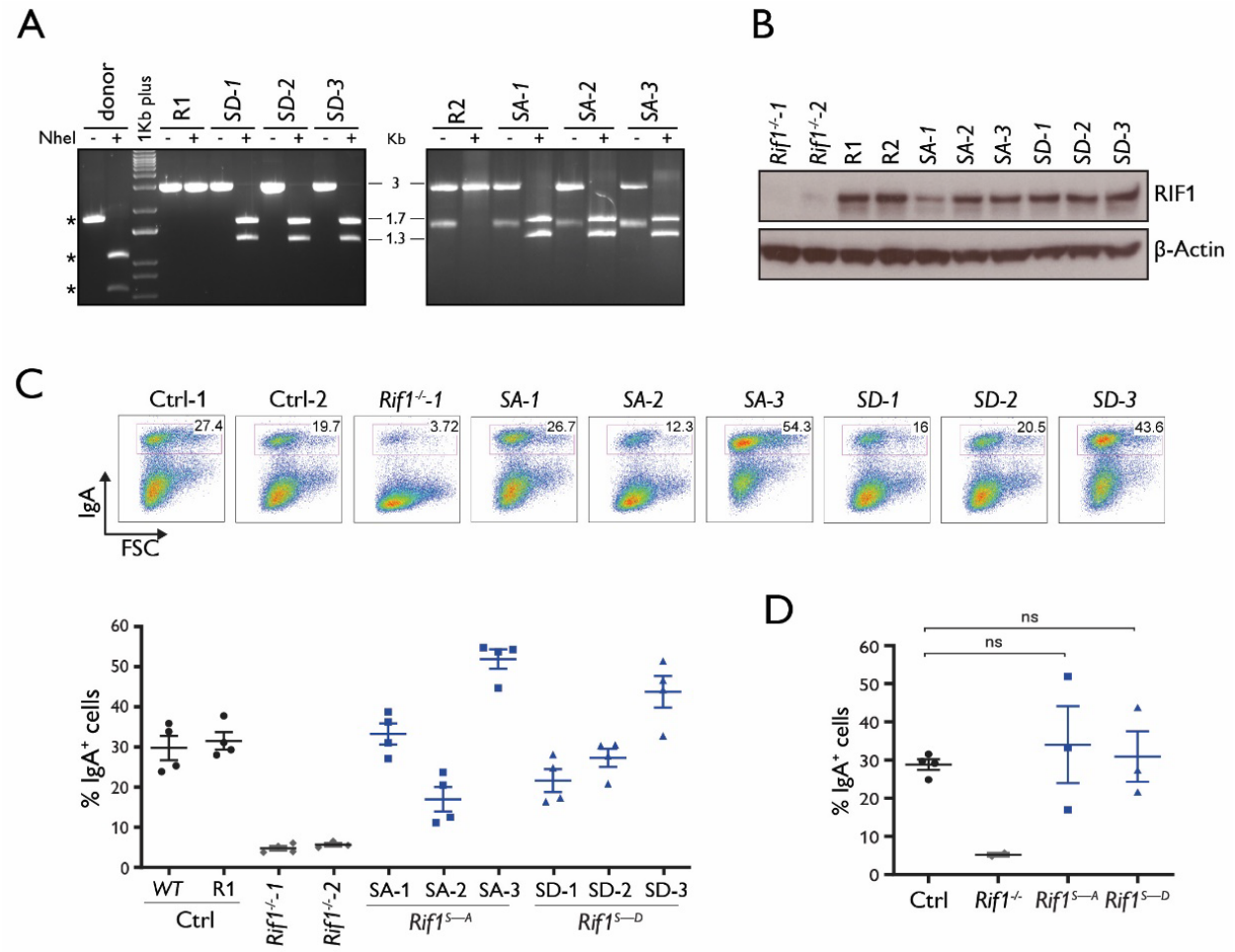

Figure 17: RIF1 phospho-deficient and phospho-mutant CH12 cell lines undergo efficient CSR. (A) Confirmatory PCR screen performed on controls and three independent clones per genotype (*SA-1, SA-2, SA-3 / SD-1, SD-2, SD-3*). *SA* = phospho-deficient clone; *SD* = phospho-mimetic clone. Controls: HDR donor plasmid DNA (donor) and gDNA from two different clones derived from targeting of CH12 cells with a random (R) gRNA that does not anneal with any region in the murine genome (R1, R2). *Expected bands from amplification of 10ng of HDR donor plasmid (uncut: 1.8 kb; cut: 1.1 kb + 0.7 kb) **(B)** Western blot analysis controls and three independent $Rif1^{S \rightarrow A}$ and $Rif1^{S \rightarrow D}$ cell lines. Controls: two different *Rif1* knock-out cell lines ($Rif1^{-/-}$-1 and $Rif1^{-/-}$-2) and two different Random cell lines (R1, R2).

(C) Top: Representative flow cytometry plots measuring CSR to IgA in activated CH12 cells of the indicated genotype. Right: Dot plot summarizing %CSR efficiency (% IgA^+ cells) of three independent *Rif1*$^{S\rightarrow A}$ and *Rif1*$^{S\rightarrow D}$ clones in four independent experiments. Controls: wild-type (WT) CH12 cell line, three independent Random (R1, R2, R3) CH12 cell lines and two independent *Rif1*$^{-/-}$ CH12 cell lines. **(D)** Representation of results from (C) with cell lines grouped by genotype. Significance in panel D was calculated with the Mann–Whitney U test (ns: non-significant). Error bars in the graphs represent SEM.

4.2.6. Phosphorylation of RIF1 at the conserved SQ cluster does not alter genomic instability in PARPi-treated *Brca1*$^{-/-}$ cells

It was reported that a fraction of breast and ovarian cancers that developed resistance to PARPi treatments displayed downregulation or depletion of *Tp53bp1* or *Rif1* genes[195]. From a molecular perspective, this is explained by a loss of DSB end protection leading to the re-establishment of the HR pathway and, consequently, tumor cell survival[195,196] (Fig. 18) (see 1.5 for more details).

In a collaborative effort, Sandhya Balasubramanian (S.B., from my lab) and I investigated whether the modification of the SQ-CII by ATM kinase is required for RIF1-mediated synthetic lethality of *Brca1*-deficient cells treated with PARPi. Answering this question could potentially help us clarifying whether RIF1-mediated DSB end protection is differently regulated based on the cellular context. S.B. generated the *Brca1*$^{mut/mut}$ (HR deficiency model) and *Brca1*$^{mut/mut}$ *Rif1*$^{-/-}$ (PARP1 resistance model) cell lines that will be mentioned in this part of the dissertation.

To study the involvement of RIF1 SQ-CII in the aberrant repair of DSB in PARPi-treated *Brca1*-deficient cells, serine to alanine/aspartate mutations were introduced in the *Brca1*$^{mut/mut}$ cell line by the same CRISPR/Cas9 strategy used to mutated RIF1 in wild-type CH12 cells (Fig. 16A).

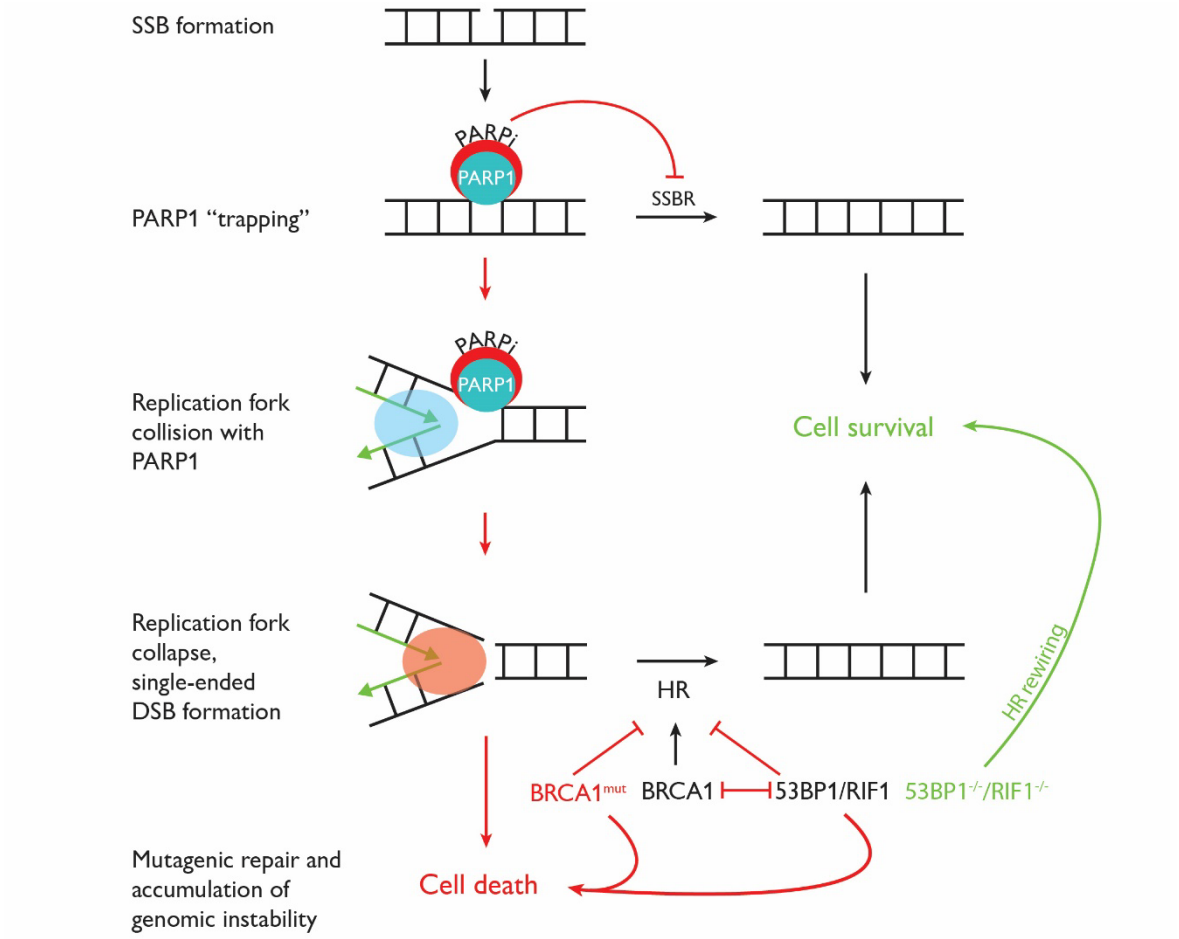

Figure 18: Scheme representing the concept of BRCA1 and PARP1 synthetic lethality.

As it is well described in literature, BRCA1 is required for displacement of 53BP1 from DSBs in order to promote HR repair[44]. This clearly represents an obstacle to gene editing techniques relying on HDR. Surprisingly, we obtained knock-in rates similar to those in the wild-type genetic background: 21% for *Brca1*$^{mut/mut}$ *Rif1*$^{S \rightarrow A}$ clones and 19% for *Brca1*$^{mut/mut}$ *Rif1*$^{S \rightarrow D}$ (data not shown). Three clones of each genotype were characterized, to confirm the successful introduction of the mutated sequence in both copies of *Rif1* gene (Fig. 19A) and that protein levels were not negatively affected by the knocked-in sequence (Fig. 19B).

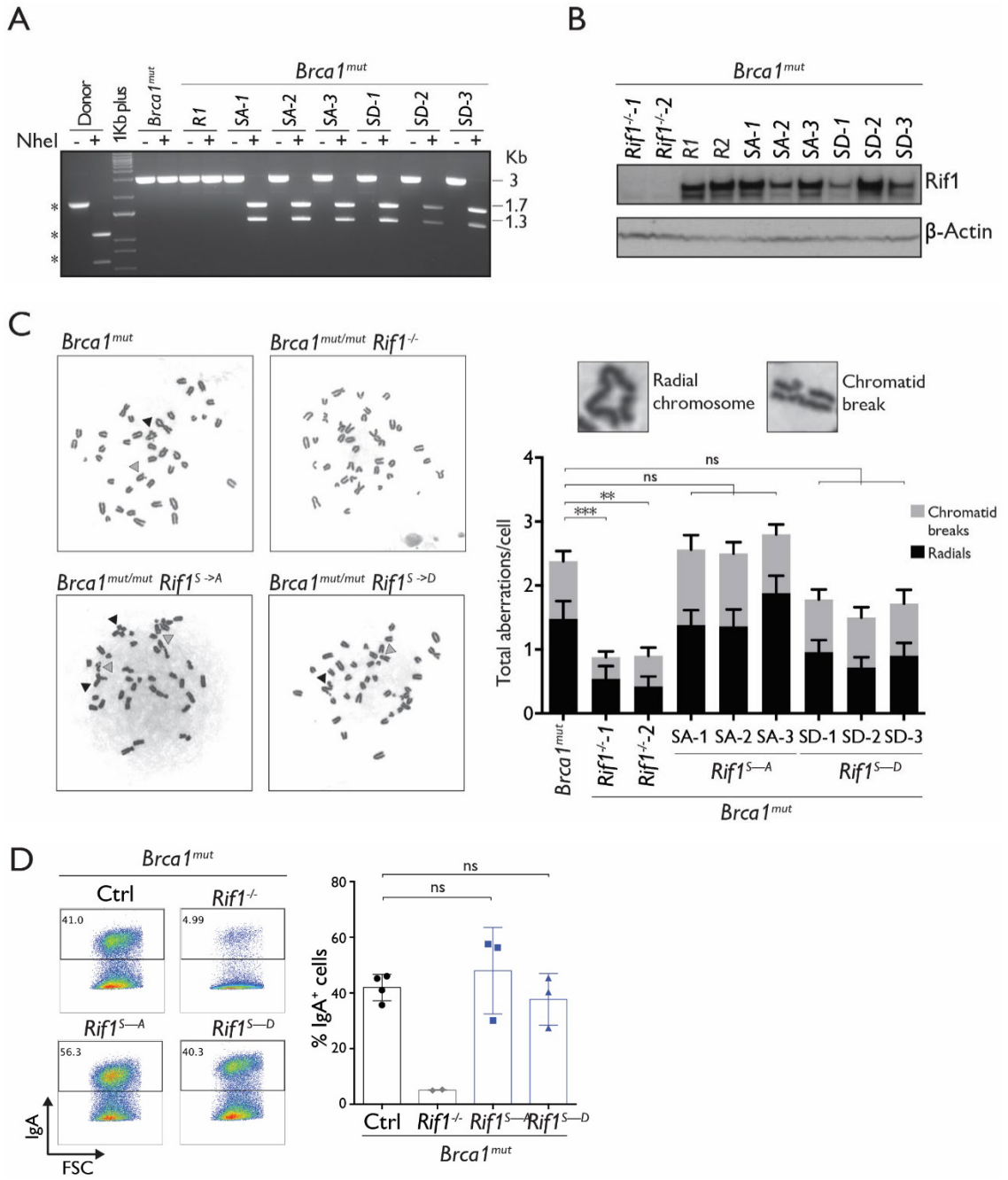

Figure 19: *Brca1 mut Rif1 S→A* and *Brca1 mut Rif1 S→D* CH12 clones are sensitive to PARPi treatment. (A) Confirmatory PCR screen performed on controls and three independent *Brca1 mut Rif1 S→A* and *Brca1 mut Rif1 S→D* CH12 clones per genotype (*SA* = phospho-deficient clone; *SD* = phospho-mimetic clone). Controls: HDR donor plasmid DNA (donor) and gDNA from a random (R) clone. *Expected bands from amplification of 10ng of HDR donor plasmid (uncut: 1.8 kb; cut: 1.1 kb + 0.7 kb) **(B)** Western blot analysis of controls and three independent *Brca1 mut Rif1S→A* and *Brca1 mut Rif1S→D* cell lines. Controls: two different *Brca1 mut Rif1* knock-out cell lines (*Rif1-/-*-1 and *Rif1-/-*-2) and two different Random cell lines (R1, R2). **(C)** Analysis of genomic instability in metaphases from PARPi-treated *Brca1mut* RIF1 phosphomutant cell lines. Chromosome radials and chromatid breaks are indicated with black and grey arrows, respectively (n = 50 metaphases per genotype). Left: Representative metaphase spreads from PARPi-treated

cells of the indicated genotype. Right: representative chromosomal aberrations (top) and graph (bottom) summarizing the mean number of radial chromosomes (black bar) and chromatid breaks (grey bars) per cell of each indicated genotype. **(D)** Representative flow cytometry plots (left) and dot plot (right) summarizing the % CSR efficiency (% IgA^+ cells) of three independent *Brca1*^{mut} *Rif1*$^{S\rightarrow A}$ and *Brca1*^{mut} *Rif1*$^{S\rightarrow D}$ clones. Controls: *Brca1*^{mut} CH12 cell line, three independent Random (R1, R2, R3) CH12 cell lines and two independent *Brca1*^{mut} *Rif1*$^{-/-}$ CH12 cell lines. Significance in panels C and D was calculated with the Mann–Whitney U test (ns: non-significant). Error bars in the graphs represent SEM.

To study the levels of genomic instability leading to PARPi-induced cell death, we performed metaphase spread analysis. This robust assay, established by S.B., allows visualizing chromatid breaks and chromosome radials, the main hallmarks of genomic instability. In line with the loss of aberrant NHEJ, double knock-out cell lines (*Brca1*$^{mut/mut}$ *Rif1*$^{-/-}$) rescued the load of both genomic aberrations (Fig. 19C). *Brca1*$^{mut/mut}$ *Rif1*$^{S \rightarrow A}$ and *Brca1*$^{mut/mut}$ *Rif1*$^{S \rightarrow D}$ clones displayed no significant difference in the number of both chromosome radials and chromatid breaks (Fig. 19C). These results indicate that the phosphorylation status of SQ-CII does not affect RIF1 contribution to genomic instability of PARP-treated *Brca1*-deficient cells.

Considering the results obtained in the wild-type phosphomutant clones, we conclude that SQ-CII is not involved in the phosphoregulation of RIF1 DSB end protection function during CSR as well as in the context of aberrant NHEJ repair of replication-associated DSBs in *Brca1*-null cells.

The results of this collaborative project are currently being combined with those presented in the second part (4.2) of this dissertation into a scientific paper.

5. Discussion

The effective response to DNA damage is essential for the preservation of DNA integrity and for cell survival. The repair of both spontaneous and programmed DSBs partly relies on RIF1, a component of the 53BP1-dependent pathway that is designed to limit DSB end resection and promote NHEJ repair. An important aspect of this repair pathway is that it is essential for CSR, the deletional-recombination process leading to the expression of different antibody isotypes in B cells. RIF1 is a conserved, multi-functional protein lacking any enzymatic activity[150-152]. Despite years of research, many are the open questions regarding the actual mechanism of DSB end protection. This hints at the existence of as-yet-unknown factor(s) mediating this mechanism. In the present work, RIF1 interactome has been investigated to shed light on the complexity of this process.

Additionally, the mechanism of action of RIF1 remained poorly described for many years after its discovery, especially from a structural and biochemical point of view. Recently, major advances have been made in the investigation of RIF1 structure in the context of different RIF1 functions[160,172,174,175], but the molecular mechanisms/switches by which RIF1 function during NHEJ (and consequently, CSR) is regulated remain unclear. This work provides evidence that conserved ATM kinase target sites in RIF1 IDR are phosphorylated *in vivo*, but do not affect its function in DSB end protection.

This study took advantage of the dependency of CSR on the NHEJ repair process, exploiting the ability of stimulated CH12 cells to produce IgA antibody isotype as an output for DSB end protection efficiency.

5.1 Investigation of the RIF1 interactome via a loss-of-CSR screen

The CRISPR/Cas9-based functional screen employed to investigate RIF1 interactome was developed in such a way to efficiently screen a large number of candidates and, at the same time, to maximize the chances of knocking down the candidate genes. The major contribution to its efficiency laid in the model used, the murine B lymphoma-derived CH12 cell line[205]. CH12 are the only cells that can be stimulated to undergo CSR at relatively high levels *in vitro*, enabling to identify CSR defects with an adequate dynamic range.

To increase the confidence of each knock-out, I chose to target either exons encoding for functional domains or exons that were previously disrupted to successfully generate knock-out models (depending on the availability of the information in literature or in mouse models repositories). Due to the size of the screen, I decided not to test the ability of each gRNA to induce Cas9 cut on its target gene, but rather to pool three gRNAs per candidate and simultaneously express them in CH12 cell (Fig. 8A).

CSR relies on the inhibitory effect of RIF1 and the other pro-NHEJ factors to limit resection[124]. Hence, the eventual hits could have been as-yet-unknown factors, which have implications in DSB end protection. Nonetheless, as studies from our lab suggest, RIF1 contribution to CSR may go beyond its function in protecting S-region DSBs. In fact, we raised the possibility that RIF1 may be involved in the CSR-related transcriptional regulation[147] and showed that the regulation of DSB resection by 53BP1 and RIF1 marginally impacts CSR, despite the fact that the depletion of the two proteins almost completely impairs the process[147,148] (see 1.3.4). This evidence indicates that candidates resulting positive in the screen might be involved in novel RIF1-dependent mechanisms promoting CSR. Surprisingly, the somatic targeting of only 2 out of 42 candidates showed a consistent, albeit not severe reduction in IgA-switched cells (Fig. 8B). However,

two considerations may explain why most of the candidate interactors resulted negative in the CSR screen.

On one hand, taking into account the experimental conditions of the SILAC-based pull-down that generated the list of candidates, we cannot exclude the possibility that some of the potential interactors may have a role in any of the RIF1-mediated processes other than CSR (e.g., regulation of replication timing; see 1.4). Additionally, the material used to perform the iDIRT was composed of primary splenocytes stimulated with cytokines to undergo CSR. Besides inducing GLT and the expression of AID[122], cytokine stimulation increases the proliferation rate of these cells[124]. As a consequence, these cells are more likely to incur into replication stress[215]. Since RIF1 has a role in both replication timing and replication stress response, it is possible that potential interactors have a role in those processes rather than in CSR.

On the other hand, it cannot be ruled out that, in some cases, CRISPR/Cas9 failed to efficiently target the candidate gene. All three gRNAs used to target a specific candidate may have been inefficient in localizing Cas9 to the target sites; effective targeting may have occurred on a single allele which, in the case of an haplosufficient gene, would have led to the expression of a functional protein[216]. Lastly, we could speculate that residual levels of proteins with long turnover times may have been present at the time of cytokine stimulation, thus maintaining physiological levels of CSR. This assumption is supported by the observation that trace levels of RIF1 can support CSR (see 4.2.2).

Somatic targeting of NDUFB7 caused a moderate, but variable reduction (20-40%) of CSR efficiency (Fig. 9D). NDUFB7 is a subunit of the NADH:ubiquinone oxidoreductase (complex I), which catalyzes the oxidation of NADH and the reduction of ubiquinone in the mitochondrial inner membrane. The specific subunit stabilizes the membrane domain of the complex and together with other

25 accessory subunits, it is important for the maintenance of complex I structure and function[217,218]. Of note, Stroud et al. proved that depletion of the membrane arm subunits of complex I (NDUFB7 is one of them) causes severe mitochondrial respiratory chain defects and affects metabolism, transporter activity, translation, and DNA replication pathways[218].

Due to the importance of respiration for cellular metabolism, we could argue that the depletion of a key subunit of the complex I may affect CSR indirectly. In line with this assumption, NDUFB7 may not interact with RIF1 and this could be as well justified by the low number of peptides recognized in the mass-spec following the iDIRT (Table 2). For this reason no replicate CSR experiment was performed for this candidate (Fig. 9D).

CRISPR/Cas9-mediated depletion of ARPC1A, a subunit of the ARP2/3 complex, caused a minimal yet consistent reduction (25%) of CSR levels in the first screen and in the following CSR assays (Fig. 9E). As for the mitochondrial complex I, the main biological processes supported by the ARP2/3 complex appear to be unrelated from CSR.

The ARP2/3 complex is essential for cell migration, endocytosis, and phagocytosis, due to its ability to polymerize actin filaments[219,220]. WASP (Wiskott-Aldrich syndrome protein) is one of the main proteins facilitating actin polymerization by ARP2/3 and both were found to physically associate with RNA-pol II and mediate RNA-pol II-dependent transcriptional regulation *in vitro* and *in vivo*[221]. Different studies confirmed that actin branching affects chromatin remodeling complexes including SWI/SNF, INO80, SRCAP/SWR1, and the combined remodeler/histone acetyltransferase complex TIP60/NuA4[222-224]; consequently, affecting actin-mediated chromatin remodeling can impact DNA transcription[225,226], replication[227,228] or repair[229-231].

Interestingly, a recent study showed that nuclear actin filaments are formed upon DNA damage[232-234]. In Drosophila, nucleation of F-actin filaments by Arp2/3 complex appeared to allow the relocation of heterochromatic DSBs to the nuclear periphery and to aid heterochromatic DSB repair[233]. In mammalian cells ARP2/3 and WASP inhibition reduced HR, whereas MMEJ and NHEJ pathways remained unaltered[234].

Taken together, the recent insights into the potential contribution of actin polymerization in nuclear processes suggest that these proteins may also directly contribute to aspects of the dynamic process of CSR. Nonetheless, the fact that NHEJ was not affected by the inhibition ARP2/3 and WASP[234], may indicate that the CSR defect seen upon ARPC1A knock-out (Fig. 9E) could be an indirect effect, due to the disruption of epigenetic regulators' activity instead. In fact, the chromatin remodeling complex INO80 was also shown to regulate CSR in humans and in CH12 cells[235]. These results were supported by previous studies describing CSR deficiency upon depletion of the cohesion complex, which is known to be modulated by INO80 during sister chromatid cohesion[236,237]. Additionally, the depletion of the INO80 complex was shown to reduce 53BP1 accumulation to DSBs in different cell lines[231]. Opposingly, INO80 was also shown to promote DSB end resection in support of HR repair[238].

In summary, this evidence highlights the need to further investigate the role of INO80 and cohesin complexes at damaged chromatin and to further explore the connection between actin-mediated chromatin remodeling, RIF1, and CSR.

5.2 The structural study of RIF1 in B cells and its challenges

Although the role of mammalian RIF1 in different nuclear processes has been studied for almost two decades, its mechanisms of function remain elusive. The diverging functions that mammalian RIF1, compared to its yeast ortholog, has developed throughout the evolution hinder the study of RIF1 conserved domains. Direct interactions and structural determinants at the base of both yeast and mammalian RIF1 mechanism of action have been well described only in the context of replication timing[159,162,163,166,172,174,175,239].

Escribano-Diaz et al. provided the first comprehensive domain study of RIF1, proving that its localization to DSBs is dependent on its N-terminal HEAT domain and that its antagonizing activity towards BRCA1 focal accumulation additionally requires its C-terminus (excluded the SILK-RVxF motifs)[85]. In this and in a later study, to investigate the required structural features for RIF1 function, adherent cells were transfected with different mutant versions of a construct expressing human RIF1[85,240]. The same approach was used to identify a specific CHK1-mediated phosphorylation event that appeared to inhibit RIF1-PP1 interaction in the context of DNA replication[164].

However, regardless of the numerous functional studies published[68,85,88,89], no structural information regarding RIF1 role in CSR has been reported so far. Presumably, the explanation lies in the difficulties related to the transfection or viral transduction of B lymphocytes with RIF1-full length and mutant constructs (up to 15 kb in size). In fact, it is well known than B cells are refractory to most transfection methods (e.g. Lipofectamine, calcium phosphate, etc.) and that viral packaging limit is a constraint for the efficient delivery of large constructs[241-243].

In this study, the attempt to transfect the large RIF1-encoding plasmids in CH12 cells and primary B cells *via* electroporation was unsuccessful. Furthermore, the expression of a smaller vector containing full-length RIF1 resulted toxic to

different *E. Coli* strains. This toxicity hampered the amplification of the desired vector and favored the introduction of stop codons or frameshift mutations in RIF1 coding sequence, a rare event previously described in literature[244]. Altogether, these aspects complicated the experimental design required to identify the domains that are essential for RIF1 role in CSR. CRISPR/Cas9 gene editing represented an alternative to endogenously express modified versions of RIF1 in CH12 single cell clones.

A number of RIF1 mutants that I planned to generate would have lacked the NLS, predicted to lay in the C-terminus[76,151,152,154,240] as well as the epitope for our custom-made RIF1 antibody (#2034) (Fig. 6). Of note, no available commercial anti-murine RIF1 antibody performed similarly to #2034 in all the required applications (i.e. western blot, IRIF, coIP). Accordingly, I first generated a cell line expressing a version of RIF1 bearing a NLS followed by a 3xHA-tag at the N-terminus by CRISPR/Cas9-mediated knock-in (Fig. 12A). The decision to include the new peptides at the N-terminus - rather than the C-terminus - of the protein was based on a previously generated mouse model (*Rif1*$^{FH/FH}$) expressing a 1xFLAG-2xHA tag at the amino-terminus of RIF1[159]. B cells isolated from *Rif1*$^{FH/FH}$ mice express physiological levels of the epitope-tagged RIF1, which recapitulates the endogenous RIF1 abilities to accumulate at DSBs and to support CSR[147,159] This was an indication that the introduction of a peptide sequence of similar length at the N-terminal RIF1 would have not affected its levels of expression, recruitment to the damaged chromatin and function in CSR. Surprisingly, despite the integrity of both RIF1 alleles at the regions surrounding the knocked-in sequences and the unaltered ability to undergo CSR of the different clones tested, NLS-3xHA-RIF1 protein levels were almost undetectable (Fig. 13A-B). The same phenomenon was observed in additional knock-in clones in which RIF1 bore only the 3xHA epitope at its N-terminus.

The possible cause underlying the dramatic decrease in protein expression in both knock-in sets was not investigated. Nonetheless, I hypothesized that the addition

of the specific N-terminal tags affected negatively the stability of the protein. The biochemical characteristics of the extra amino acid residues at the N-terminus may have caused problems in protein folding or constituted "*N*-degrons", leading to enhanced protein degradation. *N*-degrons represent modified or unmodified destabilizing N-terminal residues of proteins that, in the so-called "N-end rule pathway", are recognized as degradation signals by specific E3 ubiquitin ligases (*N*-recognin), leading to 26S proteasome-mediated degradation[245,246]. Certain *N*-degrons can be repressed by steric shielding, mediated by protein folding or interaction with other proteins[247]. Unlike NLS-3xHA-RIF1, 3xHA-RIF1 displays a potential type of *N*-degrons (i.e. bulky hydrophobic residues, Fig. S3). Further testing would be required, for example using proteasomal inhibitors. However, considering the absence of an *N*-degron in NLS-3xHA-RIF1, we could exclude that the knocked-in sequences promote RIF1 protein degradation *via* the N-end rule pathway.

Lastly, in spite of the fact that these cell lines could not be further employed for RIF1 structural studies, this unexpected phenomenon gave a first clue regarding the sensitivity of CSR to RIF1 dosage. In reference to this point, a recent study showed that halving RIF1 levels (in *Rif1* hemizygous mESCs) negatively affected chromatin architecture but not replication timing, suggesting that only certain functions of RIF1 are sensitive to its dosage[239].

5.3 Intrinsic disorder and phosphorylation of RIF1 during DSB end protection

ATM is a conserved as well as essential kinase for the DDR signaling[19]. As a consequence, ATM is required for the effective repair of S-region breaks during CSR[248]. Its kinase activity is indirectly required for 53BP1 recruitment to DSBs (*via* the phosphorylation of H2AX and the recruitment of RNF8/168) and directly required for RIF1 accumulation through the interaction with phosphorylated 53BP1[19]. RIF1, similarly to 53BP1, contains ATM phosphorylation consensus motifs, mostly concentrated in three different clusters located in the RIF1 IDR (Fig. 6).

The potential influence of this unstructured region on RIF1 function has not been investigated in the past years, though it represents one of the major structural differences between the yeast and the mammalian orthologs and may justify most of their functional differences. Consistently with this idea, disordered domains may play a role in the evolution of protein functions[181]. Additionally, the interaction of RIF1 mutants with BLM helicase was enhanced by the addition of the entire IDR to the C-terminal domain[154]. This further hints at the possibility that the IDR may contribute to mediate the interactions between RIF1 and other proteins.

In agreement with the first indication that a serine residue in a highly conserved SQ cluster (S^{1525}) was phosphorylated in UV- and IR-treated 293T cells[186], our mass-spec data indicated that all conserved SQ sites of the cluster (S^{1394}, S^{1423}, S^{1535}) were phosphorylated in activated, IR-treated primary B cells (Fig. 15). Despite these indications, the abrogation of ATM-mediated phosphorylation of the conserved SQ cluster, as well as its mimicking, did not affect the levels of IgA-switched CH12 cells (Fig. 17D). Similarly, mutation of the conserved SQ sites did not affect the ability of RIF1 to promote aberrant NHEJ repair leading to genomic instability in PARPi-treated *Brca1*-deficient B cells (Fig. 19C). Therefore, we

conclude that the phosphorylation status of the conserved SQ cluster does not affect RIF1 ability to protect DSB ends.

The unaltered phenotype observed in RIF1 phosphomutants, as compared to the control cell lines, may indicate that the cluster was not phosphorylated in response to cytokine activation or IR treatment. This possibility cannot be ruled out due to the lack of mass spec data from untreated cells. In fact, the dataset used to identify phosphorylated residues was generated from a SILAC-based pull-down of RIF1 interactors (iDIRT)[147]. This experiment was designed to prioritize the specificity of the interactions, rather than their dependency on the IR-treatment or the cytokine stimulation, the latter being a prerequisite for the proliferation and survival of primary B cells[249].

The fact that the DSB end protection function of RIF1 phospho-deficient mutants was not impaired in both wild-type and *Brca1*$^{-/-}$ cells may also suggest that additional phosphorylated SQ/TQ sites in the IDR were sufficient to support the conformation required for RIF1 function, even when the phosphorylation of one cluster is abrogated. Considering the 74% coverage of our analysis (Fig. 15), the additional phosphoresidues may have not been identified.

Lastly, the observation that RIF1 SQ-CII is phosphorylated *in vivo* suggests that this phosphorylation event may be essential for other RIF1 functions than the one promoting B cell isotype switching or genome instability in *Brca1*-deficient background. Considering that the data was obtained from highly proliferating cells, it would be interesting to investigate whether phosphorylation of RIF1 SQ-CII is required for its reported functions in replication timing, at stalled replication forks or at anaphase bridges, which are all dependent on its interaction with PP1[157,161,164,250]. In agreement with the partial requirement of the IDR for the RIF1-BLM interaction[154], the ATM phosphorylation-driven conformation of the IDR may also enhance RIF1 binding to PP1.

In conclusion, additional efforts are needed to understand how phosphorylation affects RIF1 DSB end protection function. Among these efforts, a new proteomic analysis of DNA damage- or CSR-induced RIF1 PTMs may clarify whether other clusters are phosphorylated in a DNA damage- or CSR-dependent manner. This approach would help to determine whether RIF1 phosphoregulation differs between the repair of global damage (induced by IR) and the repair of programmed DSBs at the *IgH* locus (induced by cytokine stimulation). Multi-step phosphorylation regulates a variety of proteins and transduced signals[251-254] and was shown to regulate IDRs[255,256]. For this reason, it will be necessary to obtain full protein coverage in future proteomic studies, to identify the full landscape of RIF1 phosphorylation. Eventually, thanks to the new approach and full coverage, the contribution of other PTMs in DSB repair and CSR may come into focus. Alternatively, stepping away from B cells CSR, light could be shed on the phosphoregulation of RIF1 in the context of replication. Such a study would clarify the regulation of mammalian RIF1 function during replication, an aspect that has been investigated only recently[160,164].

6. Supplementary information

6.1 List of abbreviations

53BP1	p53-binding protein
A	
A-EJ	alternative end joining
AID	activation induced deaminase
ATM	ataxia telangiectasia mutated
B	
BARD1	BRCA1-associated ring domain protein 1
BER	base excision repair
BLM	Bloom syndrome RECQ like helicase
Bp	base pair
BRCA1/BRCA2	breast cancer type 1/2 susceptibility protein
BSA	bovine serum albumin
C	
$Cas9^{D10A}$	nickase Cas9
$Cas9^{D10A}$	Cas9 nickase mutant
CD40L	CD40 ligand
CDK	cyclin-dependent kinase
C_H	immunoglobulin heavy chain constant region
CHFR	checkpoint with forkhead and ring finger domains
CHK	checkpoint kinase 1
CRISPR	clustered regularly interspaced short palindromic repeats
CSR	class-switch recombination
CTC1	conserved telomere maintenance component 1
CTD	bacterial RNA polymerase α subunit
CtIP	CTBP-interacting protein
Ctrl	control
D	
DDK	DBF4-dependent kinase
DDR	DNA damage response
DDT	1,4-dithiothreitol
dHJ	double Holliday junction
DISPHOS	disorder-enhanced phosphorylation site
DMSO	dimethyl sulfoxide
DNA	deoxyribonucleic acid
DNA2	DNA replication helicase/nuclease 2

DNA-PKcs	DNA-dependent protein kinase catalytic subunit
DSB	double-strand break
dsDNA	double-stranded DNA
E	
EDTA	ethylenediaminetetraacetic acid
ERA	end-resection assay
EXO1	exonuclease 1
Eμ	enhancer region
F	
FBS	fetal bovine serum
FH	FLAG-2xHA
G	
G4	G-quadruplex secondary DNA structures
GC	germline transcription
gDNA	genomic DNA
GFP	green fluorescent protein
GLT	germline transcription
gRNA	guide RNA
H	
h	hour(s)
H/H+L	SILAC ratio
H2A.X	H2A histone family member X
HA[1]	homology arm
HA[2]	hemagglutinin
HDR	homology-directed repair
HEAT	Huntingtin, elongation factor 3, protein phosphatase 2A, TOR1)-like repeats domain
HEPES	4-(2-hydroxylethyl)-1-piperazineethanesulfonic acid
HR	homologous recombination
HRP	horseradish peroxidase
HTS	high-throughput samples
I	
I-DIRT	isotopic differentiation of interactions as random or targeted
IDR	intrinsically disordered region
I-exon	intervening exon
Ig	immunoglobulin
IgH	immunoglobulin heavy chain
IgL	immunoglobulin light chain
IL-4	interleukin-4

IR	ionizing radiation
IRIF	ionizing radiation-induced foci
ISD	internal switch deletion
J	
JMJD2	lysine-specific demethylase 4A
K	
KI	knock-in
KO	knock-out
L	
L3MBTL1	lethal(3)malignant brain tumor-like protein 1
LC	liquid chromatography
LIG4	DNA ligase 4
LPS	lipopolysaccharide
M	
MDC1	mediator of DNA damage checkpoint 1
MEF	mouse embryonic fibroblast
min	minute(s)
MMEJ	microhomology-mediated end joining
MMR	mismatch repair
MRE11	meiotic recombination 11 homolog 1
MS/MS	tandem mass spectrometry
N	
NBS1	Nijmegen breakage syndrome 1
NDUFB7	NADH:ubiquinone oxidoreductase subunit b7
NHEJ	non-homologous end joining
NLS	nuclear localization signal
O	
OS	overall survival
P	
PAPRi	PARP inhibitor
PAR	poly-ADP ribose
PARP1	poly(ADP-ribose) polymerase-1
PBS	phosphate-buffered saline
PCR	polymerase-chain reaction
PEP	posterior error probability
PFS	progression-free survival
phomim	*Rif1*$^{S\rightarrow D}$ mutant
phonull	*Rif1*$^{S\rightarrow A}$ mutant
PIAS1/4	protein inhibitor of activated STAT

Pol α-primase	polymerase alpha-primase
PP1	protein phosphatase 1
PPP4C	serine/threonine-protein phosphatase 4 catalytic subunit
PTIP	PAX transcription activation domain interacting protein
PTM	post-translational modification
R	
R	random
RAG1/RAG2	recombination activating genes 1/2
RIF1	Rap1-interacting factor 1
RMPI	Roswell park memorial institute
RNF4/ RNF8/ RNF11/ RNF20/ RNF40/ RNF138/ RNF168	ring finger protein 4/8/11/20/40/138/168
ROS	reactive oxygen species
RPA	replication protein A
RT	room temperature
S	
S → A	serine to alanine mutation
S → D	serine to aspartate
SCAI	suppressor of cancer cell invasion
SD	standard deviation
SDS	sodium dodecyl sulfate
sec	second(s)
SEM	standard error of the mean
SHLD1/ SHLD2/ SHLD3	shieldin complex subunit 1/2/3
SHM	somatic hyper mutation
SILAC	stable isotope labeling by/with amino acids in cell culture
SMARCAD1	SWI/SNF-related matrix-associated actin-dependent regulator of chromatin subfamily a containing DEAD/H box 1
SQ-C	IRF1 SQ site cluster
SSB	single-strand break
ssDNA	single-stranded DNA
STN1	suppressor of CDC thirteen homolog
SV40	Simian virus 40
T	
TEN1	telomere length regulation protein TEN1 homolog
TGFβ	transforming growth factor β
TIP60	histone acetyltransferase KAT5
TIRR	Tudor-interacting repair regulator protein

U	
UDR	ubiquitylation-dependent recruitment
UFB	anaphase ultrafine bridge
UHRF1	ubiquitin like with PHD and RING finger domains 1
UNG	uracil-DNA glycosylase
UV	ultraviolet radiation
V	
V(D)J	variable, diversity and joining genes
W	
WASP	Wiskott-Aldrich syndrome protein
WB	western blot
WT	wild-type
X	
XLF	XRCC4-like factor
XRCC4	x-ray repair cross complementing 4
Z	
ZMYND8	zinc finger MYND-type containing 8
γH2AX	phosphorylated histone H2AX

6.2 Supplemental figures and table

```
wt          GAAGAGCAAATGGAAAGTACTATTTTCATCCATCAAGATGCCCCGGAGAACTGTGGAATA
phonull     GAAGAGCAAATGGAAAGTACTATTTTCATCCATCAAGATGCCCCGGAGAACTGTGGAATA
phomim      GAAGAGCAAATGGAAAGTACTATTTTCATCCATCAAGATGCCCCGGAGAACTGTGGAATA
            ************************************************************

wt          GATGAACATTCTGAGAATGCTTCTTTACCAAATTGTGGTGGCTCTGTTGCTGAAACCAAT
phonull     GATGAACATTCTGAGAATGCTTCTTTACCAAATTGTGGTGGCTCTGTTGCTGAAACCAAT
phomim      GATGAACATTCTGAGAATGCTTCTTTACCAAATTGTGGTGGCTCTGTTGCTGAAACCAAT
            ************************************************************

wt          CCAGAAACATTGATCACTGGTTTTGATGCTAGAAAAGAAGTATTAATTTCATCAAAGATA
phonull     CCAGAAACATTGATCACTGGTTTTGATGCTAGAAAAGAAGTATTAATTTCATCAAAGATA
phomim      CCAGAAACATTGATCACTGGTTTTGATGCTAGAAAAGAAGTATTAATTTCATCAAAGATA
            ************************************************************

wt          TTGTCTGCTGAAAGTTCATCTAGTACAGAAACTTCGGTGGTCAGCAGTAGTTCAGTTTCT
phonull     TTGTCTGCTGAAAGTTCATCTAGTACAGAAACTTCGGTGGTCAGCAGTAGTTCAGTTTCT
phomim      TTGTCTGCTGAAAGTTCATCTAGTACAGAAACTTCGGTGGTCAGCAGTAGTTCAGTTTCT
            ************************************************************

wt          AATGCCACTTTTTCTGGAACTCCTCCACAGCCTACAAGTCGGAGACAAACCTTTATTACT
phonull     AATGCCACTTTTTCTGGAACTCCTCCACAGCCTACAAGTCGGAGACAAACCTTTATTACT
phomim      AATGCCACTTTTTCTGGAACTCCTCCACAGCCTACAAGTCGGAGACAAACCTTTATTACT
            ************************************************************

wt          TTGGAGAAATTTGATGGCTCAGAAACTAGACCTTTTAGTCCATCCCCCTTGAATAACATA
phonull     TTGGAGAAATTTGATGGCTCAGAAACTAGACCTTTTAGTCCATCCCCCTTGAATAACATA
phomim      TTGGAGAAATTTGATGGCTCAGAAACTAGACCTTTTAGTCCATCCCCCTTGAATAACATA
            ************************************************************

wt          TCTTCCACTGTTACAGTGAGAAATAACCAGGATAACACAACTAACACTGACATGCCACCA
phonull     TCTTCCACTGTTACAGTGAGAAATAACCAGGATAACACAACTAACACTGACATGCCACCA
phomim      TCTTCCACTGTTACAGTGAGAAATAACCAGGATAACACAACTAACACTGACATGCCACCA
            ************************************************************

wt          AAAGCAAGGAAAAGAGAAGTGACGAACTCAAAATCTGATTCAGAAAATTTAGCGAATGCA
phonull     AAAGCAAGGAAAAGAGAAGTGACGAACTCAAAATCTGATTCAGAAAATTTAGCGAATGCA
phomim      AAAGCAAGGAAAAGAGAAGTGACGAACTCAAAATCTGATTCAGAAAATTTAGCGAATGCA
            ************************************************************

wt          GGTAAGAAATCAAGTCGGAGATGGAGTAAAGCTGAGCAGTCAGTTACTAAAAAGTCTAAG
phonull     GGTAAGAAATCAAGTCGGAGATGGAGTAAAGCTGAGCAGTCAGTTACTAAAAAGTCTAAG
phomim      GGTAAGAAATCAAGTCGGAGATGGAGTAAAGCTGAGCAGTCAGTTACTAAAAAGTCTAAG
            ************************************************************

wt          CCATCACTGACATCTGAACAGGAAGAGCACTCATCCGAAAATAACTCTCCTGATCTGCTC
phonull     CCATCACTGACATCTGAACAGGAAGAGCACTCATCCGAAAATAACTCTCCTGATCTGCTC
phomim      CCATCACTGACATCTGAACAGGAAGAGCACTCATCCGAAAATAACTCTCCTGATCTGCTC
            ************************************************************

wt          AGCCCAACAGAACATGTGTCAGAAAATGATGATCATCCTTCTGAAGCTACCCTAGAGCAT
phonull     AGCCCAACAGAACATGTGTCAGAAAATGATGATCATCCTTCTGAAGCTACCCTAGAGCAT
phomim      AGCCCAACAGAACATGTGTCAGAAAATGATGATCATCCTTCTGAAGCTACCCTAGAGCAT
            ************************************************************
```

```
wt          AAAGATGGAGATCCTAAACCAGCAGTAGAAAATGCTTCATTGGAAGACTTAACAACAGAA
phonull     AAAGATGGAGATCCTAAACCAGCAGTAGAAAATGCTTCATTGGAAGACTTAACAACAGAA
phomim      AAAGATGGAGATCCTAAACCAGCAGTAGAAAATGCTTCATTGGAAGACTTAACAACAGAA
            ************************************************************

wt          GAGAAAAATGTAGGCATTAATATGGAATCTAAAGAAAGTACAGCCTCAGTTGTAGCACGA
phonull     GAGAAAAATGTAGGCATTAATATGGAATCTAAAGAAAGTACAGCCTCAGTTGTAGCACGA
phomim      GAGAAAAATGTAGGCATTAATATGGAATCTAAAGAAAGTACAGCCTCAGTTGTAGCACGA
            ************************************************************

wt          ACAGAACAAATAGTAAATGAAGATAGTCAGGCTGCTGCACTAGCCCCAAATCCAAAAACA
phonull     ACAGAACAAATAGTAAATGAAGATGCTCAGGCTGCTGCGCTAGCCCCAAATCCAAAAACA
phomim      ACAGAACAAATAGTAAATGAAGATGATCAGGCTGCTGCGCTAGCCCCAAATCCAAAAACA
            ************************  ************ ********************

wt          CTCCGACGGTCTTCGAGGCGGCGTTCAGAAGCTGTAGATTCTTGCAGTGACAGCCAAGAG
phonull     CTCCGTCGGAGTTCTCGCCGGCGTTCAGAAGCTGTAGATTCTTGCAGTGACGCCCAAGAG
phomim      CTCCGTCGGAGTTCTCGCCGGCGTTCAGAAGCTGTAGATTCTTGCAGTGACGACCAAGAG
            ***** ***   ***   * ********************************   *******

wt          AGAGAGAGTGGTCAGCAAAAAAAGGAAAGACGAAAGGAAGAAGAAAAAATAATCTCCAAG
phonull     AGAGAGAGTGGTCAGCAAAAAAAGGAAAGACGAAAGGAAGAAGAAAAAATAATCTCCAAG
phomim      AGAGAGAGTGGTCAGCAAAAAAAGGAAAGACGAAAGGAAGAAGAAAAAATAATCTCCAAG
            ************************************************************

wt          AGTCCGTTGCGTATCAAAGATGATAAGTTGCCCACGCAAAAACTAACTGATGAGTCACCT
phonull     AGTCCGTTGCGTATCAAAGATGATAAGTTGCCCACGCAAAAACTAACTGATGAGTCACCT
phomim      AGTCCGTTGCGTATCAAAGATGATAAGTTGCCCACGCAAAAACTAACTGATGAGTCACCT
            ************************************************************

wt          ATACAGGAAAATTTAACTGAAAAGGGAAATACTTTACCTGAGAGAACTTCAGGGGAACCC
phonull     ATACAGGAAAATTTAACTGAAAAGGGAAATACTTTACCTGAGAGAACTTCAGGGGAACCC
phomim      ATACAGGAAAATTTAACTGAAAAGGGAAATACTTTACCTGAGAGAACTTCAGGGGAACCC
            ************************************************************

wt          AGTGTTAATGCTGAAATTGACCAAAATAGAAGAAAACCAGACCTTGAGAATGTTAGTTCT
phonull     AGTGTTAATGCTGAAATTGACCAAAATAGAAGAAAACCAGACCTTGAGAATGTTAGTTCT
phomim      AGTGTTAATGCTGAAATTGACCAAAATAGAAGAAAACCAGACCTTGAGAATGTTAGTTCT
            ************************************************************

wt          GAAGGAGGTGGTGGTACCCTGGACAATCTAGACAAGTCGTCTGAGAAACCTTTAAGAGGA
phonull     GAAGGAGGTGGTGGTACACTTGATAACTTAGACAAGTCGTCTGAGAAACCTTTAAGAGGA
phomim      GAAGGAGGTGGTGGTACACTTGATAACTTAGACAAGTCGTCTGAGAAACCTTTAAGAGGA
            ***************** ** ** **  ********************************


wt          CGGACACGTTATCAAACAAGAAGAGCTTCGCAGGGTTTGATTTCTGCTGTTGAAAACTCA
phonull     CGGACACGTTATCAAACAAGAAGAGCTGCGCAGGGTTTGATTTCTGCTGTTGAAAACTCA
phomim      CGGACACGTTATCAAACAAGAAGAGCTGATCAGGGTTTGATTTCTGCTGTTGAAAACTCA
            ***************************   ******************************

wt          GAATCTGACAGTTCTGAGGCAAAGGAAGAAGTTTCTAGAAAGAAACGATCAGGGAAATGG
phonull     GAATCTGACAGTTCTGAGGCAAAGGAAGAAGTTTCTAGAAAGAAACGATCAGGGAAATGG
phomim      GAATCTGACAGTTCTGAGGCAAAGGAAGAAGTTTCTAGAAAGAAACGATCAGGGAAATGG
            ************************************************************

wt          AAAAATAGAAGCAGTGACAGTGTTGACATTGAAGAACAAGAAGAAAAAAAGGCTGAAGAG
phonull     AAAAATAGAAGCAGTGACAGTGTTGACATTGAAGAACAAGAAGAAAAAAAGGCTGAAGAG
phomim      AAAAATAGAAGCAGTGACAGTGTTGACATTGAAGAACAAGAAGAAAAAAAGGCTGAAGAG
            ************************************************************
```

```
wt          GAAGTTATGAAAACTGCAAATCAGACACTCGATGGCCAGGCAGTTCCTGATGTTGATGTA
phonull     GAAGTTATGAAAACTGCAAATCAGACACTCGATGGCCAGGCAGTTCCTGATGTTGATGTA
phomim      GAAGTTATGAAAACTGCAAATCAGACACTCGATGGCCAGGCAGTTCCTGATGTTGATGTA
            ************************************************************

wt          AATGCAGCGGCTCAGGTTTGTGAAAAAAGTACAAATAACAACAGGGTCATCCTCCAGGAT
phonull     AATGCAGCGGCTCAGGTTTGTGAAAAAAGTACAAATAACAACAGGGTCATCCTCCAGGAT
phomim      AATGCAGCGGCTCAGGTTTGTGAAAAAAGTACAAATAACAACAGGGTCATCCTCCAGGAT
            ************************************************************

wt          TCTGCTGGGCCTGCAGATTCACTGCAAGCTCCACCCAAAGGCGAGGAGAAAAGTAAGATT
phonull     TCTGCTGGGCCTGCAGATTCACTGCAAGCTCCACCCAAAGGCGAGGAGAAAAGTAAGATT
phomim      TCTGCTGGGCCTGCAGATTCACTGCAAGCTCCACCCAAAGGCGAGGAGAAAAGTAAGATT
            ************************************************************

wt          AACAAATGTGTAGACAGTTCATTTGTAAGTCTACCTGTGCCAGAGTCAAACCTCAGGACT
phonull     AACAAATGTGTAGACAGTTCATTTGTAAGTCTACCTGTGCCAGAGTCAAACCTCAGGACT
phomim      AACAAATGTGTAGACAGTTCATTTGTAAGTCTACCTGTGCCAGAGTCAAACCTCAGGACT
            ************************************************************

wt          AGGAATGCCAGTAAGAGATTATTATATAAACAAGATAATGATAGTAATGTGAGGGTATCA
phonull     AGGAATGCCAGTAAGAGATTATTATATAAACAAGATAATGATAGTAATGTGAGGGTATCA
phomim      AGGAATGCCAGTAAGAGATTATTATATAAACAAGATAATGATAGTAATGTGAGGGTATCA
            ************************************************************

wt          GACAGCTCTCTGTCTCCCGAAAAATTCACCCAAGTTGAATGCCAACACAAGAGAAGTAGG
phonull     GACAGCTCTCTGTCTCCCGAAAAATTCACCCAAGTTGAATGCCAACACAAGAGAAGTAGG
phomim      GACAGCTCTCTGTCTCCCGAAAAATTCACCCAAGTTGAATGCCAACACAAGAGAAGTAGG
            ************************************************************

wt          AGAGTCAGGAGATCTAAAAGTTGTGACTGCTGTGGCGAAAAATCACAGTCCCAGGAAAAG
phonull     AGAGTCAGGAGATCTAAAAGTTGTGACTGCTGTGGCGAAAAATCACAGTCCCAGGAAAAG
phomim      AGAGTCAGGAGATCTAAAAGTTGTGACTGCTGTGGCGAAAAATCACAGTCCCAGGAAAAG
            ************************************************************

wt          TCATTTATTGGGTTAAAGAACACAGAAAGTTATGCTATAAAGAGTGTGGAGAAAAAAAAG
phonull     TCATTTATTGGGTTAAAGAACACAGAAAGTTATGCTATAAAGAGTGTGGAGAAAAAAAAG
phomim      TCATTTATTGGGTTAAAGAACACAGAAAGTTATGCTATAAAGAGTGTGGAGAAAAAAAAG
            ************************************************************

wt          ACAGATCTACAAGTACCTGAGACTGCCCCTGAAACTCGTGAAGCTCGTGACCATGCTGAA
phonull     ACAGATCTACAAGTACCTGAGACTGCCCCTGAAACTCGTGAAGCTCGTGACCATGCTGAA
phomim      ACAGATCTACAAGTACCTGAGACTGCCCCTGAAACTCGTGAAGCTCGTGACCATGCTGAA
            ************************************************************


wt          ACAAAGTTGGCAGGCGAAGAGCCTCTTGTGAATTTTCATGTGGGTCTTAAAGAAGAGAAT
phonull     ACAAAGTTGGCAGGCGAAGAGCCTCTTGTGAATTTTCATGTGGGTCTTAAAGAAGAGAAT
phomim      ACAAAGTTGGCAGGCGAAGAGCCTCTTGTGAATTTTCATGTGGGTCTTAAAGAAGAGAAT
            ************************************************************

wt          TGTACTACTGGTGATTCAGTTAAGTCTGAGGCTGAGTTGCAAGAAGCTTCCCTTCCACCT
phonull     TGTACTACTGGTGATTCAGTTAAGTCTGAGGCTGAGTTGCAAGAAGCTTCCCTTCCACCT
phomim      TGTACTACTGGTGATTCAGTTAAGTCTGAGGCTGAGTTGCAAGAAGCTTCCCTTCCACCT
            ************************************************************

wt          GAAATAGTAACTGTGAAAGAGAAGACTTACGATACAGACGCTAGTGAAGCAGTGTCTGAA
phonull     GAAATAGTAACTGTGAAAGAGAAGACTTACGATACAGACGCTAGTGAAGCAGTGTCTGAA
phomim      GAAATAGTAACTGTGAAAGAGAAGACTTACGATACAGACGCTAGTGAAGCAGTGTCTGAA
            ************************************************************
```

```
wt          ATCCAAGGGCCATGTAGTGAGAACCACAGCCCTGCTGAGGACCCAGGCTTAAGTGAGTGC
phonull     ATCCAAGGGCCATGTAGTGAGAACCACAGCCCTGCTGAGGACCCAGGCTTAAGTGAGTGC
phomim      ATCCAAGGGCCATGTAGTGAGAACCACAGCCCTGCTGAGGACCCAGGCTTAAGTGAGTGC
            ************************************************************

wt          AAAGACATTTCACAGAAGCAGCTTTCAGAGAACGGAGAGCTTGACATCAGCGATGTAGGG
phonull     AAAGACATTTCACAGAAGCAGCTTTCAGAGAACGGAGAGCTTGACATCAGCGATGTAGGG
phomim      AAAGACATTTCACAGAAGCAGCTTTCAGAGAACGGAGAGCTTGACATCAGCGATGTAGGG
            ************************************************************

wt          AAGGCATGCAA
phonull     AAGGCATGCAA
phomim      AAGGCATGCAA
            ***********
```

Figure S1: Multiple nucleotide sequence alignment (Clustal Ω) of sequenced alleles from *Rif1*$^{S \rightarrow A}$ (phonull) and *Rif1*$^{S \rightarrow D}$ (phomim) CH12 clones. The represented region spans from nt 3376 to nt 5606 of *Rif1* CDS (Ref. gene: ENSMUSG00000036202) Wild-type CH12 genome (wt) was used as a reference. S → A / S → D nonsynonymous mutations are indicated in green; silent mutations for the introduction of the NheI site, protospacer disruption and PAM sequence disruption are indicated in yellow, grey and turquoise, respectively. Reference genome for ENSMUSG00000036202: GRCm38:CM000995.2.

```
wt          EEQMESTIFIHQDAPENCGIDEHSENASLPNCGGSVAETNPETLITGFDARKEVLISSKI
phonull     EEQMESTIFIHQDAPENCGIDEHSENASLPNCGGSVAETNPETLITGFDARKEVLISSKI
phomim      EEQMESTIFIHQDAPENCGIDEHSENASLPNCGGSVAETNPETLITGFDARKEVLISSKI
            ************************************************************

wt          LSAESSSSTETSVVSSSSVSNATFSGTPPQPTSRRQTFITLEKFDGSETRPFSPSPLNNI
phonull     LSAESSSSTETSVVSSSSVSNATFSGTPPQPTSRRQTFITLEKFDGSETRPFSPSPLNNI
phomim      LSAESSSSTETSVVSSSSVSNATFSGTPPQPTSRRQTFITLEKFDGSETRPFSPSPLNNI
            ************************************************************

wt          SSTVTVRNNQDNTTNTDMPPKARKREVTNSKSDSENLANAGKKSSRRWSKAEQSVTKKSK
phonull     SSTVTVRNNQDNTTNTDMPPKARKREVTNSKSDSENLANAGKKSSRRWSKAEQSVTKKSK
phomim      SSTVTVRNNQDNTTNTDMPPKARKREVTNSKSDSENLANAGKKSSRRWSKAEQSVTKKSK
            ************************************************************

wt          PSLTSEQEEHSSENNSPDLLSPTEHVSENDDHPSEATLEHKDGDPKPAVENASLEDLTTE
phonull     PSLTSEQEEHSSENNSPDLLSPTEHVSENDDHPSEATLEHKDGDPKPAVENASLEDLTTE
phomim      PSLTSEQEEHSSENNSPDLLSPTEHVSENDDHPSEATLEHKDGDPKPAVENASLEDLTTE
            ************************************************************

wt          EKNVGINMESKESTASVVARTEQIVNEDSQAAALAPNPKTLRRSSRRRSEAVDSCSDSQE
phonull     EKNVGINMESKESTASVVARTEQIVNEDAQAAALAPNPKTLRRSSRRRSEAVDSCSDAQE
phomim      EKNVGINMESKESTASVVARTEQIVNEDDQAAALAPNPKTLRRSSRRRSEAVDSCSDDQE
            *************************** *************************** **

wt          RESGQQKKERRKEEEKIISKSPLRIKDDKLPTQKLTDESPIQENLTEKGNTLPERTSGEP
phonull     RESGQQKKERRKEEEKIISKSPLRIKDDKLPTQKLTDESPIQENLTEKGNTLPERTSGEP
phomim      RESGQQKKERRKEEEKIISKSPLRIKDDKLPTQKLTDESPIQENLTEKGNTLPERTSGEP
            ************************************************************

wt          SVNAEIDQNRRKPDLENVSSEGGGGTLDNLDKSSEKPLRGRTRYQTRRASQGLISAVENS
phonull     SVNAEIDQNRRKPDLENVSSEGGGGTLDNLDKSSEKPLRGRTRYQTRRAAQGLISAVENS
phomim      SVNAEIDQNRRKPDLENVSSEGGGGTLDNLDKSSEKPLRGRTRYQTRRADQGLISAVENS
            ********************************************** **********
```

```
wt          ESDSSEAKEEVSRKKRSGKWKNRSSDSVDIEEQEEKKAEEEVMKTANQTLDGQAVPDVDV
phonull     ESDSSEAKEEVSRKKRSGKWKNRSSDSVDIEEQEEKKAEEEVMKTANQTLDGQAVPDVDV
phomim      ESDSSEAKEEVSRKKRSGKWKNRSSDSVDIEEQEEKKAEEEVMKTANQTLDGQAVPDVDV
            ************************************************************

wt          NAAAQVCEKSTNNNRVILQDSAGPADSLQAPPKGEEKSKINKCVDSSFVSLPVPESNLRT
phonull     NAAAQVCEKSTNNNRVILQDSAGPADSLQAPPKGEEKSKINKCVDSSFVSLPVPESNLRT
phomim      NAAAQVCEKSTNNNRVILQDSAGPADSLQAPPKGEEKSKINKCVDSSFVSLPVPESNLRT
            ************************************************************

wt          RNASKRLLYKQDNDSNVRVSDSSLSPEKFTQVECQHKRSRRVRRSKSCDCCGEKSQSQEK
phonull     RNASKRLLYKQDNDSNVRVSDSSLSPEKFTQVECQHKRSRRVRRSKSCDCCGEKSQSQEK
phomim      RNASKRLLYKQDNDSNVRVSDSSLSPEKFTQVECQHKRSRRVRRSKSCDCCGEKSQSQEK
            ************************************************************

wt          SFIGLKNTESYAIKSVEKKKTDLQVPETAPETREARDHAETKLAGEEPLVNFHVGLKEEN
phonull     SFIGLKNTESYAIKSVEKKKTDLQVPETAPETREARDHAETKLAGEEPLVNFHVGLKEEN
phomim      SFIGLKNTESYAIKSVEKKKTDLQVPETAPETREARDHAETKLAGEEPLVNFHVGLKEEN
            ************************************************************

wt          CTTGDSVKSEAELQEASLPPEIVTVKEKTYDTDASEAVSEIQGPCSENHSPAEDPGLSEC
phonull     CTTGDSVKSEAELQEASLPPEIVTVKEKTYDTDASEAVSEIQGPCSENHSPAEDPGLSEC
phomim      CTTGDSVKSEAELQEASLPPEIVTVKEKTYDTDASEAVSEIQGPCSENHSPAEDPGLSEC
            ************************************************************

wt          KDISQKQLSENGELDISDVGKACKVIAGSSPEGVETMELNVRNDAFVAADSEKSTQMDVS
phonull     KDISQKQLSENGELDISDVGKAC--------------------------------------
phomim      KDISQKQLSENGELDISDVGKAC--------------------------------------
            ***********************
```

Figure S2: Multiple protein sequence alignment (Clustal Ω) of translated nucleotide sequences from Fig. S1 (ExPASy translate tool). Wild-type RIF1 protein sequence was used as reference (accession: NP_780447 XP_283721). S → A / S → D nonsynonymous mutations are indicated in green; silent mutations for the introduction of the NheI site, protospacer disruption and PAM sequence disruption are indicated in yellow, grey and turquoise, respectively.

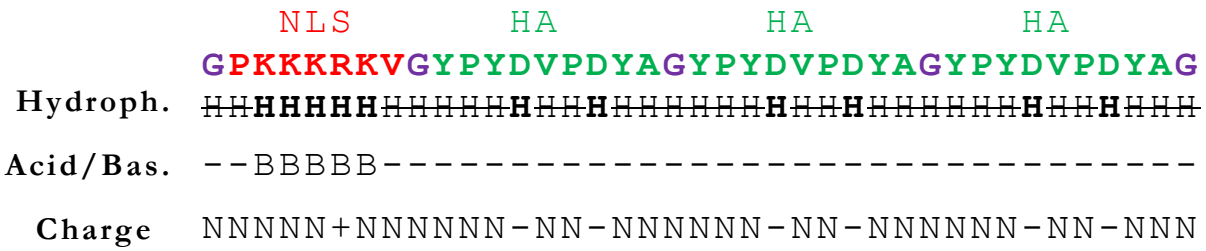

Figure S3: Biochemical characteristics of the amino acids composing the NLS-3xHA peptides knocked-in at RIF1 N-terminus. ~~H~~ (struck through H): hydrophobic residues. B: basic amino acid; N: neutral amino acid. Glycine linkers are indicated in purple.

gRNA	Protospacer sequence
CD36 #1	TCAATAAGCATGTCTCCGAC (-)
CD36 #2	CGGAACTGTGGGCTCATTGC (+)
CD36 #3	CTGTTCTTTGCCACGTCATC (-)
MGA #1	AGGAATAGCTCCGATCAAGA (+)
MGA #2	GTAAGACGAACACGATGAGC (-)
MGA #3	ACCACGCCGACGCCGCTCAT (-)
LYD #1	CACGTGACATCGAAGTGCCC (-)
LYD #2	TGACCAGCCTCTCGTTGCAT (+)
LYD #3	CCATGTCAGCAGTGGTTCCG (+)
BACH2 #1	CTGTGACGTGACGCTGATCG (+)
BACH2 #2	TCCGTTGGTCATTGAGGCCC (-)
BACH2 #3	ACCAATTCCAGTGACGAGTC (+)
PLD4 #1	CATGATCCACATAGCGGACT (+)
PLD4 #2	TCATGGGCACTTGTCGTATC (-)
PLD4 #3	CGTGCTGGACAATGCGCTAC (+)
EIF5 #1	ACGTTGCAAAGGCGCTTAAT (+)
EIF5 #2	GTATGATGCCGACCTGTTAG (+)
EIF5 #3	GACCTCCTCCTCTAACAGGT (-)
CHMP5 #1	TGACAAAAAGATTTCCCGGC (+)
CHMP5 #2	TGAGCAACAGCGAGACAACC (+)
CHMP5 #3	TCCGCTCCTGCAATTCCGGA (+)
RNF31 #1	GCCCGCAGCGGCCCCGGTAT (+)
RNF31 #2	GTCTCGGGTTCGGTTGCACA (-)
RNF31 #3	TGGGCACGAGACTTGGTTAC (-)
ANHAK #1	AACTCCCCTGCGGCCCGCAC (+)
ANHAK #2	ACCACCCCAGTGCGGGCCGC (-)
ANHAK #3	CTGGGCAATGGTCAGCCCGT (-)
TIMELESS #1	CCACAAGGAGCCGGATTGCC (+)
TIMELESS #2	CTAGCCACGTGTAGCGCCCT (+)
TIMELESS #3	AGGATTTGATCCGATACCTG (+)
POLE #1	ACTTACGGTTTGGTTTCGAA (+)
POLE #2	GTGATATCCCCTGCCGGTTT (+)
POLE #3	GATGCTGAGACCTACGTCGG (+)
TLK2 #1	CAGTTAGCGCCACGGGGAGC (+)
TLK2 #2	TAAAGTGGCCTAATCGCAAT (+)
TLK2 #3	TAAAGTGGCCTAATCGCAAT (-)
NAA50 #1	CTTGCACCTTACCGAAGACT (-)
NAA50 #2	CTAGTCTTCGGTAAGGTGCA (+)
NAA50 #3	ATTCTACAAGGATGTGCTAG (-)
RNF2 #1	GTGTTTACATCGGTTTTGCG (+)
RNF2 #2	AGTGCATCAAAGTTCGGGTC (-)
RNF2 #3	TGATGAGTATGAAGCGCATC (+)
TEX10 #1	AATGTGTTCAGTTCGTATTT (+)
TEX10 #2	TGAGAAGTGACTCTCCGATT (+)
TEX10 #3	TGAGAAGTGACTCTCCGATT (+)
LAS1L #1	TGGATCGCGTGTGGCGTGCG (+)
LAS1L #2	CCAAGAGACGACGATACCCC (-)
LAS1L #3	CGCTGAACCGAATTACAGTA (+)
PYHIN1 #1	ATACTGCTGGACGGTCTTTT (-)
PYHIN1 #2	AAGACCGTCCAGCAGTATTC (+)
PYHIN1 #3	CTAGAGGAACTCCTAGTGCC (-)
CD55 # 1	CGAAAACAACCTCCACTCCC (+)
CD55 # 2	TCAAGGCAAGTTGCTTTTCC (-)
CD55 # 3	CACAGGAAATACTGTTGATT (+)
SPCS2 #1	TCCCACTTATCAATTTTTAC (-)
SPCS2 #2	GCCAAAACTGGCTTGGACTC (-)
SPCS2 #3	GAATGGATCCTGATGATATT (+)
CPM #1	CCCCATGGAGATTCGCAGAG (-)
CPM #2	GTGCTGTAAATATCCTCGCG (+)
CPM #3	TCCACGATTACATTCGGTAA (-)
COXB5 #1	TAGCCTGCTCCTCATCAGTG (-)
COXB5 #2	TGTCCCCACTGATGAGGAGC (+)
COXB5 #3	GTGCCTGAAGCTGCCTTTGG (-)
MS4A4A #1	TATATGTGAATTCGCATTCA (+)
MS4A4A #2	ATAATTGCCACTGTGTCGAC (+)
MS4A4A #3	GCTGATTACGATCCCCGAGA (-)
PDLIM2 #1	TGGGGCTTCCGAATTAGCGG (+)
PDLIM2 #2	AGAGAACATGCTACACGCGG (+)
PDLIM2 #3	GCCTTGGGGCGGCCCGTCCC (-)

EXOSC8 #1	TGGAGCCGCTGGAGTATTAC (+)
EXOSC8 #2	AAGGAAAACTGCCGTCCTGA (+)
EXOSC8 #3	AGCGGTGGTAGATCCACATT (-)
SYK #1	AATTGCGGCTCTGGCGTAGC (-)
SYK #2	TACTCCCGGGGGCCGGTTGA (-)
SYK #3	CCGGCCCAAAGAGGTCTACC (+)
GBAS #1	CGGGTGTTGCTCGCGCGAGG (+)
GBAS #2	TTGTCAGAAAGGTCGATCCA (+)
GBAS #3	GCTTGTGCCAGGCCGCGTTC (-)
PSMD4 #1	AGCAACCCTGAGAATAACGT (+)
PSMD4 #2	CTTCTGCACTGGCATCCGCG (+)
PSMD4 #3	AGCAGGAGTTTGGCCGTCCT (+)
IFIH1 #1	TTGACATAGCGCGCGGCTAG (-)
IFIH1 #2	TGCCGCGCTGGTGTTACCAC (-)
IFIH1 #3	CAGAGAAGTGTTATTAACGA (-)
DPP4 #1	AACTATTGGCACGGTGATGA (-)
DPP4 #2	TAGTACTCCCACCGTGACAC (-)
DPP4 #3	CTGCCGTTCCATGAATAAGG (-)
APRT #1	CGCGCCACCAGTTTCAACTC (-)
APRT #2	GTCGATCTTGCCGCTGTGCG (-)
APRT #3	CTGTGTGCTCATCCGGAAAC (+)
ARPC1A #1	GACGAAAGCGCACGAGCTGA (+)
ARPC1A #2	CAGACCGCAACGCCTATGTC (+)
ARPC1A #3	TGGCTGCACGGTTAATCCTC (-)
SLC2A1 #1	GGTGACGGGCCGCCTCATGT (+)
SLC2A1 #2	GGATGGGCTCTCCGTAGCGG (-)
SLC2A1 #3	GTTGACGATACCGGAGCCGA (-)
TCEB1 #1	AGGGCCTTCACAGCCACCAT (-)
TCEB1 #2	GGAGAGGAGAAGACCTATGG (+)
TCEB1 #3	ACAATAAAGGCTATGTTGAG (+)
NDUFB7 #1	CCCGCCGGACCTCGGCTTTC (+)
NDUFB7 #2	CCCACAGATAGCGCCGGGTC (-)
NDUFB7 #3	CAAGCACGAGCAGCACGACT (+)
IGLV2 #1	AGAGAGTATAAGTGAAGTCC (-)
IGLV2 #2	GTGAGTATGACTGTTCCACC (-)
IGLV2 #3	AACACCTGGAGCTCGGTTGC (-)
PAG #1	GTGGGGAAGTCTGGCTGCCG (+)
PAG #2	TGGTCCCCGCTATGCTGCCG (-)
PAG #3	GATCCCGCCTGAGAACGCCG (+)
ZRANB2 #1	TCCGAGTCAGTGACGGGGAC (+)
ZRANB2 #2	CATTGGCACTAAATAAGCCC (-)
ZRANB2 #3	TGGCCCTGCATCTATATTAA (+)
BMP2K #1	GTTCGCCGTCGGCCGCTACC (+)
BMP2K #2	TCCCACTGTGAGTCCGCACC (-)
BMP2K #3	CAAAAATATTGTCGGTTATT (+)
GBP3 #1	ATTGTTGGTTTATATCGTAC (+)
GBP3 #2	AATCCGAAACCAAGGGTATC (+)
GBP3 #3	CATGAGCACCATCAACCAGC (+)
EIF2B5 #1	CGAACAACGTTGGGGGACGT (+)
EIF2B5 #2	ACTCGAGATGATTTTGTACG (+)
EIF2B5 #3	AAAGCGTGCAGCTGACCACT (+)
CISD1 #1	GCACAGCGGAGTTGGAGCTG (-)
CISD1 #2	GGTGCATGCCTTCGACATGG (+)
CISD1 #3	GAAGAGACTGGCGACAACGT (+)

Table S1: List of gRNAs designed for the somatic targeting of each RIF1 interactor candidate.

7. Bibliography

1. Watson JD, Crick FH. The structure of DNA. *Cold Spring Harb Symp Quant Biol.* 1953;18:123-131.
2. Lindahl T, Nyberg B. Rate of depurination of native deoxyribonucleic acid. *Biochemistry.* 1972;11(19):3610-3618.
3. Lindahl T. Instability and decay of the primary structure of DNA. *Nature.* 1993;362(6422):709-715.
4. Lindahl T, Barnes DE. Repair of endogenous DNA damage. *Cold Spring Harb Symp Quant Biol.* 2000;65:127-133.
5. Jackson SP, Bartek J. The DNA-damage response in human biology and disease. *Nature.* 2009;461(7267):1071-1078.
6. Friedberg EC. A brief history of the DNA repair field. *Cell Res.* 2008;18(1):3-7.
7. Milligan JR, Ng JY, Wu CC, Aguilera JA, Fahey RC, Ward JF. DNA repair by thiols in air shows two radicals make a double-strand break. *Radiat Res.* 1995;143(3):273-280.
8. Her J, Bunting SF. How cells ensure correct repair of DNA double-strand breaks. *The Journal of biological chemistry.* 2018;293(27):10502-10511.
9. Ling AK, So CC, Le MX, Chen AY, Hung L, Martin A. Double-stranded DNA break polarity skews repair pathway choice during intrachromosomal and interchromosomal recombination. *Proceedings of the National Academy of Sciences of the United States of America.* 2018;115(11):2800-2805.
10. Kakarougkas A, Ismail A, Klement K, et al. Opposing roles for 53BP1 during homologous recombination. *Nucleic acids research.* 2013;41(21):9719-9731.
11. Papamichos-Chronakis M, Peterson CL. Chromatin and the genome integrity network. *Nat Rev Genet.* 2013;14(1):62-75.
12. Yang G, Liu C, Chen SH, et al. Super-resolution imaging identifies PARP1 and the Ku complex acting as DNA double-strand break sensors. *Nucleic acids research.* 2018;46(7):3446-3457.
13. Caron MC, Sharma AK, O'Sullivan J, et al. Poly(ADP-ribose) polymerase-1 antagonizes DNA resection at double-strand breaks. *Nature communications.* 2019;10(1):2954.
14. Jungmichel S, Rosenthal F, Altmeyer M, Lukas J, Hottiger MO, Nielsen ML. Proteome-wide identification of poly(ADP-Ribosyl)ation targets in different genotoxic stress responses. *Molecular cell.* 2013;52(2):272-285.
15. Gibson BA, Zhang Y, Jiang H, et al. Chemical genetic discovery of PARP targets reveals a role for PARP-1 in transcription elongation. *Science.* 2016;353(6294):45-50.
16. Langelier MF, Planck JL, Roy S, Pascal JM. Crystal structures of poly(ADP-ribose) polymerase-1 (PARP-1) zinc fingers bound to DNA: structural and functional insights into DNA-dependent PARP-1 activity. *The Journal of biological chemistry.* 2011;286(12):10690-10701.
17. Strickfaden H, McDonald D, Kruhlak MJ, et al. Poly(ADP-ribosyl)ation-dependent Transient Chromatin Decondensation and Histone Displacement following Laser Microirradiation. *The Journal of biological chemistry.* 2016;291(4):1789-1802.
18. Haince JF, McDonald D, Rodrigue A, et al. PARP1-dependent kinetics of recruitment of MRE11 and NBS1 proteins to multiple DNA damage sites. *The Journal of biological chemistry.* 2008;283(2):1197-1208.
19. Blackford AN, Jackson SP. ATM, ATR, and DNA-PK: The Trinity at the Heart of the DNA Damage Response. *Molecular cell.* 2017;66(6):801-817.

20. Rogakou EP, Pilch DR, Orr AH, Ivanova VS, Bonner WM. DNA double-stranded breaks induce histone H2AX phosphorylation on serine 139. *The Journal of biological chemistry.* 1998;273(10):5858-5868.
21. Falck J, Coates J, Jackson SP. Conserved modes of recruitment of ATM, ATR and DNA-PKcs to sites of DNA damage. *Nature.* 2005;434(7033):605-611.
22. Sun J, Lee KJ, Davis AJ, Chen DJ. Human Ku70/80 protein blocks exonuclease 1-mediated DNA resection in the presence of human Mre11 or Mre11/Rad50 protein complex. *The Journal of biological chemistry.* 2012;287(7):4936-4945.
23. Branzei D, Foiani M. Regulation of DNA repair throughout the cell cycle. *Nature reviews Molecular cell biology.* 2008;9(4):297-308.
24. Britton S, Coates J, Jackson SP. A new method for high-resolution imaging of Ku foci to decipher mechanisms of DNA double-strand break repair. *The Journal of cell biology.* 2013;202(3):579-595.
25. Panier S, Durocher D. Push back to respond better: regulatory inhibition of the DNA double-strand break response. *Nature reviews Molecular cell biology.* 2013;14(10):661-672.
26. Blier PR, Griffith AJ, Craft J, Hardin JA. Binding of Ku protein to DNA. Measurement of affinity for ends and demonstration of binding to nicks. *The Journal of biological chemistry.* 1993;268(10):7594-7601.
27. Mimori T, Hardin JA. Mechanism of interaction between Ku protein and DNA. *The Journal of biological chemistry.* 1986;261(22):10375-10379.
28. Myler LR, Gallardo IF, Soniat MM, et al. Single-Molecule Imaging Reveals How Mre11-Rad50-Nbs1 Initiates DNA Break Repair. *Molecular cell.* 2017;67(5):891-898 e894.
29. Symington LS, Gautier J. Double-strand break end resection and repair pathway choice. *Annu Rev Genet.* 2011;45:247-271.
30. Pannunzio NR, Watanabe G, Lieber MR. Nonhomologous DNA end-joining for repair of DNA double-strand breaks. *The Journal of biological chemistry.* 2018;293(27):10512-10523.
31. Betermier M, Bertrand P, Lopez BS. Is non-homologous end-joining really an inherently error-prone process? *PLoS Genet.* 2014;10(1):e1004086.
32. Chang HH, Watanabe G, Gerodimos CA, et al. Different DNA End Configurations Dictate Which NHEJ Components Are Most Important for Joining Efficiency. *The Journal of biological chemistry.* 2016;291(47):24377-24389.
33. Casellas R, Nussenzweig A, Wuerffel R, et al. Ku80 is required for immunoglobulin isotype switching. *The EMBO journal.* 1998;17(8):2404-2411.
34. Soulas-Sprauel P, Le Guyader G, Rivera-Munoz P, et al. Role for DNA repair factor XRCC4 in immunoglobulin class switch recombination. *The Journal of experimental medicine.* 2007;204(7):1717-1727.
35. Nussenzweig A, Chen C, da Costa Soares V, et al. Requirement for Ku80 in growth and immunoglobulin V(D)J recombination. *Nature.* 1996;382(6591):551-555.
36. Grawunder U, Zimmer D, Fugmann S, Schwarz K, Lieber MR. DNA ligase IV is essential for V(D)J recombination and DNA double-strand break repair in human precursor lymphocytes. *Molecular cell.* 1998;2(4):477-484.
37. Ma Y, Pannicke U, Schwarz K, Lieber MR. Hairpin opening and overhang processing by an Artemis/DNA-dependent protein kinase complex in nonhomologous end joining and V(D)J recombination. *Cell.* 2002;108(6):781-794.
38. Gottlieb TM, Jackson SP. The DNA-dependent protein kinase: requirement for DNA ends and association with Ku antigen. *Cell.* 1993;72(1):131-142.
39. Nick McElhinny SA, Snowden CM, McCarville J, Ramsden DA. Ku recruits the XRCC4-ligase IV complex to DNA ends. *Molecular and cellular biology.* 2000;20(9):2996-3003.

40. Ahnesorg P, Smith P, Jackson SP. XLF interacts with the XRCC4-DNA ligase IV complex to promote DNA nonhomologous end-joining. *Cell.* 2006;124(2):301-313.
41. Graham TG, Walter JC, Loparo JJ. Two-Stage Synapsis of DNA Ends during Non-homologous End Joining. *Molecular cell.* 2016;61(6):850-858.
42. Lobrich M, Jeggo P. A Process of Resection-Dependent Nonhomologous End Joining Involving the Goddess Artemis. *Trends Biochem Sci.* 2017;42(9):690-701.
43. Chang HH, Watanabe G, Lieber MR. Unifying the DNA end-processing roles of the artemis nuclease: Ku-dependent artemis resection at blunt DNA ends. *The Journal of biological chemistry.* 2015;290(40):24036-24050.
44. Scully R, Panday A, Elango R, Willis NA. DNA double-strand break repair-pathway choice in somatic mammalian cells. *Nature reviews Molecular cell biology.* 2019;20(11):698-714.
45. Lovett ST. Between sisters: Watching replication-associated recombinational DNA repair. *The Journal of cell biology.* 2018;217(7):2225-2227.
46. Karanam K, Kafri R, Loewer A, Lahav G. Quantitative live cell imaging reveals a gradual shift between DNA repair mechanisms and a maximal use of HR in mid S phase. *Molecular cell.* 2012;47(2):320-329.
47. Huertas P, Jackson SP. Human CtIP mediates cell cycle control of DNA end resection and double strand break repair. *The Journal of biological chemistry.* 2009;284(14):9558-9565.
48. Sturzenegger A, Burdova K, Kanagaraj R, et al. DNA2 cooperates with the WRN and BLM RecQ helicases to mediate long-range DNA end resection in human cells. *The Journal of biological chemistry.* 2014;289(39):27314-27326.
49. Ciccia A, Elledge SJ. The DNA damage response: making it safe to play with knives. *Molecular cell.* 2010;40(2):179-204.
50. Li X, Heyer WD. Homologous recombination in DNA repair and DNA damage tolerance. *Cell Res.* 2008;18(1):99-113.
51. Ceccaldi R, Rondinelli B, D'Andrea AD. Repair Pathway Choices and Consequences at the Double-Strand Break. *Trends in cell biology.* 2016;26(1):52-64.
52. Simsek D, Jasin M. Alternative end-joining is suppressed by the canonical NHEJ component Xrcc4-ligase IV during chromosomal translocation formation. *Nature structural & molecular biology.* 2010;17(4):410-416.
53. Zhang Y, Jasin M. An essential role for CtIP in chromosomal translocation formation through an alternative end-joining pathway. *Nature structural & molecular biology.* 2011;18(1):80-84.
54. Beucher A, Birraux J, Tchouandong L, et al. ATM and Artemis promote homologous recombination of radiation-induced DNA double-strand breaks in G2. *The EMBO journal.* 2009;28(21):3413-3427.
55. Rothkamm K, Kruger I, Thompson LH, Lobrich M. Pathways of DNA double-strand break repair during the mammalian cell cycle. *Molecular and cellular biology.* 2003;23(16):5706-5715.
56. Shahar OD, Raghu Ram EV, Shimshoni E, Hareli S, Meshorer E, Goldberg M. Live imaging of induced and controlled DNA double-strand break formation reveals extremely low repair by homologous recombination in human cells. *Oncogene.* 2012;31(30):3495-3504.
57. Reynolds P, Anderson JA, Harper JV, et al. The dynamics of Ku70/80 and DNA-PKcs at DSBs induced by ionizing radiation is dependent on the complexity of damage. *Nucleic acids research.* 2012;40(21):10821-10831.
58. Shibata A, Conrad S, Birraux J, et al. Factors determining DNA double-strand break repair pathway choice in G2 phase. *The EMBO journal.* 2011;30(6):1079-1092.
59. Bothmer A, Phadke T, Barrera LA, et al. Characterization of the interplay between DNA repair and CRISPR/Cas9-induced DNA lesions at an endogenous locus. *Nature communications.* 2017;8:13905.

60. Orthwein A, Fradet-Turcotte A, Noordermeer SM, et al. Mitosis inhibits DNA double-strand break repair to guard against telomere fusions. *Science.* 2014;344(6180):189-193.
61. Amaral N, Ryu T, Li X, Chiolo I. Nuclear Dynamics of Heterochromatin Repair. *Trends Genet.* 2017;33(2):86-100.
62. Hauer MH, Gasser SM. Chromatin and nucleosome dynamics in DNA damage and repair. *Genes & development.* 2017;31(22):2204-2221.
63. Marini F, Rawal CC, Liberi G, Pellicioli A. Regulation of DNA Double Strand Breaks Processing: Focus on Barriers. *Front Mol Biosci.* 2019;6:55.
64. Symington LS. Mechanism and regulation of DNA end resection in eukaryotes. *Crit Rev Biochem Mol Biol.* 2016;51(3):195-212.
65. Wang W, Daley JM, Kwon Y, et al. A DNA nick at Ku-blocked double-strand break ends serves as an entry site for exonuclease 1 (Exo1) or Sgs1-Dna2 in long-range DNA end resection. *The Journal of biological chemistry.* 2018;293(44):17061-17069.
66. Chanut P, Britton S, Coates J, Jackson SP, Calsou P. Coordinated nuclease activities counteract Ku at single-ended DNA double-strand breaks. *Nature communications.* 2016;7:12889.
67. Bunting SF, Callen E, Kozak ML, et al. BRCA1 functions independently of homologous recombination in DNA interstrand crosslink repair. *Molecular cell.* 2012;46(2):125-135.
68. Chapman JR, Barral P, Vannier JB, et al. RIF1 is essential for 53BP1-dependent nonhomologous end joining and suppression of DNA double-strand break resection. *Molecular cell.* 2013;49(5):858-871.
69. Stucki M, Clapperton JA, Mohammad D, Yaffe MB, Smerdon SJ, Jackson SP. MDC1 directly binds phosphorylated histone H2AX to regulate cellular responses to DNA double-strand breaks. *Cell.* 2005;123(7):1213-1226.
70. Jungmichel S, Clapperton JA, Lloyd J, et al. The molecular basis of ATM-dependent dimerization of the Mdc1 DNA damage checkpoint mediator. *Nucleic acids research.* 2012;40(9):3913-3928.
71. Chapman JR, Jackson SP. Phospho-dependent interactions between NBS1 and MDC1 mediate chromatin retention of the MRN complex at sites of DNA damage. *EMBO Rep.* 2008;9(8):795-801.
72. Thorslund T, Ripplinger A, Hoffmann S, et al. Histone H1 couples initiation and amplification of ubiquitin signalling after DNA damage. *Nature.* 2015;527(7578):389-393.
73. Panier S, Boulton SJ. Double-strand break repair: 53BP1 comes into focus. *Nature reviews Molecular cell biology.* 2014;15(1):7-18.
74. Fradet-Turcotte A, Canny MD, Escribano-Diaz C, et al. 53BP1 is a reader of the DNA-damage-induced H2A Lys 15 ubiquitin mark. *Nature.* 2013;499(7456):50-54.
75. Botuyan MV, Lee J, Ward IM, et al. Structural basis for the methylation state-specific recognition of histone H4-K20 by 53BP1 and Crb2 in DNA repair. *Cell.* 2006;127(7):1361-1373.
76. Zimmermann M, de Lange T. 53BP1: pro choice in DNA repair. *Trends in cell biology.* 2014;24(2):108-117.
77. Becker JR, Cuella-Martin R, Barazas M, et al. The ASCIZ-DYNLL1 axis promotes 53BP1-dependent non-homologous end joining and PARP inhibitor sensitivity. *Nature communications.* 2018;9(1):5406.
78. Noordermeer SM, Adam S, Setiaputra D, et al. The shieldin complex mediates 53BP1-dependent DNA repair. *Nature.* 2018;560(7716):117-121.
79. Hustedt N, Durocher D. The control of DNA repair by the cell cycle. *Nat Cell Biol.* 2016;19(1):1-9.
80. Her J, Ray C, Altshuler J, Zheng H, Bunting SF. 53BP1 Mediates ATR-Chk1 Signaling and Protects Replication Forks under Conditions of Replication Stress. *Molecular and cellular biology.* 2018;38(8).

81. Schmid JA, Berti M, Walser F, et al. Histone Ubiquitination by the DNA Damage Response Is Required for Efficient DNA Replication in Unperturbed S Phase. *Molecular cell.* 2018;71(6):897-910 e898.
82. Dimitrova N, Chen YC, Spector DL, de Lange T. 53BP1 promotes non-homologous end joining of telomeres by increasing chromatin mobility. *Nature.* 2008;456(7221):524-528.
83. Kibe T, Zimmermann M, de Lange T. TPP1 Blocks an ATR-Mediated Resection Mechanism at Telomeres. *Molecular cell.* 2016;61(2):236-246.
84. Munoz IM, Jowsey PA, Toth R, Rouse J. Phospho-epitope binding by the BRCT domains of hPTIP controls multiple aspects of the cellular response to DNA damage. *Nucleic acids research.* 2007;35(16):5312-5322.
85. Escribano-Diaz C, Orthwein A, Fradet-Turcotte A, et al. A cell cycle-dependent regulatory circuit composed of 53BP1-RIF1 and BRCA1-CtIP controls DNA repair pathway choice. *Molecular cell.* 2013;49(5):872-883.
86. Zimmermann M, Lottersberger F, Buonomo SB, Sfeir A, de Lange T. 53BP1 regulates DSB repair using Rif1 to control 5' end resection. *Science.* 2013;339(6120):700-704.
87. Feng L, Fong KW, Wang J, Wang W, Chen J. RIF1 counteracts BRCA1-mediated end resection during DNA repair. *The Journal of biological chemistry.* 2013;288(16):11135-11143.
88. Di Virgilio M, Callen E, Yamane A, et al. Rif1 prevents resection of DNA breaks and promotes immunoglobulin class switching. *Science.* 2013;339(6120):711-715.
89. Callen E, Di Virgilio M, Kruhlak MJ, et al. 53BP1 mediates productive and mutagenic DNA repair through distinct phosphoprotein interactions. *Cell.* 2013;153(6):1266-1280.
90. Callen E, Zong D, Wu W, et al. 53BP1 Enforces Distinct Pre- and Post-resection Blocks on Homologous Recombination. *Molecular cell.* 2019.
91. Xu G, Chapman JR, Brandsma I, et al. REV7 counteracts DNA double-strand break resection and affects PARP inhibition. *Nature.* 2015;521(7553):541-544.
92. Boersma V, Moatti N, Segura-Bayona S, et al. MAD2L2 controls DNA repair at telomeres and DNA breaks by inhibiting 5' end resection. *Nature.* 2015;521(7553):537-540.
93. Dev H, Chiang TW, Lescale C, et al. Shieldin complex promotes DNA end-joining and counters homologous recombination in BRCA1-null cells. *Nat Cell Biol.* 2018;20(8):954-965.
94. Gupta R, Somyajit K, Narita T, et al. DNA Repair Network Analysis Reveals Shieldin as a Key Regulator of NHEJ and PARP Inhibitor Sensitivity. *Cell.* 2018;173(4):972-988 e923.
95. Findlay S, Heath J, Luo VM, et al. SHLD2/FAM35A co-operates with REV7 to coordinate DNA double-strand break repair pathway choice. *The EMBO journal.* 2018;37(18).
96. Tomida J, Takata KI, Bhetawal S, et al. FAM35A associates with REV7 and modulates DNA damage responses of normal and BRCA1-defective cells. *The EMBO journal.* 2018;37(12).
97. Gao S, Feng S, Ning S, et al. An OB-fold complex controls the repair pathways for DNA double-strand breaks. *Nature communications.* 2018;9(1):3925.
98. Ghezraoui H, Oliveira C, Becker JR, et al. 53BP1 cooperation with the REV7-shieldin complex underpins DNA structure-specific NHEJ. *Nature.* 2018;560(7716):122-127.
99. Setiaputra D, Durocher D. Shieldin - the protector of DNA ends. *EMBO Rep.* 2019;20(5).
100. Mirman Z, Lottersberger F, Takai H, et al. 53BP1-RIF1-shieldin counteracts DSB resection through CST- and Polalpha-dependent fill-in. *Nature.* 2018;560(7716):112-116.
101. Mallette FA, Mattiroli F, Cui G, et al. RNF8- and RNF168-dependent degradation of KDM4A/JMJD2A triggers 53BP1 recruitment to DNA damage sites. *The EMBO journal.* 2012;31(8):1865-1878.
102. Pellegrino S, Michelena J, Teloni F, Imhof R, Altmeyer M. Replication-Coupled Dilution of H4K20me2 Guides 53BP1 to Pre-replicative Chromatin. *Cell reports.* 2017;19(9):1819-1831.

103. Acs K, Luijsterburg MS, Ackermann L, Salomons FA, Hoppe T, Dantuma NP. The AAA-ATPase VCP/p97 promotes 53BP1 recruitment by removing L3MBTL1 from DNA double-strand breaks. *Nature structural & molecular biology.* 2011;18(12):1345-1350.
104. Zhang A, Peng B, Huang P, Chen J, Gong Z. The p53-binding protein 1-Tudor-interacting repair regulator complex participates in the DNA damage response. *The Journal of biological chemistry.* 2017;292(16):6461-6467.
105. Drane P, Brault ME, Cui G, et al. TIRR regulates 53BP1 by masking its histone methyl-lysine binding function. *Nature.* 2017;543(7644):211-216.
106. Dai Y, Zhang A, Shan S, Gong Z, Zhou Z. Structural basis for recognition of 53BP1 tandem Tudor domain by TIRR. *Nature communications.* 2018;9(1):2123.
107. Guo X, Bai Y, Zhao M, et al. Acetylation of 53BP1 dictates the DNA double strand break repair pathway. *Nucleic acids research.* 2018;46(2):689-703.
108. Renaud E, Barascu A, Rosselli F. Impaired TIP60-mediated H4K16 acetylation accounts for the aberrant chromatin accumulation of 53BP1 and RAP80 in Fanconi anemia pathway-deficient cells. *Nucleic acids research.* 2016;44(2):648-656.
109. Fontana GA, Hess D, Reinert JK, et al. Rif1 S-acylation mediates DNA double-strand break repair at the inner nuclear membrane. *Nature communications.* 2019;10(1):2535.
110. Cortez D, Wang Y, Qin J, Elledge SJ. Requirement of ATM-dependent phosphorylation of brca1 in the DNA damage response to double-strand breaks. *Science.* 1999;286(5442):1162-1166.
111. Mallery DL, Vandenberg CJ, Hiom K. Activation of the E3 ligase function of the BRCA1/BARD1 complex by polyubiquitin chains. *The EMBO journal.* 2002;21(24):6755-6762.
112. Zhu Q, Pao GM, Huynh AM, et al. BRCA1 tumour suppression occurs via heterochromatin-mediated silencing. *Nature.* 2011;477(7363):179-184.
113. Densham RM, Garvin AJ, Stone HR, et al. Human BRCA1-BARD1 ubiquitin ligase activity counteracts chromatin barriers to DNA resection. *Nature structural & molecular biology.* 2016;23(7):647-655.
114. Zhang H, Liu H, Chen Y, et al. A cell cycle-dependent BRCA1-UHRF1 cascade regulates DNA double-strand break repair pathway choice. *Nature communications.* 2016;7:10201.
115. Isono M, Niimi A, Oike T, et al. BRCA1 Directs the Repair Pathway to Homologous Recombination by Promoting 53BP1 Dephosphorylation. *Cell reports.* 2017;18(2):520-532.
116. Feng L, Li N, Li Y, et al. Cell cycle-dependent inhibition of 53BP1 signaling by BRCA1. *Cell Discov.* 2015;1:15019.
117. Isobe SY, Nagao K, Nozaki N, Kimura H, Obuse C. Inhibition of RIF1 by SCAI Allows BRCA1-Mediated Repair. *Cell reports.* 2017;20(2):297-307.
118. Dantuma NP, van Attikum H. Spatiotemporal regulation of posttranslational modifications in the DNA damage response. *The EMBO journal.* 2016;35(1):6-23.
119. Polo SE, Jackson SP. Dynamics of DNA damage response proteins at DNA breaks: a focus on protein modifications. *Genes & development.* 2011;25(5):409-433.
120. von Stechow L, Olsen JV. Proteomics insights into DNA damage response and translating this knowledge to clinical strategies. *Proteomics.* 2017;17(3-4).
121. Xu Z, Zan H, Pone EJ, Mai T, Casali P. Immunoglobulin class-switch DNA recombination: induction, targeting and beyond. *Nat Rev Immunol.* 2012;12(7):517-531.
122. Mesin L, Ersching J, Victora GD. Germinal Center B Cell Dynamics. *Immunity.* 2016;45(3):471-482.
123. Briney B, Inderbitzin A, Joyce C, Burton DR. Commonality despite exceptional diversity in the baseline human antibody repertoire. *Nature.* 2019;566(7744):393-397.

124. Methot SP, Di Noia JM. Molecular Mechanisms of Somatic Hypermutation and Class Switch Recombination. *Adv Immunol.* 2017;133:37-87.
125. Stavnezer J, Schrader CE. IgH chain class switch recombination: mechanism and regulation. *Journal of immunology.* 2014;193(11):5370-5378.
126. Matthews AJ, Zheng S, DiMenna LJ, Chaudhuri J. Regulation of immunoglobulin class-switch recombination: choreography of noncoding transcription, targeted DNA deamination, and long-range DNA repair. *Adv Immunol.* 2014;122:1-57.
127. Yancopoulos GD, DePinho RA, Zimmerman KA, Lutzker SG, Rosenberg N, Alt FW. Secondary genomic rearrangement events in pre-B cells: VHDJH replacement by a LINE-1 sequence and directed class switching. *The EMBO journal.* 1986;5(12):3259-3266.
128. Snapper CM, Finkelman FD, Paul WE. Regulation of IgG1 and IgE production by interleukin 4. *Immunol Rev.* 1988;102:51-75.
129. Le Q, Maizels N. Cell Cycle Regulates Nuclear Stability of AID and Determines the Cellular Response to AID. *PLoS Genet.* 2015;11(9):e1005411.
130. Sharbeen G, Yee CW, Smith AL, Jolly CJ. Ectopic restriction of DNA repair reveals that UNG2 excises AID-induced uracils predominantly or exclusively during G1 phase. *The Journal of experimental medicine.* 2012;209(5):965-974.
131. Petersen S, Casellas R, Reina-San-Martin B, et al. AID is required to initiate Nbs1/gamma-H2AX focus formation and mutations at sites of class switching. *Nature.* 2001;414(6864):660-665.
132. Alt FW, Zhang Y, Meng FL, Guo C, Schwer B. Mechanisms of programmed DNA lesions and genomic instability in the immune system. *Cell.* 2013;152(3):417-429.
133. Boboila C, Yan C, Wesemann DR, et al. Alternative end-joining catalyzes class switch recombination in the absence of both Ku70 and DNA ligase 4. *The Journal of experimental medicine.* 2010;207(2):417-427.
134. Han L, Yu K. Altered kinetics of nonhomologous end joining and class switch recombination in ligase IV-deficient B cells. *The Journal of experimental medicine.* 2008;205(12):2745-2753.
135. Yan CT, Boboila C, Souza EK, et al. IgH class switching and translocations use a robust non-classical end-joining pathway. *Nature.* 2007;449(7161):478-482.
136. Cortizas EM, Zahn A, Hajjar ME, Patenaude AM, Di Noia JM, Verdun RE. Alternative end-joining and classical nonhomologous end-joining pathways repair different types of double-strand breaks during class-switch recombination. *Journal of immunology.* 2013;191(11):5751-5763.
137. Bothmer A, Robbiani DF, Di Virgilio M, et al. Regulation of DNA end joining, resection, and immunoglobulin class switch recombination by 53BP1. *Molecular cell.* 2011;42(3):319-329.
138. Bothmer A, Robbiani DF, Feldhahn N, Gazumyan A, Nussenzweig A, Nussenzweig MC. 53BP1 regulates DNA resection and the choice between classical and alternative end joining during class switch recombination. *The Journal of experimental medicine.* 2010;207(4):855-865.
139. Manis JP, Morales JC, Xia Z, Kutok JL, Alt FW, Carpenter PB. 53BP1 links DNA damage-response pathways to immunoglobulin heavy chain class-switch recombination. *Nat Immunol.* 2004;5(5):481-487.
140. Lenz G, Nagel I, Siebert R, et al. Aberrant immunoglobulin class switch recombination and switch translocations in activated B cell-like diffuse large B cell lymphoma. *The Journal of experimental medicine.* 2007;204(3):633-643.
141. Reina-San-Martin B, Chen J, Nussenzweig A, Nussenzweig MC. Enhanced intra-switch region recombination during immunoglobulin class switch recombination in 53BP1-/- B cells. *European journal of immunology.* 2007;37(1):235-239.
142. Wang JH, Gostissa M, Yan CT, et al. Mechanisms promoting translocations in editing and switching peripheral B cells. *Nature.* 2009;460(7252):231-236.

143. Bothmer A, Rommel PC, Gazumyan A, et al. Mechanism of DNA resection during intrachromosomal recombination and immunoglobulin class switching. *The Journal of experimental medicine.* 2013;210(1):115-123.
144. Wuerffel R, Wang L, Grigera F, et al. S-S synapsis during class switch recombination is promoted by distantly located transcriptional elements and activation-induced deaminase. *Immunity.* 2007;27(5):711-722.
145. Dong J, Panchakshari RA, Zhang T, et al. Orientation-specific joining of AID-initiated DNA breaks promotes antibody class switching. *Nature.* 2015;525(7567):134-139.
146. Rocha PP, Raviram R, Fu Y, et al. A Damage-Independent Role for 53BP1 that Impacts Break Order and Igh Architecture during Class Switch Recombination. *Cell reports.* 2016;16(1):48-55.
147. Delgado-Benito V, Rosen DB, Wang Q, et al. The Chromatin Reader ZMYND8 Regulates Igh Enhancers to Promote Immunoglobulin Class Switch Recombination. *Molecular cell.* 2018;72(4):636-649 e638.
148. Sundaravinayagam D, Rahjouei A, Andreani M, et al. 53BP1 Supports Immunoglobulin Class Switch Recombination Independently of Its DNA Double-Strand Break End Protection Function. *Cell reports.* 2019;28(6):1389-1399 e1386.
149. Hardy CF, Sussel L, Shore D. A RAP1-interacting protein involved in transcriptional silencing and telomere length regulation. *Genes & development.* 1992;6(5):801-814.
150. Adams IR, McLaren A. Identification and characterisation of mRif1: a mouse telomere-associated protein highly expressed in germ cells and embryo-derived pluripotent stem cells. *Dev Dyn.* 2004;229(4):733-744.
151. Silverman J, Takai H, Buonomo SB, Eisenhaber F, de Lange T. Human Rif1, ortholog of a yeast telomeric protein, is regulated by ATM and 53BP1 and functions in the S-phase checkpoint. *Genes & development.* 2004;18(17):2108-2119.
152. Xu L, Blackburn EH. Human Rif1 protein binds aberrant telomeres and aligns along anaphase midzone microtubules. *The Journal of cell biology.* 2004;167(5):819-830.
153. Buonomo SB, Wu Y, Ferguson D, de Lange T. Mammalian Rif1 contributes to replication stress survival and homology-directed repair. *The Journal of cell biology.* 2009;187(3):385-398.
154. Xu D, Muniandy P, Leo E, et al. Rif1 provides a new DNA-binding interface for the Bloom syndrome complex to maintain normal replication. *The EMBO journal.* 2010;29(18):3140-3155.
155. Sreesankar E, Senthilkumar R, Bharathi V, Mishra RK, Mishra K. Functional diversification of yeast telomere associated protein, Rif1, in higher eukaryotes. *BMC genomics.* 2012;13:255.
156. Hengeveld RC, de Boer HR, Schoonen PM, de Vries EG, Lens SM, van Vugt MA. Rif1 Is Required for Resolution of Ultrafine DNA Bridges in Anaphase to Ensure Genomic Stability. *Dev Cell.* 2015;34(4):466-474.
157. Bhowmick R, Thakur RS, Venegas AB, et al. The RIF1-PP1 Axis Controls Abscission Timing in Human Cells. *Curr Biol.* 2019;29(7):1232-1242 e1235.
158. Yamazaki S, Ishii A, Kanoh Y, Oda M, Nishito Y, Masai H. Rif1 regulates the replication timing domains on the human genome. *The EMBO journal.* 2012;31(18):3667-3677.
159. Cornacchia D, Dileep V, Quivy JP, et al. Mouse Rif1 is a key regulator of the replication-timing programme in mammalian cells. *The EMBO journal.* 2012;31(18):3678-3690.
160. Hiraga S, Alvino GM, Chang F, et al. Rif1 controls DNA replication by directing Protein Phosphatase 1 to reverse Cdc7-mediated phosphorylation of the MCM complex. *Genes & development.* 2014;28(4):372-383.
161. Hiraga SI, Ly T, Garzon J, et al. Human RIF1 and protein phosphatase 1 stimulate DNA replication origin licensing but suppress origin activation. *EMBO Rep.* 2017;18(3):403-419.
162. Dave A, Cooley C, Garg M, Bianchi A. Protein phosphatase 1 recruitment by Rif1 regulates DNA replication origin firing by counteracting DDK activity. *Cell reports.* 2014;7(1):53-61.

163. Foti R, Gnan S, Cornacchia D, et al. Nuclear Architecture Organized by Rif1 Underpins the Replication-Timing Program. *Molecular cell.* 2016;61(2):260-273.
164. Moiseeva TN, Yin Y, Calderon MJ, et al. An ATR and CHK1 kinase signaling mechanism that limits origin firing during unperturbed DNA replication. *Proceedings of the National Academy of Sciences of the United States of America.* 2019;116(27):13374-13383.
165. Hayano M, Kanoh Y, Matsumoto S, Renard-Guillet C, Shirahige K, Masai H. Rif1 is a global regulator of timing of replication origin firing in fission yeast. *Genes & development.* 2012;26(2):137-150.
166. Mattarocci S, Shyian M, Lemmens L, et al. Rif1 controls DNA replication timing in yeast through the PP1 phosphatase Glc7. *Cell reports.* 2014;7(1):62-69.
167. Sreesankar E, Bharathi V, Mishra RK, Mishra K. Drosophila Rif1 is an essential gene and controls late developmental events by direct interaction with PP1-87B. *Scientific reports.* 2015;5:10679.
168. Hafner L, Lezaja A, Zhang X, et al. Rif1 Binding and Control of Chromosome-Internal DNA Replication Origins Is Limited by Telomere Sequestration. *Cell reports.* 2018;23(4):983-992.
169. Zaaijer S, Shaikh N, Nageshan RK, Cooper JP. Rif1 Regulates the Fate of DNA Entanglements during Mitosis. *Cell reports.* 2016;16(1):148-160.
170. You Z, Chahwan C, Bailis J, Hunter T, Russell P. ATM activation and its recruitment to damaged DNA require binding to the C terminus of Nbs1. *Molecular and cellular biology.* 2005;25(13):5363-5379.
171. Perry J, Kleckner N. The ATRs, ATMs, and TORs are giant HEAT repeat proteins. *Cell.* 2003;112(2):151-155.
172. Moriyama K, Yoshizawa-Sugata N, Masai H. Oligomer formation and G-quadruplex binding by purified murine Rif1 protein, a key organizer of higher-order chromatin architecture. *The Journal of biological chemistry.* 2018;293(10):3607-3624.
173. Breitkreutz A, Choi H, Sharom JR, et al. A global protein kinase and phosphatase interaction network in yeast. *Science.* 2010;328(5981):1043-1046.
174. Sukackaite R, Jensen MR, Mas PJ, Blackledge M, Buonomo SB, Hart DJ. Structural and biophysical characterization of murine rif1 C terminus reveals high specificity for DNA cruciform structures. *The Journal of biological chemistry.* 2014;289(20):13903-13911.
175. Kanoh Y, Matsumoto S, Fukatsu R, et al. Rif1 binds to G quadruplexes and suppresses replication over long distances. *Nature structural & molecular biology.* 2015;22(11):889-897.
176. Shi T, Bunker RD, Mattarocci S, et al. Rif1 and Rif2 shape telomere function and architecture through multivalent Rap1 interactions. *Cell.* 2013;153(6):1340-1353.
177. Jazayeri A, Falck J, Lukas C, et al. ATM- and cell cycle-dependent regulation of ATR in response to DNA double-strand breaks. *Nat Cell Biol.* 2006;8(1):37-45.
178. Kim ST, Lim DS, Canman CE, Kastan MB. Substrate specificities and identification of putative substrates of ATM kinase family members. *The Journal of biological chemistry.* 1999;274(53):37538-37543.
179. Cuadrado M, Martinez-Pastor B, Murga M, et al. ATM regulates ATR chromatin loading in response to DNA double-strand breaks. *The Journal of experimental medicine.* 2006;203(2):297-303.
180. Arai M, Sugase K, Dyson HJ, Wright PE. Conformational propensities of intrinsically disordered proteins influence the mechanism of binding and folding. *Proceedings of the National Academy of Sciences of the United States of America.* 2015;112(31):9614-9619.
181. Chakrabortee S, Byers JS, Jones S, et al. Intrinsically Disordered Proteins Drive Emergence and Inheritance of Biological Traits. *Cell.* 2016;167(2):369-381 e312.

182. van der Lee R, Buljan M, Lang B, et al. Classification of intrinsically disordered regions and proteins. *Chemical reviews.* 2014;114(13):6589-6631.
183. Wright PE, Dyson HJ. Intrinsically disordered proteins in cellular signalling and regulation. *Nature reviews Molecular cell biology.* 2015;16(1):18-29.
184. Iakoucheva LM, Radivojac P, Brown CJ, et al. The importance of intrinsic disorder for protein phosphorylation. *Nucleic acids research.* 2004;32(3):1037-1049.
185. Sugase K, Dyson HJ, Wright PE. Mechanism of coupled folding and binding of an intrinsically disordered protein. *Nature.* 2007;447(7147):1021-1025.
186. Matsuoka S, Ballif BA, Smogorzewska A, et al. ATM and ATR substrate analysis reveals extensive protein networks responsive to DNA damage. *Science.* 2007;316(5828):1160-1166.
187. Sridhar A, Kedziora S, Donaldson AD. At short telomeres Tel1 directs early replication and phosphorylates Rif1. *PLoS Genet.* 2014;10(10):e1004691.
188. Wang J, Zhang H, Al Shibar M, Willard B, Ray A, Runge KW. Rif1 phosphorylation site analysis in telomere length regulation and the response to damaged telomeres. *DNA repair.* 2018;65:26-33.
189. Claus EB, Schildkraut JM, Thompson WD, Risch NJ. The genetic attributable risk of breast and ovarian cancer. *Cancer.* 1996;77(11):2318-2324.
190. Bouwman P, Jonkers J. The effects of deregulated DNA damage signalling on cancer chemotherapy response and resistance. *Nat Rev Cancer.* 2012;12(9):587-598.
191. Gibson BA, Kraus WL. New insights into the molecular and cellular functions of poly(ADP-ribose) and PARPs. *Nature reviews Molecular cell biology.* 2012;13(7):411-424.
192. Fong PC, Boss DS, Yap TA, et al. Inhibition of poly(ADP-ribose) polymerase in tumors from BRCA mutation carriers. *N Engl J Med.* 2009;361(2):123-134.
193. Noordermeer SM, van Attikum H. PARP Inhibitor Resistance: A Tug-of-War in BRCA-Mutated Cells. *Trends in cell biology.* 2019;29(10):820-834.
194. Pommier Y, O'Connor MJ, de Bono J. Laying a trap to kill cancer cells: PARP inhibitors and their mechanisms of action. *Science translational medicine.* 2016;8(362):362ps317.
195. Bouwman P, Aly A, Escandell JM, et al. 53BP1 loss rescues BRCA1 deficiency and is associated with triple-negative and BRCA-mutated breast cancers. *Nature structural & molecular biology.* 2010;17(6):688-695.
196. Bunting SF, Callen E, Wong N, et al. 53BP1 inhibits homologous recombination in Brca1-deficient cells by blocking resection of DNA breaks. *Cell.* 2010;141(2):243-254.
197. Cao L, Xu X, Bunting SF, et al. A selective requirement for 53BP1 in the biological response to genomic instability induced by Brca1 deficiency. *Molecular cell.* 2009;35(4):534-541.
198. Chu VT, Graf R, Wirtz T, et al. Efficient CRISPR-mediated mutagenesis in primary immune cells using CrispRGold and a C57BL/6 Cas9 transgenic mouse line. *Proceedings of the National Academy of Sciences of the United States of America.* 2016;113(44):12514-12519.
199. Haeussler M, Schonig K, Eckert H, et al. Evaluation of off-target and on-target scoring algorithms and integration into the guide RNA selection tool CRISPOR. *Genome biology.* 2016;17(1):148.
200. Artimo P, Jonnalagedda M, Arnold K, et al. ExPASy: SIB bioinformatics resource portal. *Nucleic acids research.* 2012;40(Web Server issue):W597-603.
201. Madeira F, Park YM, Lee J, et al. The EMBL-EBI search and sequence analysis tools APIs in 2019. *Nucleic acids research.* 2019;47(W1):W636-W641.
202. Cox J, Mann M. MaxQuant enables high peptide identification rates, individualized p.p.b.-range mass accuracies and proteome-wide protein quantification. *Nat Biotechnol.* 2008;26(12):1367-1372.

203. Ran FA, Hsu PD, Wright J, Agarwala V, Scott DA, Zhang F. Genome engineering using the CRISPR-Cas9 system. *Nat Protoc.* 2013;8(11):2281-2308.
204. Tackett AJ, DeGrasse JA, Sekedat MD, Oeffinger M, Rout MP, Chait BT. I-DIRT, a general method for distinguishing between specific and nonspecific protein interactions. *Journal of proteome research.* 2005;4(5):1752-1756.
205. Nakamura M, Kondo S, Sugai M, Nazarea M, Imamura S, Honjo T. High frequency class switching of an IgM+ B lymphoma clone CH12F3 to IgA+ cells. *International immunology.* 1996;8(2):193-201.
206. Shen B, Zhang W, Zhang J, et al. Efficient genome modification by CRISPR-Cas9 nickase with minimal off-target effects. *Nature methods.* 2014;11(4):399-402.
207. Komor AC, Badran AH, Liu DR. CRISPR-Based Technologies for the Manipulation of Eukaryotic Genomes. *Cell.* 2017;168(1-2):20-36.
208. Dingwall C, Laskey RA. Nuclear targeting sequences--a consensus? *Trends Biochem Sci.* 1991;16(12):478-481.
209. Kalderon D, Richardson WD, Markham AF, Smith AE. Sequence requirements for nuclear location of simian virus 40 large-T antigen. *Nature.* 1984;311(5981):33-38.
210. Ishida T, Kinoshita K. PrDOS: prediction of disordered protein regions from amino acid sequence. *Nucleic acids research.* 2007;35(Web Server issue):W460-464.
211. Kelley LA, Mezulis S, Yates CM, Wass MN, Sternberg MJ. The Phyre2 web portal for protein modeling, prediction and analysis. *Nat Protoc.* 2015;10(6):845-858.
212. Kuhn R, Chu VT. Pop in, pop out: a novel gene-targeting strategy for use with CRISPR-Cas9. *Genome biology.* 2015;16:244.
213. Hsu PD, Scott DA, Weinstein JA, et al. DNA targeting specificity of RNA-guided Cas9 nucleases. *Nat Biotechnol.* 2013;31(9):827-832.
214. Zhang Y, Ge X, Yang F, et al. Comparison of non-canonical PAMs for CRISPR/Cas9-mediated DNA cleavage in human cells. *Scientific reports.* 2014;4:5405.
215. Zeman MK, Cimprich KA. Causes and consequences of replication stress. *Nat Cell Biol.* 2014;16(1):2-9.
216. Kondrashov FA, Koonin EV. A common framework for understanding the origin of genetic dominance and evolutionary fates of gene duplications. *Trends Genet.* 2004;20(7):287-290.
217. Szklarczyk R, Wanschers BF, Nabuurs SB, Nouws J, Nijtmans LG, Huynen MA. NDUFB7 and NDUFA8 are located at the intermembrane surface of complex I. *FEBS Lett.* 2011;585(5):737-743.
218. Stroud DA, Surgenor EE, Formosa LE, et al. Accessory subunits are integral for assembly and function of human mitochondrial complex I. *Nature.* 2016;538(7623):123-126.
219. Komano J, Miyauchi K, Matsuda Z, Yamamoto N. Inhibiting the Arp2/3 complex limits infection of both intracellular mature vaccinia virus and primate lentiviruses. *Molecular biology of the cell.* 2004;15(12):5197-5207.
220. Fenn S, Breitsprecher D, Gerhold CB, Witte G, Faix J, Hopfner KP. Structural biochemistry of nuclear actin-related proteins 4 and 8 reveals their interaction with actin. *The EMBO journal.* 2011;30(11):2153-2166.
221. Yoo Y, Wu X, Guan JL. A novel role of the actin-nucleating Arp2/3 complex in the regulation of RNA polymerase II-dependent transcription. *The Journal of biological chemistry.* 2007;282(10):7616-7623.
222. Gerhold CB, Gasser SM. INO80 and SWR complexes: relating structure to function in chromatin remodeling. *Trends in cell biology.* 2014;24(11):619-631.
223. Kapoor P, Chen M, Winkler DD, Luger K, Shen X. Evidence for monomeric actin function in INO80 chromatin remodeling. *Nature structural & molecular biology.* 2013;20(4):426-432.

224. Olave IA, Reck-Peterson SL, Crabtree GR. Nuclear actin and actin-related proteins in chromatin remodeling. *Annu Rev Biochem.* 2002;71:755-781.
225. Shen X, Mizuguchi G, Hamiche A, Wu C. A chromatin remodelling complex involved in transcription and DNA processing. *Nature.* 2000;406(6795):541-544.
226. Urnov FD, Wolffe AP. Chromatin remodeling and transcriptional activation: the cast (in order of appearance). *Oncogene.* 2001;20(24):2991-3006.
227. Niimi A, Chambers AL, Downs JA, Lehmann AR. A role for chromatin remodellers in replication of damaged DNA. *Nucleic acids research.* 2012;40(15):7393-7403.
228. Falbo KB, Shen X. Function of the INO80 chromatin remodeling complex in DNA replication. *Front Biosci (Landmark Ed).* 2012;17:970-975.
229. Fritsch O, Benvenuto G, Bowler C, Molinier J, Hohn B. The INO80 protein controls homologous recombination in Arabidopsis thaliana. *Molecular cell.* 2004;16(3):479-485.
230. Morrison AJ, Highland J, Krogan NJ, et al. INO80 and gamma-H2AX interaction links ATP-dependent chromatin remodeling to DNA damage repair. *Cell.* 2004;119(6):767-775.
231. Gospodinov A, Vaissiere T, Krastev DB, Legube G, Anachkova B, Herceg Z. Mammalian Ino80 mediates double-strand break repair through its role in DNA end strand resection. *Molecular and cellular biology.* 2011;31(23):4735-4745.
232. Belin BJ, Lee T, Mullins RD. DNA damage induces nuclear actin filament assembly by Formin -2 and Spire-(1/2) that promotes efficient DNA repair. [corrected]. *eLife.* 2015;4:e07735.
233. Caridi CP, D'Agostino C, Ryu T, et al. Nuclear F-actin and myosins drive relocalization of heterochromatic breaks. *Nature.* 2018;559(7712):54-60.
234. Schrank BR, Aparicio T, Li Y, et al. Nuclear ARP2/3 drives DNA break clustering for homology-directed repair. *Nature.* 2018;559(7712):61-66.
235. Kracker S, Di Virgilio M, Schwartzentruber J, et al. An inherited immunoglobulin class-switch recombination deficiency associated with a defect in the INO80 chromatin remodeling complex. *The Journal of allergy and clinical immunology.* 2015;135(4):998-1007 e1006.
236. Enervald E, Du L, Visnes T, et al. A regulatory role for the cohesin loader NIPBL in nonhomologous end joining during immunoglobulin class switch recombination. *The Journal of experimental medicine.* 2013;210(12):2503-2513.
237. Thomas-Claudepierre AS, Schiavo E, Heyer V, et al. The cohesin complex regulates immunoglobulin class switch recombination. *The Journal of experimental medicine.* 2013;210(12):2495-2502.
238. Min JN, Tian Y, Xiao Y, Wu L, Li L, Chang S. The mINO80 chromatin remodeling complex is required for efficient telomere replication and maintenance of genome stability. *Cell Res.* 2013;23(12):1396-1413.
239. Gnan S, Flyamer IM, Klein KN, et al. Nuclear organisation and replication timing are coupled through RIF1-PP1 interaction. *bioRxiv.* 2019:812156.
240. Batenburg NL, Walker JR, Noordermeer SM, Moatti N, Durocher D, Zhu XD. ATM and CDK2 control chromatin remodeler CSB to inhibit RIF1 in DSB repair pathway choice. *Nature communications.* 2017;8(1):1921.
241. Kumar M, Keller B, Makalou N, Sutton RE. Systematic determination of the packaging limit of lentiviral vectors. *Human gene therapy.* 2001;12(15):1893-1905.
242. Wu Z, Yang H, Colosi P. Effect of genome size on AAV vector packaging. *Molecular therapy : the journal of the American Society of Gene Therapy.* 2010;18(1):80-86.
243. Dong JY, Fan PD, Frizzell RA. Quantitative analysis of the packaging capacity of recombinant adeno-associated virus. *Human gene therapy.* 1996;7(17):2101-2112.
244. Forns X, Bukh J, Purcell RH, Emerson SU. How Escherichia coli can bias the results of molecular cloning: preferential selection of defective genomes of hepatitis C virus during the

cloning procedure. *Proceedings of the National Academy of Sciences of the United States of America.* 1997;94(25):13909-13914.

245. Bachmair A, Finley D, Varshavsky A. In vivo half-life of a protein is a function of its amino-terminal residue. *Science.* 1986;234(4773):179-186.
246. Varshavsky A. The N-end rule pathway and regulation by proteolysis. *Protein science : a publication of the Protein Society.* 2011;20(8):1298-1345.
247. Shemorry A, Hwang CS, Varshavsky A. Control of protein quality and stoichiometries by N-terminal acetylation and the N-end rule pathway. *Molecular cell.* 2013;50(4):540-551.
248. Reina-San-Martin B, Chen HT, Nussenzweig A, Nussenzweig MC. ATM is required for efficient recombination between immunoglobulin switch regions. *The Journal of experimental medicine.* 2004;200(9):1103-1110.
249. Manis JP, Tian M, Alt FW. Mechanism and control of class-switch recombination. *Trends Immunol.* 2002;23(1):31-39.
250. Mukherjee C, Tripathi V, Manolika EM, et al. RIF1 promotes replication fork protection and efficient restart to maintain genome stability. *Nature communications.* 2019;10(1):3287.
251. Deshaies RJ, Ferrell JE, Jr. Multisite phosphorylation and the countdown to S phase. *Cell.* 2001;107(7):819-822.
252. Varedi KS, Ventura AC, Merajver SD, Lin XN. Multisite phosphorylation provides an effective and flexible mechanism for switch-like protein degradation. *PloS one.* 2010;5(12):e14029.
253. Ji Z, Gao H, Jia L, Li B, Yu H. A sequential multi-target Mps1 phosphorylation cascade promotes spindle checkpoint signaling. *eLife.* 2017;6.
254. Valk E, Venta R, Ord M, Faustova I, Koivomagi M, Loog M. Multistep phosphorylation systems: tunable components of biological signaling circuits. *Molecular biology of the cell.* 2014;25(22):3456-3460.
255. Holt LJ, Tuch BB, Villen J, Johnson AD, Gygi SP, Morgan DO. Global analysis of Cdk1 substrate phosphorylation sites provides insights into evolution. *Science.* 2009;325(5948):1682-1686.
256. Tyanova S, Cox J, Olsen J, Mann M, Frishman D. Phosphorylation variation during the cell cycle scales with structural propensities of proteins. *PLoS computational biology.* 2013;9(1):e1002842.

8. Appendix

8.1 Selbstständigkeitserklärung

Hiermit erkläre ich, dass ich die vorliegende Arbeit mit dem Titel "Molecular Requirements for RIF1 Role in DNA Double-Strand Break End Protection" selbstständig und ohne Hilfe Dritter angefertigt habe (sofern nicht anders angegeben). Sämtliche Hilfsmittel, Hilfen sowie Literaturquellen sind als solche kenntlich gemacht. Außerdem erkläre ich hiermit, dass ich mich nicht anderweitig um einen entsprechenden Doktorgrad beworben habe. Die Promotionsordnung des Fachbereichs Biologie, Chemie und Pharmazie der Freien Universität Berlin habe ich gelesen und akzeptiert.

8.2 Curriculum Vitae

For reasons of data protection, the curriculum vitae is not published in the electronic version.

For reasons of data protection, the curriculum vitae is not published in the electronic version.

For reasons of data protection, the curriculum vitae is not published in the electronic version.

8.3 List of publications

- **The Chromatin Reader ZMYND8 Regulates Igh Enhancers to Promote Immunoglobulin Class Switch Recombination.**

  Delgado-Benito V., Rosen DB., Wang Q., Gazumyan A., Pai JA., Oliveira TY., Sundaravinayagam D., Zhang W., **Andreani M.**, Keller L., Kieffer-Kwon KR., Pękowska A., Jung S., Driesner M., Subbotin RI., Casellas R., Chait BT., Nussenzweig MC., Di Virgilio M. *Mol. Cell. 72(4):636-649 (2018)*

- **53BP1 supports Immunoglobulin Class Switch Recombination independently of its DNA Double Strand Break End Protection function.**

  Sundaravinayagam D., Rahjouei A., **Andreani M.**, Tupina D., Balasubramanian S., Saha T., Delgado-Benito V., Coralluzzo V., Daumke O., and Di Virgilio M. Cell Rep., 28, pp. 1389-1399 (2019). Paper was previewed by J. Chaudhuri (MSKCC, NY)

8.4 Acknowledgements

Some people told me that doing a PhD would have been a hard road, some others that it is pointless. Now, at the end of my personal 5-years' experience, I do agree with the first ones, but not with the second ones.

In the past 5 years I have met amazing people, and, despite the hard times and the different experimental roadblocks, I grew personally...and I had a blast.

It has been essential to have great people close to me (not necessarily in physical proximity): to help me, when I felt lost; to talk science when science had become either a nightmare or pleasantly intriguing or simply awkward; to talk about anything else but science, always at the right time when I needed a break (and to laugh); or simply to look at each other, without saying anything and share a smile.

So here you are.

Thank you, Michela, for choosing me to be part of your team. Without the opportunity you gave me, I may have not been writing these words now. It was exciting to start the lab together and see our team grow with fantastic people. Thanks for your support and motivation you never failed to give to me.

Thanks to my great team: Dev, Ali, Bob, Madlen, Lisa, Vio, Jas, Maria, Tannu, Sandhya and Vero. Really, thank you guys for your support and help, for the fun we had together, for the jokes, the great food,…

Thanks to my committee members, Claus Scheidereit and Jana Wolf, and to Oliver Daumke for the constructive critics and the precious suggestions you gave me.

Thank you. Annette and Michaela. Without you, any PhD student would be lost.

Thank you, Hans, for the constant support and great vibes you provide at the FACS facility.

Thanks to Gaetano Gargiulo and Kathrin de la Rosa for the scientific feedback and motivation.

Thanks to VD and SB. You are my little sisters. You are my little bullies, too! Thanks for always having time for my questions, my dramas, and my indecisions. Without you, I would have probably not have made it.

Thank you, My Man. You are my big Bro instead. But a big bully, too! Thanks for the great time we had together and for always having ears for me.

Thanks to my 2.0 family. You are just too many and if I start writing all your names, I will probably not manage to print my thesis on time. Anyways, thank you for making any moment special, because you are all so different and have so many qualities.

Thanks to Cri and Jules, you always made me look forward to coming home and you always managed to change my worst mood into a smile.

Thank you, Cara, for sticking with me all these years. With you, distance has never been so insignificant, and emotions have never been so strong. I love you.

Grazie Renzo, Manny, Fox, Leo e a tutti gli altri fioi. Gli anni e le distanze non ci dividono e non ci cambiano, ma rafforzano il nostro legame.

Grazie Rletz. Grazie per credere in me e per valorizzare il mio occhio fotografico. E grazie per il Vino.

Grazie a Mom&Dad per avermi supportato e aver creduto in me. Grazie Sista per ricordarti sempre i nomi delle proteine che studio.

Thanks to Trypanosoma brucei for not infecting me for real.